Copyright Warning & Restrictions

The copyright law of the United States (Title 17, United States Code) governs the making of photocopies or other reproductions of copyrighted material.

Under certain conditions specified in the law, libraries and archives are authorized to furnish a photocopy or other reproduction. One of these specified conditions is that the photocopy or reproduction is not to be "used for any purpose other than private study, scholarship, or research." If a, user makes a request for, or later uses, a photocopy or reproduction for purposes in excess of "fair use" that user may be liable for copyright infringement,

This institution reserves the right to refuse to accept a copying order if, in its judgment, fulfillment of the order would involve violation of copyright law.

Please Note: The author retains the copyright while the New Jersey Institute of Technology reserves the right to distribute this thesis or dissertation

Printing note: If you do not wish to print this page, then select "Pages from: first page # to: last page #" on the print dialog screen

ABSTRACT

DYNAMIC RESPONSE OF HIGHWAY BRIDGES UNDER A MOVING TRUCK AND DEVELOPMENT OF A RATIONAL SERVICEABILITY REQUIREMENT

by
Shabnam Darjani

Through the development and usage of high-strength materials, the design of more flexible bridges is unavoidable. It is assumed that limiting a bridge static deflection would control the excessive vibration caused by more flexible design. However, results of prior studies indicate that deflection limits do not necessarily address bridges vibrational issue.

This dissertation addresses the parameters affecting bridge vibration and provides simple equations to compute bridge dynamic acceleration, velocity and displacement in both transient and steady state parts of the vibration. These equations can then be used to control bridges excessive vibration; and provide human comfort and structural performance.

A comprehensive analytical study was performed to evaluate dynamic response of bridges under a moving truck load. The effect of bridge dynamic parameters and vehicle moving conditions are investigated, which includes bridge frequency, damping ratio, span length, girders distance, bracing, support conditions, truck speed, load sequence, axle's weight, and number of spans. Bridge and vehicle k-parameters, which represent the number of vibration cycles before the next excitation occurs, are developed to better explain the vibrational behavior of a bridge. The proposed equations include bridge frequency, static deflection for one axle load, and k-parameters. Finally, a case study is presented to highlight the application of the new approach.

DYNAMIC RESPONSE OF HIGHWAY BRIDGES UNDER A MOVING TRUCK AND DEVELOPMENT OF A RATIONAL SERVICEABILITY REQUIREMENT

by
Shabnam Darjani

Advisor: Dr. Ala Saadeghvaziri

A Dissertation
Submitted to the Faculty of
New Jersey Institute of Technology
in Partial Fulfillment of the Requirements for the Degree of
Doctor of Philosophy in Civil Engineering

Department of Civil and Environmental Engineering

January 2013

.

APPROVAL PAGE

DYNAMIC RESPONSE OF HIGHWAY BRIDGES UNDER A MOVING TRUCK AND DEVELOPMENT OF A RATIONAL SERVICEABILITY REQUIREMENT

Shabnam Darjani

Dr. Mohamad A. Saadeghvaziri, Dissertation Advisor — Date
Professor of Civil and Environmental Engineering, NJIT

Dr. Bakhtiar Feizi, Committee Member — Date
Structural Engineer, AECOM Corporation, New York, NY

Dr. C. T. Thomas Hsu, Committee Member — Date
Professor of Civil and Environmental Engineering, NJIT

Dr. Rajendra Navalurkar, Committee Member — Date
Structural Dep. Manager, URS Corporation, Paramus, NJ

Dr. John R. Schuring, Committee Member — Date
Professor of Civil and Environmental Engineering, NJIT

Dr. Methi Wecharatana, Committee Member — Date
Professor of Civil and Environmental Engineering, NJIT

BIOGRAPHICAL SKETCH

Author: Shabnam Darjani

Degree: Doctor of Philosophy

Date: January 2013

Undergraduate and Graduate Education:

- Doctor of Philosophy in Civil Engineering,
  New Jersey Institute of Technology, Newark, NJ, 2013

- Master of Science in Civil Engineering,
  New Jersey Institute of Technology, Newark, NJ, 2012

- Bachelor of Science in Civil Engineering,
  Amirkabir University of Technology (Tehran Polytechnic) Tehran, Iran, 2008

Major: Civil Engineering

Presentations and Publications:

Darjani, S., Saadeghvaziri, M. A., and Aboobaker, N. (2010). "Serviceability considerations of high performance steel bridges." *Structures Congress/North American Steel Construction Conference, ASCE*, Orlando, FL, 752-761.

Darjani, S., Saadeghvaziri, M. A., Saigal, S., Aboobaker, N., and Khan, M. A. (2010)."Toward a more rational serviceability considerations for high performance steel bridges." *IABMAS2010, The Fifth International Conference on Bridge Maintenance, Safety and Management*, Philadelphia, PA, 610-617.

Darjani, S., Saadeghvaziri, M. A., Saigal, S., Aboobaker, N., and Khan, M. A. (2011). "Dynamic response of highway bridges subjected to moving load." *TRB2011 Nineteenth Annual Meeting, Transportation Research Board*, Washington, D.C, 1-16.

Darjani, S. and Saadeghvaziri, M. A. (2011). "Dynamic response and serviceability considerations of bridges under moving load." *ICAS2011, the Second International Conference on Architecture and Structure*, Tehran, Iran.

Darjani, S., Saadeghvaziri, M. A., Aboobaker, N. and Khan, M. A. (2012). "Bridge dynamic response due to truck load sequence." *IABMAS2012 Sixth International Conference on Bridge Maintenance, Safety and Management*, Villa Erba, Lake Como, Italy.

Saadeghvaziri, M. A., Darjani, S., Saigal, S., and Khan, M. A. (2012). "Design for Deflection Control vs. Use of Specified Span to Depth Ration Limitation." *Report FHWA/NJ-2012-0XX*, NJ Department of Transportation, Trenton, NJ.

Darjani, S. (2009). "Performance and Serviceability of High Performance Steel Bridges." *Dana Knox Student Research Showcase*, NJIT, Newark, NJ.

Darjani, S. (2011). "Dynamic Response of a Bridge under Moving Truck and Vibration Control." *NSF CMMI Research and Innovation Conference*, Atlanta, Georgia.

Darjani, S. (2010). "Design for Deflection Control vs. Use of Specified Span to Depth Ratio Limitations." *Twelfth Annual NJDOT Research Showcase*, Trenton, NJ.

To Aghdas Gholam Mirzaei Moghadar and Mohamad Taghi Darjani:
the most wonderful parents in the world.
I love you most of all.

تقدیم به اقدس غلام میرزایی مقدر و محمد تقی درجانی:
بهترین مادر و پدر دنیا.
با تمام وجودم دوستتان دارم.

ACKNOWLEDGMENT

Preparing a dissertation is a lot like planning a house party. You work incredibly hard and use all of your training and know-how to prepare something acceptable to the palettes of your peers and colleagues, while at the same time hoping to surprise everyone with work that will be talked about for years to come. There's inevitably some frustration, moments where you feel that this can't possibly work out in the end; there's an earned sense of confidence as everything finally comes together into a cohesive whole. Finally, once everything is finished, the meal eaten, the guests seated, there comes a moment of revelation: you are surrounded by friends, companions, a family of sorts. That has been one of the great joys of my studies, culminating in this dissertation- the colleagues I've found, the relationships I have forged, and the people I find myself surrounded by as I write the final words of this work.

Dr. Ala Saadeghvaziri, my advisor, who has stood by me through every phase of my work, without whose knowledge, experience and devotion this work would still be so many unrealized dreams. There are not words in either English or Persian to express my gratitude for his patience, humor and enthusiasm.

I would like to express my appreciation to my committee members, Professors Thomas Hsu, John Schuring, Methi Wecharatana, Drs. Bakhtiar Feizi, and Rajendra Navalurkar, whose advice, opinions and acceptance I so dearly cherish. Their trust in my abilities honors me.

My special thanks go to Dr. Taha Marhaba, Civil and Environmental Engineering department Chair, and Dr. Sunil Saigal, Dean of Newark College of Engineering, who graciously guided me through many of the challenges of my studies with their wisdom

and experience. I am also indebted to Dr. Xanthos, Ms. Gonzalez-Lenahan, and Mr. Grundy for showing me the way, step by step, through the last year of my study, ensuring I never lost my way. I appreciate Heidi Young, Robert Morris, Allyn Luke, Dallas Link, Marion Balavender, Lillian Quiles, Marlene Masi, and Annie Brown who assisted me with the myriad administrative issues and questions I faced during the four years of my study.

I would also like to extend my gratitude to all faculty members and staff in the Civil and Environmental Engineering Department; Graduate, International & Financial Aid Offices. Some of the faculty members in the Mechanical Engineering Department also helped me a lot; I would like to thank Professors Herli Surjanhata, Bernard Koplik, and Rong-yaw Chen for teaching me the knowledge I could hardly have obtained without them.

Without the New Jersey Department of Transportation, the following pages would likely be blank. It is only through their generous funding and opportunity that I was able to embark on this journey of discovery. Chief among those are Nazhat Aboobaker and Xiaohua Cheng. However, I must extend my thanks to all those working at the NJDOT who assisted me and similar PhD students. Your investment will surely benefit the infrastructure of this great country.

Friends: Shilan Motamedvaziri, Navid Allahverdi, Oruba Rabie, Chitra Sridhar, Yazdan Majdi, Jila Mosahebi, Mehdi Zarei, Mahnaz, Farzad, and Reza have made the last four years some of the most enjoyable and rewarding of my life. Their support and encouragement through every moment of my work and life has proven invaluable and remains cherished.

I appreciate my colleagues, Nickolas Carlson, Ashish Borgaonkar, Sheng Yan Gao, and Nimrat Sandho, for sharing their experience and insight, showing me the path.

Every great party, as with any great action or undertaking, requires inspiration before it can germinate into something well-remembered; a guiding force that permeates every atom of accomplishment. Mohammad Taghi Darjani and Aghdas Gholam Mirzaei Moghadar, my beloved parents, are that inspiration. They have been my bridge through this life, ensuring I cross all obstacles, with a minimum amount of discomfort and vibration. I appreciate them with every fiber of my being. Also, all thanks to Shaghayegh Darjani and Shahin Darjani, my beloved sister and brother, for the unlimited happiness and enthusiasm they bring to my life by their existence.

Finally, I greatly thank Maxwell Lux, my best friend, partner, support and strength, who has helped me during this time of crisis and stress. His support and encouragement through all my difficulties mean a lot to me and will not ever be forgotten.

TABLE OF CONTENTS

Chapter		Page
1	INTRODUCTION…….	1
	1.1 Problem Statement…….….	1
	1.2 High Performance Steel (HPS) vs. Conventional Steel …….….	2
	1.2.1 Deflection Criteria vs. Economical Use of HPS…….……..	4
	1.2.2 Vibration vs. Deflection Criteria……...	5
	1.3 Objectives…….……..	7
2	Literature review……	9
	2.1 Vibration and Human Comfort……...	11
	2.2 Vibration and Structural Performance……	20
	2.2.1 Girder Cracking……	20
	2.2.2 Deck Deterioration……	23
	2.3 Parameters Affecting Vibration…….….	28
	2.4 Alternatives Limitations…….	33
	2.4.1 Canadian Standards- Ontario Highway Bridge Code…….…..…	33
	2.4.2 European Codes……	35
	2.4.3 British Standard……..…….……	35
	2.4.4 German Code……..……	35
	2.4.5 Australian Specifications……..……	36
	2.4.6 New Zealand Code……...….	36

TABLE OF CONTENTS
(Continued)

Chapter **Page**

2.4.7 International Organization for Standards (ISO) ……..…. 37

2.4.8 Wright and Walker……..……..…… 38

3 FINITE ELEMENT MODELING…… 41

3.1 Zero Damping Exact Solution……... 41

3.2 Damped System Analysis…….. 43

3.3 Moving Load Model…….. 47

3.3.1 Time Function…….. 48

3.3.2 Time Step……. 50

4 PARAMETRIC STUDY…….…… 52

4.1 Speed Parameter and k-Parameter…… 52

4.2 Damping Ratio…….. 56

4.3 Load Sequence…… 58

4.3.1 Consecutive One-Axle Loads……... 58

4.3.2 Two-Axle Loads……... 63

4.3.3 Different Axle Weights…… 66

4.3.4 Three-Axle Trucks…… 68

4.3.5 Bridge Response Due to Truck Loads…… 71

4.4 Number of Spans…….. 78

4.5 2-Dimensional vs. 3-Dimensional Models …….…… 81

4.5.1 Stringer Spacing ……..…… 84

TABLE OF CONTENTS
(Continued)

Chapter **Page**

4.5.2 Effect of Bracing …… 85

4.6 Effect of Elastomeric Bearing …… 87

4.6.1 Test Data……..…… 88

4.6.2 Material Model…… 92

4.6.3 Dynamic Response Due to Elastomeric Bearings…… 95

5 STRUCTURAL PERFORMANCE……. 104

5.1 Fatigue Problem due to Vibration…… 104

5.1.1 Fatigue Loads……..……. 105

5.1.2 AASHTO LRFD Fatigue Criteria……..……..…….. 106

5.2 Analytical Studies on Fatigue……... 109

5.3 Fatigue Modification……. 117

6 CASE STUDIES……..…….. 119

6.1 Dynamic Response…… 119

6.1.1 Study by Yang et al…...……. 120

6.1.2 Study by Yau et al…...……. 121

6.1.3 Study by Pan and Li…...……. 122

6.2 Human Comfort and Limitation…… 124

7 RATIONAL SERVICEABILITY CRITERIA……..……... 131

7.1 Example I- Magnolia Avenue Bridge…… 133

7.2 Example II- Route 130 over Route 73…… 134

TABLE OF CONTENTS
(Continued)

Chapter **Page**

7.3 Example III and IV- Field Measurements…… 135

8 CONCLUSIONS AND FUTURE WORK…….……. 142

APPENDIX A…… 150

APPENDIX B…… 156

REFERENCES…….…… 158

LIST OF TABLES

Table **Page**

2.1 Depth-to-Span Ratios per AREA and AASHTO ……..…..….. 9

2.2 Evaluation of Deformation Requirements in Bridge Design……..…..... 11

2.3 Summary of Literature Results on Acceleration Limitation……..…. 19

2.4 Perception of Vibration According to DIN 4150…….……... 36

2.5 Peak Acceleration Limit for Human Response to Vertical Vibrations……... 40

4.1 Bridge Natural Frequency and Span Length Corresponding to $k_b = 1$……..…. 56

4.2 Calculated Bridge k-Parameters (k_b) for Some Bridges in New Jersey……..…… 56

4.3 One Stringer 3-D Model (Solid Element) vs. 2-D Model ……...…….…….…… 83

4.4 Frequency and Static Deflection of 2D and 3D Models……. 84

4.5 The Effect of Bracings on Bridge Dynamic Response……... 87

4.6 Material Constants for Yeoh Strain Energy Function……. 93

4.7 Bridge Dynamic Results with Elastomeric Bearing B1, $k_b = 2.98$…….…… 100

4.8 Bridge Dynamic Results with Elastomeric Bearing B2, $k_b = 2.89$……. 100

4.9 Bridge Dynamic Results with Elastomeric Bearing B3, $k_b = 7.34$……..101

5.1 Fatigue Constant A and Threshold Amplitude for each Detail Category……... 107

5.2 Number of Vibration Cycles per Truck by AASHTO…… 110

5.3 Cumulative Damage Due To Transient Part of the Vibration (TCD) for $k_v = 2$……. 112

5.4 Number of Cycles to Fatigue Failure for $k_b = 3$, $k_v = 2$ and $\zeta = 3\%$..... 114

6.1 Bridge Parameters in Pan and Li…….…… 123

LIST OF FIGURES

Figure		Page
1.1	Stress-strain curves for different types of steel	3
1.2	CVN transition curve for HPS-70W (70 ksi) compared to 50W steel	3
1.3	Deflection versus span to depth ratio for a sample bridge	4
2.1	Human perceptible vibration	13
2.2	Average amplitude of vibration	15
2.3	Human perceptible vibration according- Janeway, Wiss and Parmelee	16
2.4	Average peak accelerations	17
2.5	Acceptability of vertical vibrations for outdoor footbridges	18
2.6	Typical web cracking at diaphragm connections	21
2.7	Typical Relative deflection of main girders.	22
2.8	Typical fatigue cracks in plate girders	22
2.9	Deformed configuration under 3000 lb load at the center for (a) composite deck and (b) non-composite deck with and without diaphragm	24
2.10	Deflection limits per Ontario Code	34
2.11	Dynamic load allowance	34
2.12	Peak acceleration for human comfort for vibrations due to human activity	38
3.1	Moving load modeling	47
3.2	Types of time function	48
3.3	Effect of rectangular (a) and triangular (b) time function on bridge response	49
3.4	Effect of 0.04 sec (a) and 0.01 sec (b) time step on bridge response	51

LIST OF FIGURES
(Continued)

Figure **Page**

4.1 Dimensionless displacement (a), velocity (b), acceleration (c) for single moving load and 0% damping versus speed parameter……..……..……..…..... 53

4.2 Dimensionless displacement (a), velocity (b), acceleration (c) for single moving load and 0% damping versus k_b ……..……..……..…….…….. 55

4.3 The effect of damping ratio on bridge dynamic response ……...…….…….... 57

4.4 The schematic of one axle load over the bridge at a time with (a) zero arrival time and (b) with non-zero arrival time……..……...….. 59

4.5 Maximum (a) steady state and (b) transient part of the bridge dynamic response under one-axle load at a time for (1) kb = 2, (2) kb = 2.5, and (3) kb = 3…..…..… 60

4.6 Vibration due to two and three consecutive loads, one axle over the bridge at a time…….....…... 62

4.7 Two-axle load over a bridge ..……..…..... 63

4.8 The maximum (a) steady state and (b) transient part of a bridge dynamic response under two-axle loading for different arrival time …….... 65

4.9 2nd axle participation factor with respect to its arrival time.…….…….... 67

4.10 Illustration of bridges with different k_b…..……..…….…... 69

4.11 The maximum (a) steady state Response (R) and (b) transient R of a bridge dynamic displacement, velocity, and acceleration responses under a three-axle truck for different A_{t2} and A_{t3}……..... 70

4.12 The most common truck types in a randomly selected highway in New Jersey…….…….…..... 72

4.13 Dimensionless displacement for three bridges of k_b =2, k_b =3 and k_b =6.…..... 73

4.14 Dimensionless velocity for three bridges of k_b =2, k_b =3 and k_b =6.……..…..... 74

4.15 Dimensionless acceleration for three bridges of k_b =2, k_b =3 and k_b =6.……..... 74

LIST OF FIGURES
(Continued)

Figure **Page**

4.16 Transient displacement for three bridges of k_b =2, k_b =3 and k_b =6.……..... 76

4.17 Transient velocity for three bridges of k_b =2, k_b =3 and k_b =6.……..... 76

4.18 Transient acceleration for three bridges of k_b =2, k_b =3 and k_b =6.……..... 77

4.19 Dynamic load allowance compared with impact factor suggested by Canadian code……...… 78

4.20 Steady state dimensionless displacement for 1, 2, 3, 4, 5, and 6-span bridges.…... 79

4.21 Transient dimensionless displacement for 1, 2, 3, 4, 5, and 6-span bridges.…..... 79

4.22 Steady state dimensionless velocity for 1, 2, 3, 4, 5, and 6-span bridges.……..... 80

4.23 Transient dimensionless velocity for 1, 2, 3, 4, 5, and 6-span bridges…..……..... 80

4.24 Steady state dimensionless acceleration for 1, 2, 3, 4, 5, and 6-span bridges.….. 81

4.25 Transient dimensionless acceleration for 1, 2, 3, 4, 5, and 6-span bridges…….. 81

4.26 Stringers dimensions for the bridge on Rt. 130 over Rt. 73……....….... 82

4.27 Dimensionless displacement response for the sample bridge with 5 stringers spacing at 12 ft.……..……...….... 85

4.28 Three dimensional model for a sample bridge.…….……..…..…..... 86

4.29 Uniaxial tensile test data (Yoshida et al. 2004), loading velocity 69.5 mm/min.... 88

4.30 Biaxial tension test equipment and experimental data for NR ……..….. 89

4.31 Compression test data (a) and simple shear test data (b) for NR and different strain rates..……...……..... 89

4.32 Volumetric test data for NR ……..……...……..... 90

4.33 Applied strain (stretch) histories in multi-step relaxation tests for simple shear 91

LIST OF FIGURES
(Continued)

Figure **Page**

4.34 Stress history recorded in multi-step relaxation tests on Natural Rubber for simple shear ……...…….. 92

4.35 Yeoh strain energy function and test data ……...…….…….. 93

4.36 Uniaxial tensile FE model and test data.……....…….…….. 94

4.37 Simple shear test results…….....…….....…….…….. 94

4.38 Compression test results ……...…....…….…….. 95

4.39 Model of elastomeric bearing B1……...…….....…….. 96

4.40 Compressive stiffness of elastomeric bearing B1…...…….…….. 98

4.41 Different types of support conditions (a) rigid support, (b) spring support, (c) linear spring, (d) elastomeric bearing...……...……...…….. 99

4.42 Dimensionless displacement for simply supported bridge and elastomeric bearing with stiffness ratios of 0.224 and 0.03…….……...…….. 102

4.43 Dimensionless velocity for simply supported bridge and elastomeric bearing with stiffness ratios of 0.224 and 0.03…….……...…… 102

4.44 Dimensionless acceleration for simply supported bridge and elastomeric bearing with stiffness ratios of 0.224 and 0.03…….……...…….. 103

5.1 Types of fatigue loads …….……...…….. 105

5.2 Variable stress range in bridge response due to a truck……. 106

5.3 S-N curve and threshold limits for each design category (AASHTO LRFD)…... 108

5.4 Stress range for the transient with respect to the steady state part of the vibration.. 109

5.5 Stress range spectrum and S-N curve to find out the cumulative damage due to each stress range……... 111

5.6 Effective fatigue life vs. k-parameters due to both steady state and transient parts of the vibration…….. 117

LIST OF FIGURES
(Continued)

Figure **Page**

5.5 Stress range spectrum and S-N curve to find out the cumulative damage due to each stress range……. 111

5.6 Effective fatigue life vs. k-parameters due to both steady state and transient parts of the vibration…….…….…….. 117

6.1 Impact factor versus speed parameter comparison with Yang et al…….. 120

6.2 Impact factor for midspan deflection of a beam subjected to different vehicle models by Yau et al……..…… 122

6.3 Midspan displacement of simply supported beam with different vehicle speeds…. 123

6.4 Midspan velocity of simply supported beam with different vehicle speeds…….. 124

6.5 Midspan acceleration of simply supported beam with different vehicle speeds….. 124

6.6 Comparison with average amplitude of vibration suggested by Goldman…… 127

6.7 Comparison with the human perceptible vibration introduced by Reiher and Meister……..…… 128

6.8 Comparison with Ontario Code deflection limits…….. 129

7.1 Fast Fourier Transform for Rt. I-80 over Rt. I-287 steel bridge…… 139

7.2 Fast Fourier Transform for Rt. I-80 over Smith Rd. concrete bridge…… 139

7.3 Typical end diaphragm detail for steel girder bridges……... 140

7.4 Typical end diaphragm detail for concrete girder bridges……. 141

NOMENCLATURE

The following symbols are used in this dissertation:

L	—Span length
d	—Beam depth
D	—Beam depth including concrete deck thickness
f, f_b	—Bridge natural frequency
δ	—Displacement amplitude
δ_{st}	—Static displacement or deflection at the mid-span
ζ	—Damping ratio
V	—Load velocity
α	—Speed parameter
k_v	—Vehicle k-parameter
k_b	—Bridge k-parameter
IM	—Impact factor
ω	—Bridge angular frequency
T, T_b	—Bridge natural period
i	—Integer number
t_d	—Load duration
m	—Multiple presence factor
E	—Modulus of elasticity
I	—Moment of inertia
P	—Axle weight

NOMENCLATURE
(Continued)

A_t —Arrival time

L_v —The distance between the heaviest axles (Vehicle length)

PF —Participation Factor for the 2^{nd} load

R —Bridge dimensionless transient response

Vel —Velocity response

Acc —Acceleration response

P_{max} —The weight of the heaviest axle of a truck

C_{10}, C_{20}, C_{30} —Yeoh Hyperelastic material model constants

D_1, D_2, D_3 —Incompressibility parameters

E_c —Compressive modulus

G —Modulus of rigidity, shear modulus

S —Shape factor

L_s —Bearing/support length

W_s —Bearing/support width

h_{ri} —Height of the i^{th} layer elastomer

K_s —Spring stiffness constant

A_s —Support area

K_{ls} —Support stiffness per unit length

k_r —Bridge to bearing stiffness ratio

A —Detail category constant in ksi

$(\Delta F)_n$ —Allowable fatigue stress

NOMENCLATURE
(Continued)

N	—Number of bridge vibration cycles for a 75 year design life
TCD	—Transient Cumulative Damage
$(ADTT)_{SL}$	—Single-lane Average Daily Truck Traffic
$(\Delta F)_{TH}$	—Constant amplitude fatigue thresholds in ksi
n	—Number of cycles per truck passage
f_{ss}	—Stress range in the steady state part of the vibration
$f_{transient}$	—Stress range in the transient part of the vibration
u_i	—Vibration amplitude after i cycles
u_{i+j}	—Vibration amplitude after i+j cycles
j	—Number of cycles in a duration
N_i	—Number of cycles to failure
n_i	—Number of cycles during life time
C	—Minor's rule constant
f_λ	—Stress range after λ cycles
m_b	—Bridge mass per unit length
m_v	—Vehicle mass
σ	—Stress
ε	—Strain
η	—Viscosity constant
G_0	—Initial shear modulus
τ	—Relaxation time

CHAPTER 1

INTRODUCTION

1.1 Problem Statement

There have been significant advances in development of high performance materials over the past two decades. High Performance Steel (HPS) is an example that provides cost and significant weight savings when it is used as a hybrid section with conventional steel and reduces the number of stringers. HPS offers higher yield strength, enhanced weldability, and improved toughness which result in smaller cross section, lighter and much more economical designs. On the other hand, smaller cross section leads to more flexible bridges that do not satisfy the existing optional serviceability deflection criteria.

AASHTO Standard Specifications (AASHTO LFD 1996) limit live load service deflection to L/800 for general bridges and to L/1000 for bridges that are used by pedestrians. These limits were originally employed to avoid undesirable structural and psychological effects due to a bridge vibration. However, results of prior studies indicate that deflection and L/D limits do not necessarily address these objectives. Existing limits do not prevent damages in structures because they check global deflection, while the damages are more attributed to local deformations such as connection rotations and twisting of cross beams relative to support stringers (Roeder et al. 2002). Furthermore, human susceptibility is more influenced by derivatives of deflection (e.g., acceleration or velocity) rather than the deflection itself. Thus, there is a need for development of a more rational serviceability criterion that reliably controls bridge vibration while enhancing the use of HPS.

Although deflection limits have been made optional in AASHTO LRFD (1998), due to the reasons stated above, they are still being used by transportation agencies and designers mainly due to the lack of an appropriate and rational guideline that can address bridge vibration and human comfort. If the optional deflection limits are neglected in large span bridges, significant weight and cost savings, up to 20% (Clingenpeel 2001; Nagy 2008), may be realized.

Thus, there is a need for a more rational bridge vibration control guideline that enhances structural performance and human comfort while allowing the application of high strength materials. Important to this is availability of a versatile analytical model that can reliably and accurately determine vibrational response of bridges subjected to moving loads.

1.2 High Performance Steel vs. Conventional Steel

HPS offers high yield strength (Figure 1.1), high fracture toughness, good weldability, and the ease of fabrication with the choice of weathering performance (Homma et al. 2008). As a result of higher strength it can result in lighter and much more economical designs. However, live-load deflection limits of bridge design specifications negate the economical implementation of HPS.

The fracture toughness of high performance steel is much higher than the conventional bridge steel. Figure 1.2 shows the Charpy V-Notch (CNV) transition curves for HPS 70W (HPS 485W) and conventional 50W steel. The Charpy V-Notch test is a standardized high strain-rate test which determines the amount of energy absorbed by a

material during fracture. This absorbed energy for HPS 70W is much higher than 50W steel at the same temperature.

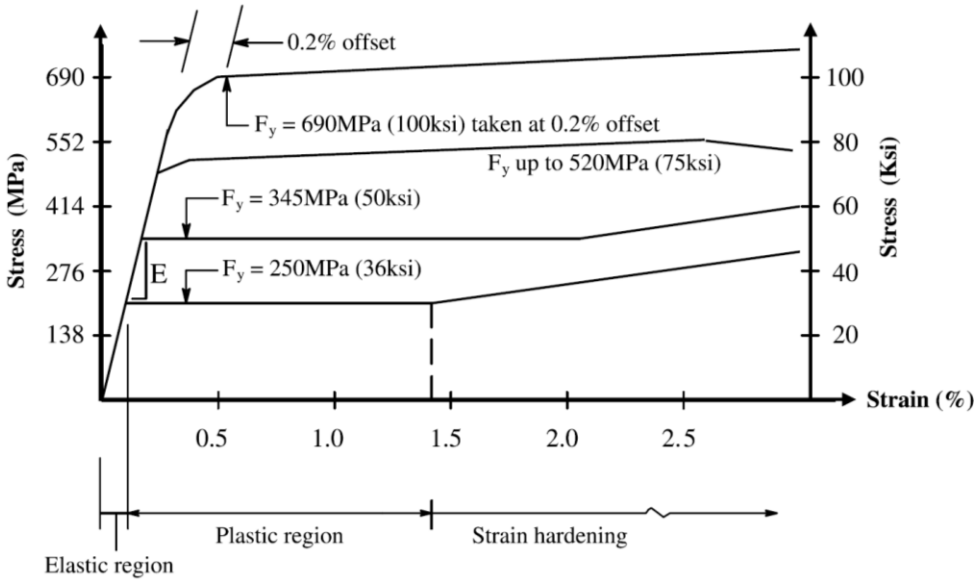

Figure 1.1 Stress-strain curves for different types of steel (Gergess and Sen 2009).

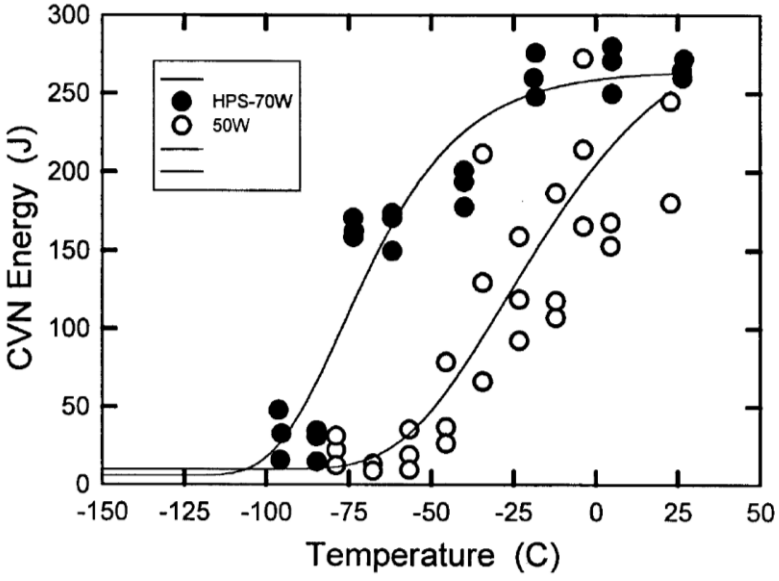

Figure 1.2 CVN transition curve for HPS-70W (70 ksi) compared to 50W steel (Fisher and Wright 2007).

As can be seen, the ductile-brittle transition temperature for HPS-70W is lower than 50W steel and HPS provides a toughness level that far exceeds the toughness for convectional steel. Although the cost of these newly invented materials is higher than ordinary grade 50W steel, the advantages due to higher strength are more than the difference in material costs (Dexter et al. 2004).

1.2.1 Deflection Criteria vs. Economical Use of HPS

Deflection control is not usually effective on design for those types of steel with the yield stress less than 50 ksi. However, when the bridge is designed for higher strength steel materials, sometimes, deflection control is the factor which appears to be critical. This is even more critical when a higher strength material such as 100W steel is used for design (Azizinamini et al. 2004; Nagy 2008; Roeder et al. 2002). Figure 1.3 shows the results obtained by Roeder et al. (2002) for the effect of span to depth ratio on deflection in different steel materials. As can be seen, when span to depth (L/d) ratio is higher than 23, the deflection control is critical in design.

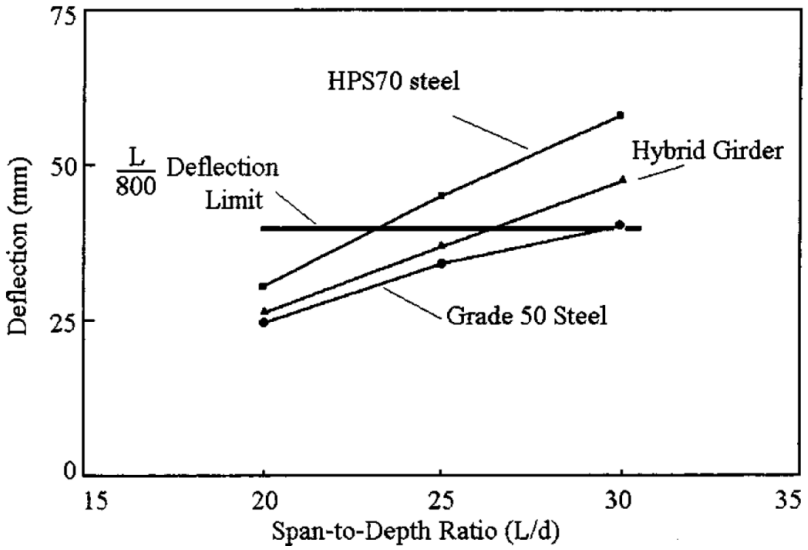

Figure 1.3 Deflection versus span to depth ratio for a sample bridge (Roeder et al. 2004).

Research shows that the use of HPS in bridges is not beneficial if deflection limits being controlled by designers. Homma (1994) performed a study on existing highway bridges and redesigned them for HPS of various strength levels. The results indicated that for efficient use of higher strength materials, a certain modification is required for the existing code criteria. Clingenpeel (2001) investigated the economy use of HPS 70W in steel bridge design using various span lengths, girders spacing and yield strength. The performed parametric studies for weight, performance, deflection, and cost indicate that the most economical use of HPS 70W is a hybrid girder with 70W flanges where a lower number of girders is used. Another study by Nagy (2008) investigated the effect of L/D and the use of HPS on deflection criteria and weight savings. It was shown in this study that span to depth ratio has a significant effect on live load deflection. All of the designs that failed L/800 deflection criteria were hybrid 70W girders with high L/D ratio.

1.2.2 Vibration vs. Deflection Criteria

Initially AASHTO specifications did not have explicit live load limits. In 1930's, Bureau of Public Roads conducted a study on impact of vibration on human. As a result of this study, live load deflection limit, L/800, was added to AASHTO Specifications in 1936 after it was found that steel highway bridges with high vibrations had static deflection greater than L/800 (Roeder et al. 2002). Note that the material and design for the bridges in that era were significantly different from the material and design for newly constructed bridges.

In 1958, a committee of American Society of Civil Engineering (ASCE 1958) reviewed the history of bridge deflection limits along with a survey of data on bridge vibration, field measurements, and human perception of vibration. Their survey showed no evidence of serious structural damage attributable to excessive live-load deflection. The report states:

> *"The few examples of damaged stringer connections or cracked concrete floors could probably be corrected more effectively by changes in design than by more restrictive limitations on deflection. Both the historical study and the results from the survey indicated clearly that unfavorable psychological reaction to bridge deflection was probably the most frequent and important source of concern regarding the flexibility of bridges. However, those characteristics of bridge vibration which are considered objectionable by pedestrians or passengers in vehicle cannot yet be defined."*

The committee recommended that no changes be made at the time, because those characteristics of bridge vibration which were considered objectionable by pedestrians or passengers in vehicle could not have been defined at the time. They recommended using a more restrictive deflection limit for bridges in which composite action was taken into account in design. It was also recommended that further attempts to be made to determine what constitutes objectionable vibration of highway bridges and to develop design criteria which will limit them. Two years later, in 1960, a more conservative limit of L/1000 was added for bridges used by pedestrians. Since then many studies were

conducted to address these goals. However, none has been adopted by AASHTO Specifications because of the lack of consensus.

1.3 Objective

While ensuring human comfort and structural performance, this dissertation offers a new and more rational serviceability requirement that will not penalize the use of high performance material. A comprehensive parametric study is performed and the results are used to propose a simple and practical method to calculate bridge vibrational parameters.

Different models for bridge are analyzed using Finite Element method, namely, time integration and modal analysis. Vehicle axles can be modeled as moving loads or moving sprung masses. However, previous research (Yau et al. 1999) shows that the use of sprung mass would decrease the bridge dynamic response. Therefore, the use of moving load model would be more conservative than the use of sprung mass model. The ratio of moving truck to bridge masses is considered small and the effect of frequency change while the mass is moving through the bridge is neglected. The pitfalls with the use of existing finite element software programs is investigated and a guideline on developing bridge models that can reliably and accurately determine bridge dynamic responses (deflection, velocity and acceleration) is provided.

Parametric study is a major task of this dissertation. The effect of bridge flexibility on the bridge vibration is investigated. It is assumed that bridge flexibility will cause excessive bridge vibration. However, the results of this study show that this is not always true. Those parameters that affect bridge vibration other than deflection will be introduced.

Moreover, the bridge structural performance due to vibration is investigated for the extreme cases. Fatigue problem is an active structural damage that occurs when a material is subjected to repeated loading and unloading. Structures with high cycles of vibration are more sensitive to fatigue failure. By manipulating the influential parameters, fatigue problem due to excessive vibration can be controlled.

Finally, the results of parametric study are compared with the corresponding literature and a new serviceability requirement will be proposed which considers not only the bridge deflection but also other parameters affecting bridge vibration. This new requirement can reliably and accurately estimate bridge responses due to moving trucks. The results of this study may be used with a combined study with human reaction to vibration and limits can be provided for bridge engineers.

CHAPTER 2

LITERATURE REVIEW

As Roeder et al. (2002) reported, deflection limitation is traced back to 1871 and was established by the Phoenix Bridge Company. These specifications limited the passage of a train traveling at 30 mph to 1/1200 the span length. In 1905, American Railway Engineering Association (AREA) restricted the depth to span ratio to 1/10 for trusses and plate girders, and 1/12 for rolled beams and channels used as girders. The history of depth to span length is as shown in Table 2.1.

Table 2.1 Depth-to-Span Ratios per AREA and AASHTO (Roeder et al. 2002)

	Year	Trusses	Plate Girders	Rolled Beams
AREA	1905	1/10	1/10	1/12
	1907-1919	1/10	1/12	1/12
	1919-1953	1/10	1/12	1/15
AASHO	1913-1931	1/10	1/12	1/20
	1931-1935	1/10	1/15	1/20
	1935-1953	1/10	1/25	1/25

In 1930, the Bureau of Public Roads conducted a study on the bridges with objectionable vibration. The attempt was to find out the reason behind the observed vibration. As a result of this study, live load deflection, L/800, was added to the design code to limit the excessive vibration. However, the bridges built in that era had wood plank decks, and the superstructures were pony trusses, simple beams, or pin connected through trusses (Roeder 2002). These bridges were non-composite, and rarely contained

continuous spans. ASTM A7 steel with 33 ksi yield strength was the accepted steel for bridge design and construction (Barker et al. 2008). L/1000 deflection limit was added in 1960 for highway bridges with side walk. This more sever deflection limit was established for the bridges open to pedestrian traffic. In 1958, a survey conducted by ASCE committee (ASCE 1958) showed no evidence of serious structural damage that could be attributed to excessive deflection. They suggested the use of deflection control at the time until a more rational vibration control being developed. However, yet, there is no rational vibration control exist that reliably and accurately can control bridge vibration.

Tilly et al. (1984) found that human were disturbed by vibration long before the bridge damaged structurally. Brown (1977) stated that all bridges except very light bridges were little affected structurally by vibrations though humans may be bothered totally. Nowak and Grouni (1988) have shown that deflection and vibration criteria should be derived by considering human reaction to vibration rather than structural performance. Wright and Walker (1971) reported that deflection limits were based on the reactions of people to the bridge vertical vibration. Therefore, it had been concluded that the deflection limitation was introduced to avoid unfavorable psychological reaction due to bridge vibration, and not to provide more structural durability for bridge structures.

It is now generally agreed that the primary factor affecting human sensitivity is acceleration, rather than deflection, velocity, or the rate of change of acceleration for bridge structures (Billing and Green 1984; Postlethwaite 1944; Blanchard et al. 1977). However, deflection limits are still utilized to provide serviceability criterion. As computing deflection was much easier than computing acceleration or velocity of the

bridge responses, it has been more practical to limit the deflection rather than bridge velocity or acceleration. Table 2.2 shows the development of deflection criteria from 1871 to 1960. Note that the deflection criteria have been optional since 1998 in AASHTO LRFD.

Table 2.2 Evaluation of Deflection Requirements in Bridge Design

Year	Agency	Deflection Limit
1871	Phoenix Bridge Company	1/1200 of span length (for train speed 30 mph)
1936	Bureau of Public Roads	1/800 of span length
1938	AASHO	1/800 of span length
1960	AASHTO	1/1000 of span length (for bridges with pedestrians)

2.1 Vibration and Human Comfort

In 2002, an NCHRP study by Roeder et al. provided comprehensive information on live load deflection, in which no evidence of serious damage on bridge structures due to flexibility was found, while the damage was invariably a consequence of local deformations such as connection rotations and twisting of cross beams relative to support members. There is a general agreement that human response to vibration is subjective and it is not directly measurable. However, it can be reported as perceptible, unpleasant, and tolerable (Wright and Green 1959).

In general, several factors influence the level of perception and the degrees of sensitivity of people to vibration. Among them, one can note position of the human body, excitation source characteristics, exposure time, floor and deck system characteristics, level of expectancy and type of activity engaged in (Griffin 2004).

Smith (1988) indicated that, in the majority of cases, reports of disturbing vibration come from pedestrians. It appeared that the reason for this is that the drivers and passengers inside the vehicles seldom notice the oscillations of bridges, perhaps because their vehicle's normal vibration obscures the vibration. Oehler (1970) confirmed this and stated that only pedestrians or occupants of stationary vehicles objected to bridge vibration. It has been noted (Moghimi and Ronagh 2008) that pedestrians are less susceptible to the vertical component of vibration when walking than when standing. Humans can tolerate less vibration vertically than in any other directions (Postlethwaite 1944). Besides, because of the frequent vibration occurrence in bridges due to moving loads, this structure is generally rigid in the horizontal plane (except the wind-induced horizontal oscillation occurring in very long suspension bridges). Reported by Moghimi and Ronagh (2008), higher values of vertical motion are acceptable in bridges, when compared to residential or office buildings; because users are out in the open area and are more aware of the presence of wind or traffic. Also, people crossing a bridge are exposed to vibration for a relatively short period of time. Therefore, the comfort threshold for bridge users is higher than the residential and office buildings.

People do not respond to vibration which persists for fewer than five cycles (Wright and Walker 1971). Therefore, only the dynamic component of the bridge motion, which does persist for a number of cycles after the loading leaves the bridge, is of the concern for human response. That is why people are less susceptible to vibration damped out rapidly. It should be noted that bridge damping ratio is relatively small and it is from 1% to 6%. Therefore, the number of cycles may be relatively large for the bridges with

lower damping ratio. British Standard (BD 37/01) recommends considering damping ratio of 0.03 for steel bridges, 0.04 for composite bridges, and 0.05 for concrete bridges.

Scales of Vibration Intensity

Human reaction to motion is very complex and cannot be consistently described in terms of any single parameter. Among the existing limits for perceptible vibration, the displacement amplitude limit is mostly considered in earlier studies. It is due to the fact that calculating deflection was much easier and more practical than calculating other characteristics such as acceleration and velocity of vibration. Most of these studies were upon floor and footbridge vibrations. Reiher and Meister (1931) suggested a base curve for acceptable human response to the vibration (Figure 2.1). In this curve, displacement amplitude is limited with respect to frequencies, and human response is ranged from imperceptible to very disturbing.

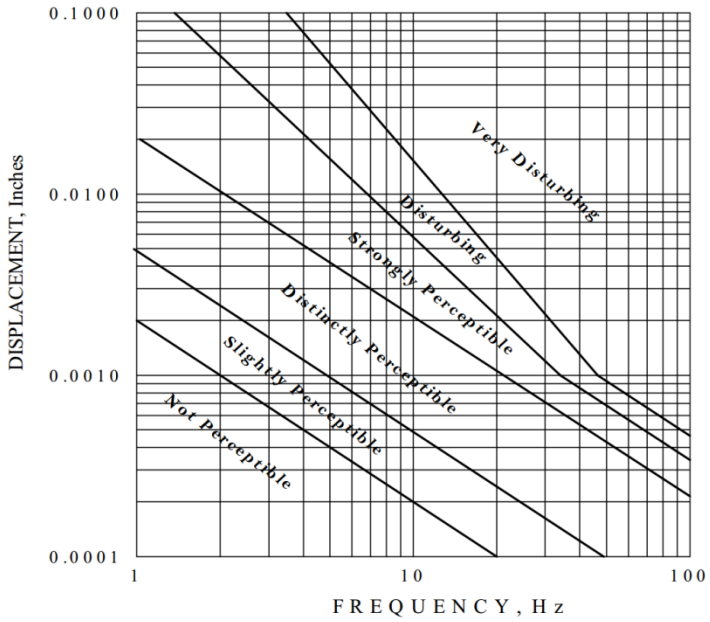

Figure 2.1 Human perceptible vibration (Reiher and Meister 1931).

In 1948, Goldman tried to construct perception curves by combining experimental results of different authors including Reiher and Meister (1931) and presented a set of revised averaged curves corresponding to three tolerance levels (Figure 2.2): I) the threshold of perception, II) the threshold of discomfort, and III) the threshold of tolerance.

One of the early efforts to find a correlation between human response and a combination of bridge frequency and displacement was made by Janeway (1950). He limited the product of vibration amplitude and cubic frequency, δf^3, to 2, for frequencies from 1 Hz to 6 Hz, and the product of vibration amplitude and squared frequency, δf^2, to 1/3 for frequencies from 6 Hz to 20 Hz (Janeway 1950; Machado 2006).

Among the 34 spans that Oehler (1957) tested to examine Janeway's suggestion, none of them was in agreement with Janeway's suggestion. The product of amplitude and frequency, δf, is investigated in another study (Wiss and Parmelee 1974) and the range was found from 0.018 to 0.062 cps-in (cycle per second inch) for distinctly perceptible and 0.18 cps-in for strongly perceptible. Figure 2.3 shows two strongly perceptible and unacceptable limits from Janeway and; Wiss and Parmelee studies. As can be seen, the limits match each other for higher frequencies.

Wright and Green (1964) compared the levels of vibration for 52 bridges to levels based on Reiher and Meister's scale and Goldman's work. They showed that 25% of the bridges reached the intolerable level indicated by Reiher and Meister's and Goldman's work. They concluded that there was no known scale of vibration intensity that may be directly related to those kinds of vibration experienced in highway bridges.

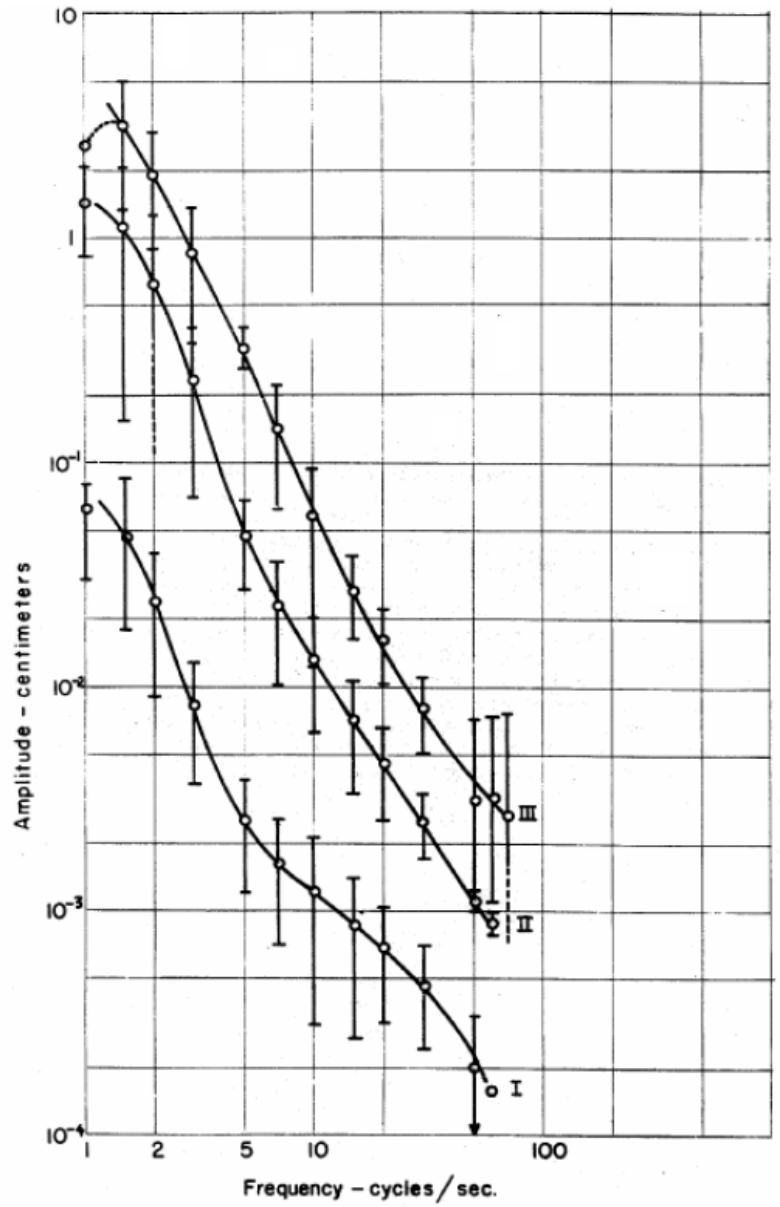

Figure 2.2 Average amplitude of vibration (Goldman 1948).

There were other scales limitation rather than deflection limitation that were doubted to influence on bridge vibration perceptible by humans. In a study by Manning (1981), it is concluded that if the time to travel the span is equal to the fundamental period of the bridge, the maximum dynamic response of the bridge occurs. Two other studies (Bartos 1979; Tilly et al. 1984) argue that the natural frequency of the bridge

should be out of the range of vehicle natural frequency (1.5-5 Hz); otherwise, unacceptable dynamic effect is unavoidable. Bartos (1979) stated that AASHTO deflection limitation leads most medium span steel bridges to have the natural frequency of 2.5 Hz which coincides with the typical truck frequency. Blanchard, Davies and Smith (1977) recommended using dampers or other means to reduce the response for the bridges with natural frequencies between 4 and 5 Hz. Ontario Code specified raising the impact value if natural frequency of the bridge is in the range of 2.0 to 5.0 Hz.

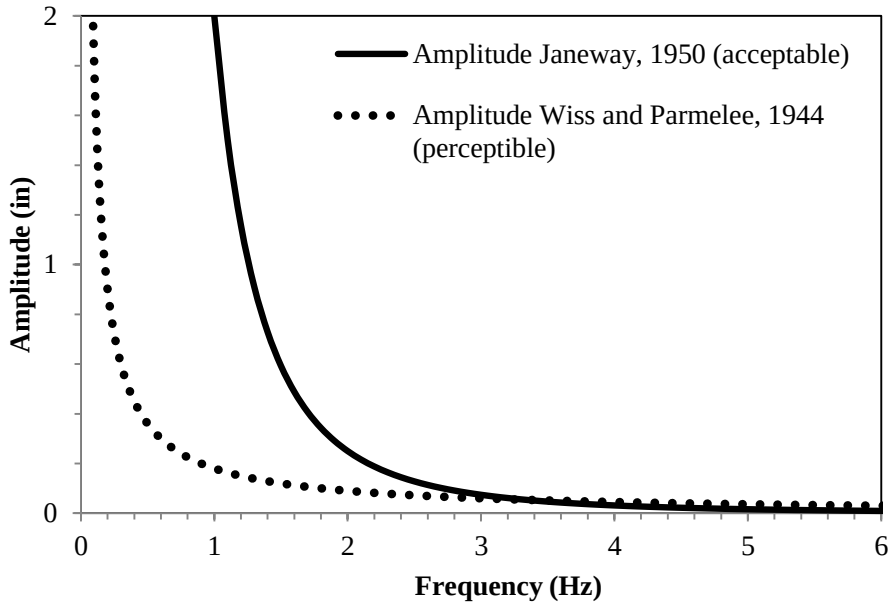

Figure 2.3 Human perceptible vibration according comparison.

In Gaunt and Sutton's (1981) study of bridge vibration, it is indicated that a human body is sensitive to the derivatives of displacement rather than the displacement. For the frequency range of 1 to 6 Hz, people are most susceptible to jerk value (the first derivation of the acceleration), for frequencies ranged from 6 to 20 Hz, acceleration, and for frequency ranged from 20 to 60 Hz, the value of velocity affect human response.

Also, according to ISO (1989), the frequency for maximum sensitivity to acceleration is in the range of 4 to 8 Hz for vibration in the vertical direction.

Most of the literature agrees with that humans respond to bridge acceleration and vibration duration rather than other vibration parameters. According to Goldman (1948) the minimum acceleration for human discomfort due to vibration is about 4.6% g (18 in/sec^2) while the perceptible value is only 0.25% g (1 in/sec^2). This minimum value occurred around a frequency of 5 Hz which is the main resonant frequency of human body (Machado 2006). Figure 2.4 shows a set of revised averaged curves corresponding to three tolerance levels: I) the threshold of perception, II) the threshold of discomfort, and III) the threshold of tolerance (Machado 2006).

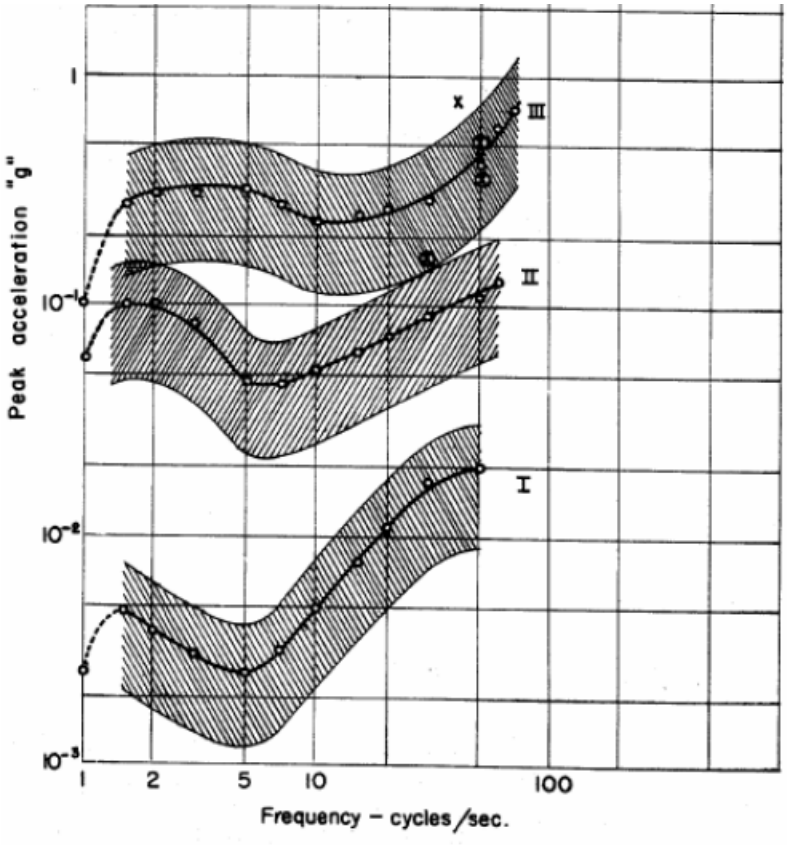

Figure 2.4 Average peak accelerations (Goldman 1948).

In a study by Postlethwaite (1944), it is suggested to limit acceleration to 0.03% g for those structures with the natural frequency less than 1 Hz. In the frequency range of 1 to 6 Hz, the value of acceleration for strongly noticeable from 1.5% g to 1.8% g and for uncomfortable vibrations is from 6% g to 16% g.

In a field study performed by Billing and Green (1984), the range of acceleration response was 1.5% g to 2.5% g for slightly perceptible, 5.2% g for distinctly perceptible and 7.6% g for strongly perceptible.

Figure 2.5 shows the comparison between three different codes in terms of acceleration limits to control undesirable bridge vibration, British Specification, Ontario Code and ISO. According to ISO, at vibration magnitude below the relevant curve, complaints regarding vibration are rare; thus, these magnitudes can be considered as acceptable limits (Moghimi and Ronagh 2008). Table 2.3 shows the summary of literature results on acceleration limitations.

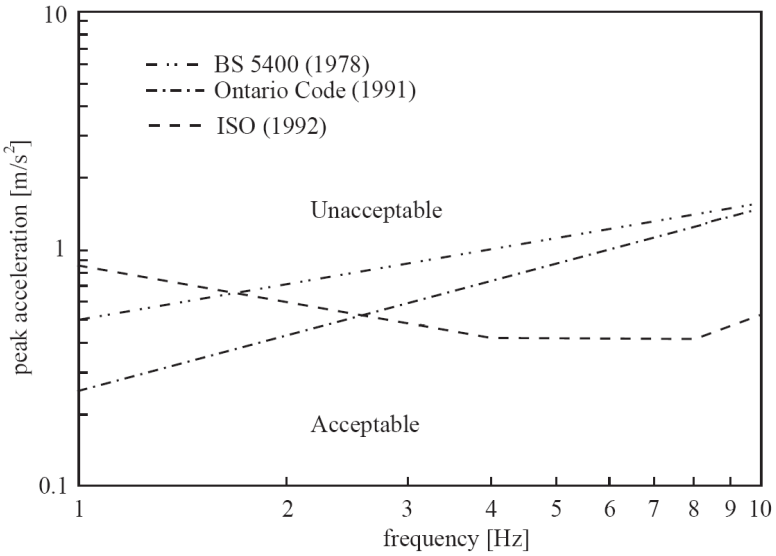

Figure 2.5 Acceptability of vertical vibrations for outdoor footbridges (Zivanovic et al. 2005).

Table 2.3 Summary of Literature Results on Acceleration Limitation

	Studied by	Postlethwaite (1941)		Billing and Green (1984)	Goldman (1948)	BS (1978)	Ontario Code (1991)	ISO (1992)
	Frequency (Hz)	< 1	1-6	___	5	5	5	5
Acceleration Threshold (g)	Slightly Perceptible	___	1.5-1.8 %	1.5-2.5%	0.4%	___	___	___
	Distinctly Perceptible			2.5-5.2%		___	___	___
	Strongly Perceptible			5.2-7.6%		___	___	___
	Acceptable	0.03%	1.8-6 %	___	8%	11%	8%	5%
	Uncomfortable	___	6-16%	___	___	___	___	___
	Tolerance	___	___	___	50%	___	___	___

A study by Tilly et al. (1984) includes a review of British Specification for footbridge written by the British Standard Institution. The acceleration is limited to one-half the square root of the first bending frequency for frequencies up to 4 Hz (this limit of $0.5\ f^{0.5}$ was developed primarily for pedestrian bridges). For frequency between 4 to 5 Hz, a reduction factor is applied to the bridge response and for frequency higher than 5 Hz, a bridge is too difficult to excite and vibration can be ignored. These limits are also suggested by Blanchard, et al. (1977).

A study by Barker et al. (2011) suggested limiting deflection to the acceleration limit over squared frequency and suggested the use of fatigue truck load to calculate the maximum deflection of a bridge. The equation provided in Barker's study is very simple and the acceleration limit is not well defined. Moreover, the results were obtained from a set of dynamic analysis for the bridge response when the vehicle is located at the mid-

span and instantaneously eliminated from the structure. The results obtained by this type of loading are not representing the actual dynamic response of a bridge under moving truck load.

Contrary to acceleration that most of the researchers tried to limit it as a concern associated with human comfort, in few studies, limiting velocity was suggested to control bridge vibration. Manning (1981) recommended that the velocity amplitude be no greater than 0.2 in/sec while New Zealand (1994) Bridge Manual limited maximum vertical velocity to 2.2 inch/sec to control vibration (Wu 2003).

2.2 Vibration and Structural Performance

Although research shows there is no evidence of damage that can be directly attributed to the bridge excessive deflection, there is a presumption that limiting deflection controls the excessive vibration which can contribute to fatigue failures and concrete deck problems. Damage in bridge superstructure can be classified as damages in still girders, connections and concrete deck. Field tests and investigations of damaged structure indicate that cracking is more common in steel girder webs close to connections and concrete bridge decks in negative moment region over interior supports.

2.2.1 Girder Cracking

Cracking of plate girder webs is one of the most common damage in bridges and occurs in the gap between the web stiffeners and the girder flanges (Figure 2.6). Among thirteen damaged bridges investigated in a study by Roeder et al. (2002), six were included to suffer from this kind of damage and all except one of them passed the AASHTO

deflection check. This damage is caused by differential girder deflections due to unequally loaded lanes. When one lane is loaded while the others are unloaded, the differential deflection between girders under the load and adjacent girders induces local stresses at the diaphragm to girder connection. Figure 2.7 shows the relative deflection between girders. To decrease these kinds of damage, more flexibility in girder web to out of plane bending and less stiffness in diaphragm connection can be beneficial (Roeder et al. 2002). These types of cracking were also called as out of plane distortional fatigue by some other researchers (Fisher 1990; Nishikawa et al. 1998).

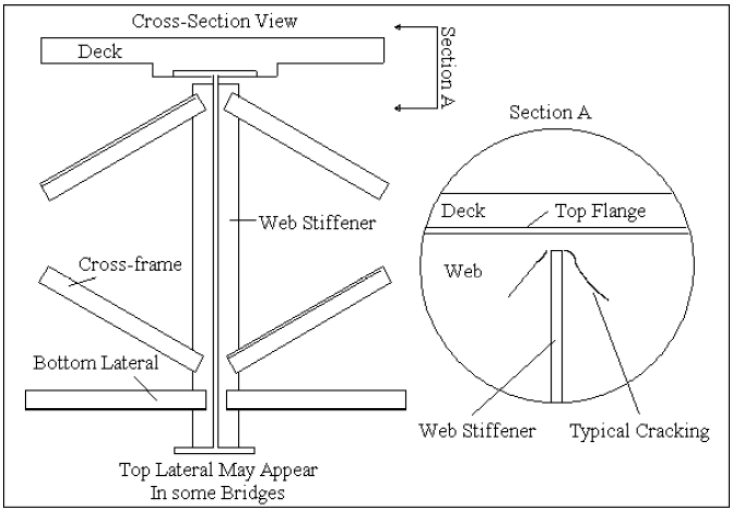

Figure 2.6 Typical web cracking at diaphragm connections (Roeder et al. 2002).

As can be seen in Figure 2.7, girders are too stiff to deform in lateral direction while cross beam is enough flexible to deform easily and affected by excessive stresses. If the cross beam is unrestrained against twisting, cracking may occur at the cross beam-superstructure connection and this damage is caused by the differential twist rotation of the cross beam relative to the small rotation and deformation expected in the bridge superstructure (Roeder et al. 2002).

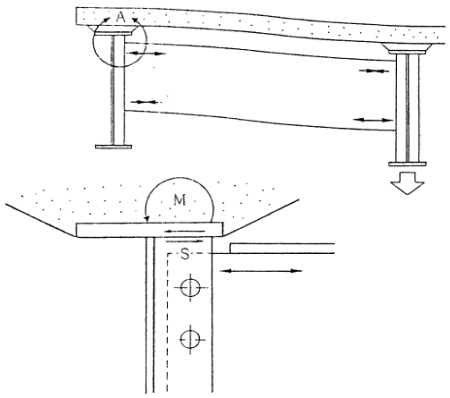

Figure 2.7 Typical relative deflection of main girders (Nishikawa et al. 1998).

In 1998, Nishikawa et al. studied the fatigue of steel highway bridges in Japan. They indicated that the deck lateral deflection and differential girders deflection significantly influence fatigue-induced girder cracking (Figure 2.8).

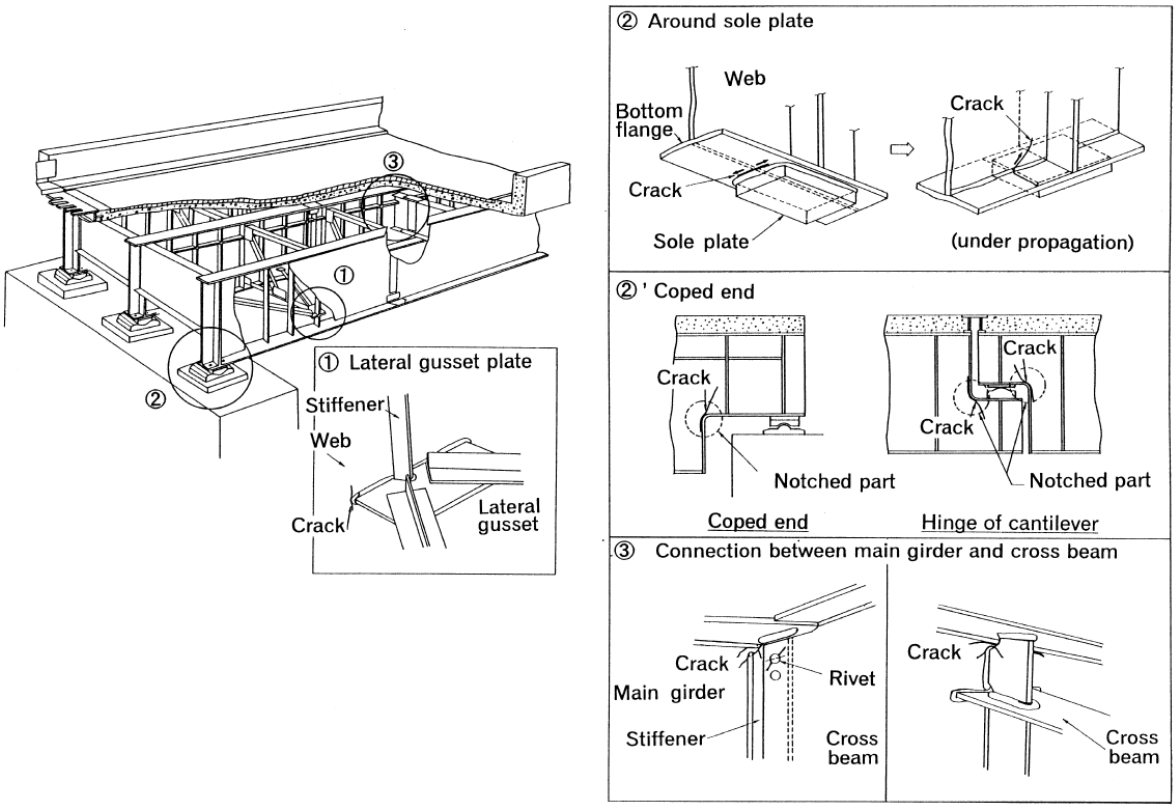

Figure 2.8 Typical fatigue cracks in plate girders (Nishikawa et al. 1998).

It was concluded that structural details should be designed to prevent fatigue problem due to distortion-induced stress. It has to be noted that the bridge damages in this study are all related to local rotations and lateral deformations (Figure 2.8). Therefore, the global deflection limits cannot reduce any of those damages as long as they are caused by transverse flexibility.

2.2.2 Deck Deterioration

Literature shows that among all bridge damages, only concrete deck deterioration can be attributed to excessive bridge deflection directly and all other damages in bridge structures caused by local deformation such as connection rotations and twisting or deformation of members relative to each other.

Concrete deck cracks occur as a result of poor mix design, change in temperature, live load effects at early ages and shrinkage in concrete. The slab thickness and distance between girders significantly affects deck transverse flexibility and directly causes longitudinal cracks in concrete slab. These cracks tend to be distributed throughout the entire length of a bridge.

Zhou et al. (2004) applied a Finite element analysis to investigate the effect of transverse flexibility on deck cracking. In their study the effect of slenderness ratio, connection between girders due to diaphragm and composite interaction between steel girders and concrete deck were investigated. It is concluded that transverse flexibility significantly influences longitudinal deck cracking. Figure 2.9 shows when composite interaction is taken into account the stresses in concrete deck are half of the stresses in the case without considering composite interaction. Furthermore, connections between

girders through diaphragms significantly reduce stresses in concrete deck. Referring to this study, what influences longitudinal cracking is related to deck transverse flexibility and limiting flexibility in longitudinal direction does not help to reduce this kind of cracking.

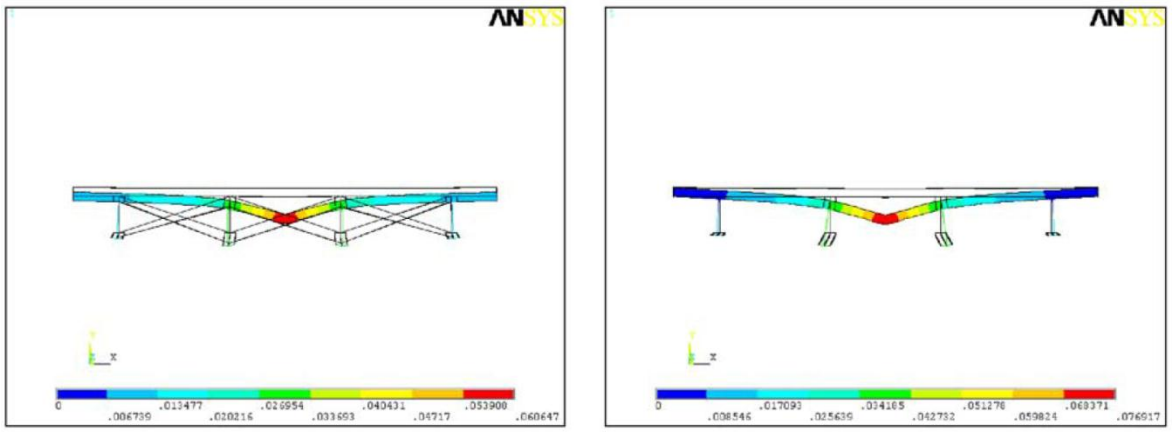

(a)

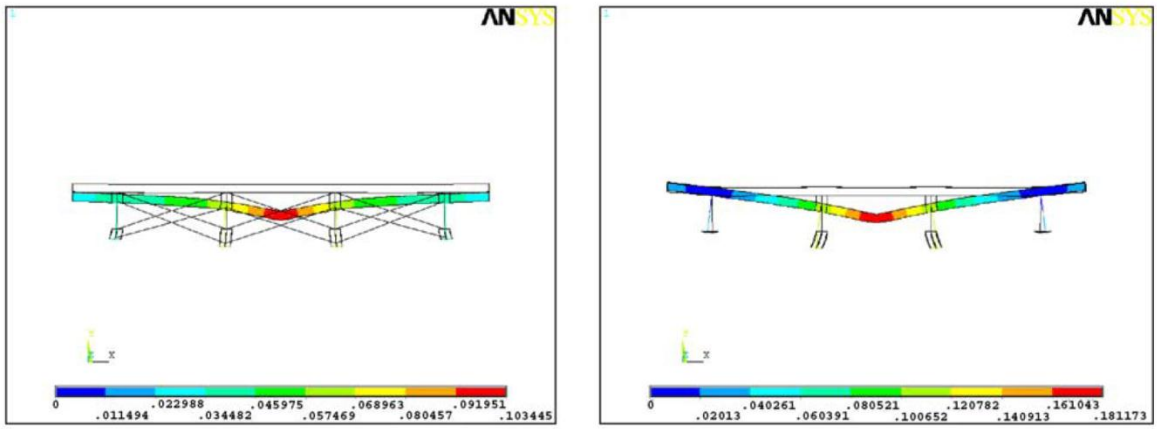

(b)

Figure 2.9 Deformed configuration under 3000 lb load at the center for (a) composite deck and (b) non-composite deck with and without diaphragm (Zhou et al. 2004).

Deflection control may only be beneficial for reducing the transverse deck cracking. This kind of deck cracking is observed to be located in negative moment region

over interior supports in continuous spans (Saadeghvaziri and Hadidi 2002). Since limiting the overall deflection would limit the negative bending moments, it may provide a beneficial effect to reduce this type of cracking.

In a study by Saadeghvaziri and Hadidi (2002), 24 bridges were surveyed in the state of New Jersey. The aim was to correlate transverse deck cracking to the bridge design parameters. It was found that "cracks in concrete occur when a restraint mass of concrete tends to change volume". The problem with deck cracking can be solved by a more flexible design for bridges at their support conditions, simply supported instead of continuous supports. They recommended to increasing the deflection limit requirement so that more flexible structures would be designed. "Analyses results indicate that more flexible superstructures have lower tendency for deck cracking. Therefore, the design should employ a more flexible superstructure."

In another study (Fountain and Thunman 1987) it is stated that stiffer deck can produce more cracking because the effects of volume change on the tensile stresses due to deck/beam interaction increase as the beam stiffness increases.

In Roeder's et al. (2002) study, among thirteen bridges, only two of them were observed to have transverse crack in deck damage. It is concluded that this cracking is attributable to shrinkage of the concrete, drying shrinkage of the hardened concrete combined with deck restraint, settlement of the finished plastic concrete around top mat of reinforcement, long term flexure of continuous spans under service loads, traffic induced repeated vibration, and environmental phenomenon.

Krauss and Rogalla's (1996) surveyed 52 transportation agencies throughout the US and Canada and conducted analytical, field and laboratory research. The longitudinal

tensile stresses in the concrete deck, which result in transverse cracking, were largely caused by concrete shrinkage, changing bridge temperature, and to lesser extent, traffic. It was concluded that cracking is more common among multi span continuous steel girder structures due to restraint provided by joints and bearings, and it is less likely to have transverse deck cracking for concrete girder bridges where deck and the girders shrink together. It was mentioned that reducing deck flexibility may potentially reduce early cracking.

Bridge flexibility in longitudinal direction is different from transverse direction. Span length, type of supports, and composite interaction influence on longitudinal flexibility; while transverse stiffness is attributed to slenderness, composite interaction and the connection between girders through diaphragms. Although some statistical studies reported deck cracking due to excessive span length and flexibility, more studies show no evidence of deck deterioration due to the longitudinal flexibility.

Goodpasture and Goodwin (1971) studied 27 bridges to determine which type of bridges exhibited the most cracking. These bridges were plate girders, rolled beams, concrete girders, pre-stressed girders, and trusses. The effect of stiffness on transverse cracking was evaluated for 10 of the continuous steel bridges. No correlation between girder flexibility and transverse cracking intensity was established.

Nevels and Hixon (1973) completed field measurements on 25 I-girder bridges to determine the causes of bridge deck deterioration. The total sample of 195 bridges consisted of simple and continuous plate girder and I-girder as well as prestressed concrete beams with span lengths ranging from 40 to 115 ft. The work showed no relationship between longitudinal flexibility and deck deterioration.

Another survey was conducted by the New York Department of Transportation (Alampalli 2001) to investigate the correlation between bridge vibration and bridge deck cracking. The study was limited to New York State steel girder superstructures built between 1990 and 1997. From 384 bridge spans (233 Bridges) inspected, 242 exhibited some form of cracking. 227 decks cracked transversely, 44 cracked longitudinally, and 29 bridge decks exhibited both forms of cracking. The effects of span length, traffic volume, type of bearing, and vibration severity were investigated. Since it was not easily possible or practical to quantitatively evaluate/ measure bridge vibration through visual inspection or with simple instrumentation by field personnel, vibration ratings in that study were more subjective and made the results of the study qualitative. The conclusion of this statistical study is as follows:

1. Vibration severity is the most significant parameter influencing bridge deck cracking. Higher severity equates to higher deck cracking. Decks with noticeable vibration cracked most severely.
2. Long spans exhibit more deck cracking than shorter spans.
3. Traffic volume is the least significant factor, of the three considered, in influencing the bridge deck cracking. However, high traffic volume generated more cracking than low traffic volume.
4. Bridge bearing do not influence the deck cracking severity.
5. Bridge with noticeable vibration combined with longer span length exhibited significant bridge deck cracking.

Through the discussion on literature review, the followings can be concluded. Differential deflection between adjacent girders causes load transfer from girder to girder by the bracing diaphragms and the bridge deck, and this transfer induces local deformation and stresses in the girder web, connections and cross beams which causes

web cracking and longitudinal concrete deck. Transverse flexibility (slenderness) can cause damage in deck and also can increase differential deflection of adjacent girders and cause damage in girders. Negative moment is higher in stiffer supports and deck cracking is increased over the internal supports in continuous spans. Therefore, less restraint in supports leads to less negative moment over superstructure. More girder flexibility in longitudinal and transverse direction would reduce the restraints in concrete deck and girder web which causes less damage on a bridge superstructure.

2.3 Parameters Affecting Vibration

Many studies prior to this study investigated the parameters affecting bridge vibration. However, the results of these studies are not consistent with each other. Each study used different methods; bridge and vehicle models; and different bridge and vehicle parameters.

Wei and Chen (2007) examined the existing deflection criteria for three different types of concrete-filled steel tubular arch bridges and concluded that the deflection limit could be eliminated. Instead, a method to estimate dynamic response and their limitation should be adapted. They stated that deflection limit could not reflect the actual vibration perception of pedestrians.

Several studies report that when the surface roughness is taken into account in analysis, vibration acceleration is amplified. For instance, Aramraks (1975) and Kou and DeWolf (1997) reported that surface roughness and vehicle velocity have the most significant effect on bridge acceleration for both simple and continuous span bridges. Vehicle speed was found to have the greatest effect on the maximum girder acceleration.

Number of axles moving on the bridge was another aspect which was considered in Aramraks study. The results indicated that maximum accelerations were approximately the same for two and three axle vehicle model, but were about two thirds of the magnitudes produced by the single axle vehicle model. Some others (Yau et al. 1999) indicate that surface roughness do not noticeably influence bridge response.

Esmailzadeh and Jalili (2003) considered a six DOF model on a simply supported single span Euler-Bernoulli beam. The effect of vehicle speed on bridge impact factor for moment and displacement was investigated. The maximum dynamic deflection occurs at the vicinity of the bridge mid-span, while the maximum bending moment occurs at ±20% of the mid-span point.

Train speed influence on the dynamic behavior of lightweight steel bridges is studies by Michaltsos and Raftoyiannis (2010). The effect of load sequence with respect to bridge frequency and rail discontinuity on bridge responses were investigated in this study. It was suggested that rail discontinuity should not be near the mid-span. If the discontinuity coincides with the critical speed, it causes continuously increase in response. Displacement response was the only response considered in this study.

The effect of train to bridge frequency, vehicle to bridge mass, axle length to span length, and damping ratios were investigated in Majka and Hartnett (2008). The train was modeled in three-dimensional with 15 DOF and a parametric analysis was carried out to establish the key variables influencing the dynamic response of railway bridges. Vehicle damping ratio was found to have negligible influence on the critical speed. The axle distance was found to be a very important parameter that may cause large amplification of the dynamic response. Bridge damping could significantly decrease acceleration.

The effect of second bending mode, vehicle speed and axle distance were investigated in a study by Museros and Alarcon (2005). The main purpose of this study was to decide whether the second mode of vibration should be taken into account for the determination of the maximum displacement and acceleration or not. It was concluded that the second mode attributes to acceleration while it does not influence deflection. The effect of higher modes on acceleration response was also investigated by Yau and yang (2006) due to a series of equally spaced moving loads at constant speed. They found that for the loads moving at resonant speeds, the higher modes can have significant influence on the acceleration amplitude. This is true especially for bridges with lower damping ratio. In the cases for which the structural damping was taken into account, the contribution of higher modes to the acceleration response tends to be damped out.

Span length is another parameter which contributes to bridge acceleration. Span length also is a parameter to evaluate bridge longitudinal flexibility. The longer span results in a more flexibility in bridge superstructure and acceleration increases by flexibility. However, flexibility was found to have a minor influence on overall dynamic bridge behavior compared to surface roughness and vehicle speed (Aramraks 1975; Kou and DeWolf 1997). Initial oscillation of the vehicle suspension was also investigated in these two studies. It is found that initial oscillation causes a 30 to 50 percent increase in the maximum acceleration (Aramraks 1975).

The impact factor was investigated experimentally by Ashebo et al. (2007) for skew bridges. The results from mounted strain gages show that dynamic impact factor is significantly related to vehicle weight. Weak correlations were found between the speed of the vehicles and the dynamic load factor. No correlation was found that attribute to the

number of axles. Moreover, it was found that the influence of skew in both the static and dynamic behaviors of the bridge within the skew angle range of 0 to 30 degrees is very small. Experimental impact factor was less than the one provided by design codes namely: AASHTO, Canadian (CHBDC), British (BS5400; BD 37/01), SDM (Hong Kong).

The effect of vehicle acceleration or deceleration was found to be significant for bridge deflection (Michaltsos 2002). Au et al. (2004) tried to describe a method for the identification of parameters of vehicle moving on multi-span continuous bridges. Each moving vehicle was modeled as a 2 DOF with sprung masses and dampers. The axle weights, stiffness and damping ratio were considered identical for both DOF. They proposed a method to identify vehicle parameters on continuous bridges based on acceleration measurement.

A three-span continuous bridge was investigated by Munirudrappa and Iyengar (1999). The effect of vehicle velocity, span length and the effect of initial vehicle oscillation on impact factor were investigated. The initial oscillation caused by the settlement in approach road was found to significantly increase impact factor. For instance when the initial value of the interacting force was assumed to be 30% greater than the static value, the impact factor was found to be 30% higher than the case without initial oscillation.

In Yau et al. (1999) study, it was found that the impact factor is drastically less for a continuous span than a simple span. According to this study, tolerance acceleration limit for suspension mass (for passengers in the car) is equal to 0.05g in Taiwan High Speed Rails code tentatively.

Moghimi and Ronagh (2008) conducted a field study on a simple span composite steel girder bridge which had significant vibration under moving truck loads. It was found that the bridge response is significantly influenced by the vehicle speed, stiffness of the elastomeric pad, continuity of the RC deck slab at pier and the ratio of vehicle weight to total weight of the superstructure. The results indicated that the vehicles heavier than 10% of the deck weight over-activate the bridge dynamics. Also, it was found that the continuity of the concrete deck on the piers reduces the perceptible vibrations of the deck. This is partly due to increasing the bridge frequency by providing continuous support conditions versus pinned support conditions; and partly due to decreasing the initial bounce of the vehicle due to deck irregularities caused by expansion joints.

Yau et al. (2001) investigated the effect of elastomeric bearing on the bridge impact factor and bridge frequency. Two extreme cases of flexible beam on rigid supports, and rigid beam on flexible supports have been considered and bridge frequency is determined for cases in between. The load sequence has been considered by two consecutive loads at a moment. Therefore, the span length is assumed to be no greater than twice the interval between two consecutive moving loads. The bearing damping was not considered in this study. They found that the installation of elastomeric bearings may amplify the impact response only over the low speed parameter range but may suppress the response for the high speed parameter range.

Kawatani et al. (2000) compared experimental data with analytical data of acceleration and displacement for a bridge supported both with steel bearings and elastomeric bearings. Analytical natural frequency of the girder bridge agrees with the measured values.

2.4 Alternatives Limitations

As many studies indicated that deflection limitation do not influence on vibration severity, alternative methods were formed to provide better ways to limit vibration.

2.4.1 Canadian Standards-Ontario Highway Bridge Code

Static deflection limitation is based on bridge natural frequency in Ontario Highway Bridge code (1991). This relationship was developed from extensive field data collection and analytical studies conducted by Wright and Green in 1964 (Wu 2003). Figure 2.10 show the Ontario deflection limitation for different types of bridges, without sidewalk, with little pedestrian and with significant pedestrian using sidewalk.

The natural frequency can be calculated using Equation 2.1.

$$f_{obs} = 0.95 f_{calc} + 0.072 \tag{2.1}$$

f_{obs} is the natural frequency of the bridge that would be observed in the field, and f_{calc} is the natural frequency calculated analytically using Equation 2.2.

$$2 \text{ Hz} < f_{calc} = \frac{\pi}{2L^2}\sqrt{\frac{EI}{m_b}} < 7 \text{ Hz} \tag{2.2}$$

L, E, I, and m_b are span length, modulus of elasticity, moment of inertia, and mass per unit length of the beam including the concrete slab, respectively.

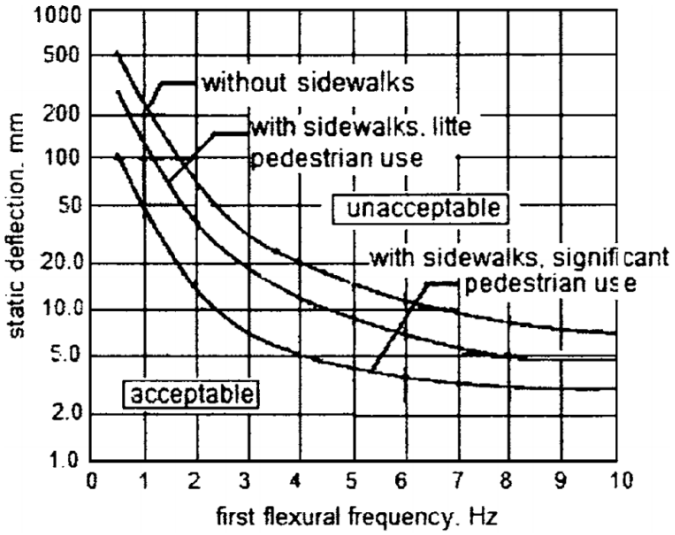

Figure 2.10 Deflection limits per Ontario Code (Aluri et al. 2005; Ontario 1991).

To compute live load deflection in Ontario code, one truck (without considering lane load) is placed at the center of a single lane. Live load factor and dynamic load allowance (Figure 2.11) must be applied to truck load and gross moment of inertia of the cross sectional area is used in calculation. To control bridge vibration, Ontario code also limits acceleration through the graph shown in Figure 2.5.

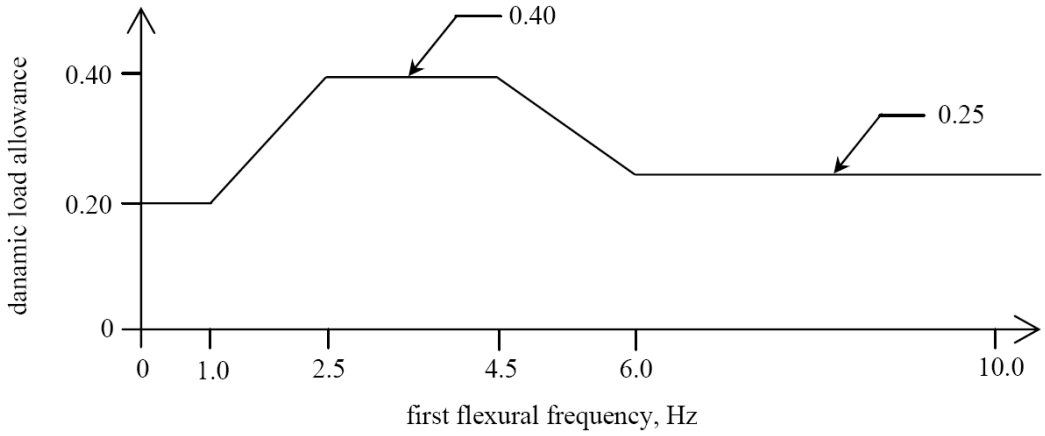

Figure 2.11 Dynamic load allowance (Ontario 1991).

2.4.2 European Codes

There is no deflection or additional checks applied for controlling bridge vibration in Europe. However, a "vibration factor" is used to account for full live load in calculating extra stresses due to vibrations in European Bridge Codes. For long span or slender pedestrian bridges, a frequency and modal analysis is performed (Wu 2003).

2.4.3 British Standard

British Design Manual (BD 2001) limits the bridge acceleration to one-half the square root of the first bending frequency for frequencies up to 4 Hz for assessing vibration serviceability of bridges. This limit of 0.5 $f^{½}$ was developed primarily for pedestrian bridges.

$$acc_{lim} = 0.5\sqrt{f}\ (m/s^2) = 20\sqrt{f}\ (in/s^2) \tag{2.3}$$

For frequencies between 4 to 5 Hz, a reduction factor is applied to the bridge response and for frequencies higher than 5 Hz, a bridge is too difficult to excite therefore vibration can be ignored. The British code recommends that in design calculations, a damping value of 0.03 should be used for steel bridges, a value of 0.04 for composite bridges and a value of 0.05 for concrete bridges (BD 37/01).

2.4.4 German Code

DIN 4150, includes the human perception of vibration chart, Table 2.4. This chart is also used by some other European countries such as Belgium and Switzerland (Elias and Villot 2010).

Table 2.4 Perception of Vibration According to DIN 4150

Acceleration (in/s^2)	Perception	
0.14	Threshold of perception	Not noticeable
		Just noticeable
0.28		
		Weakly noticeable
0.56		
1.12	Awakening threshold	Noticeable
		Clearly noticeable
2.24		
		Strongly noticeable
8.97		
		Very Strongly noticeable
140		

2.4.5 Australian Specifications

AS 5100.2 (2004) requires the deflection limits of a road bridge for Serviceability Limit State (SLS) under M1600 moving traffic load without Uniformly Distributed Load (UDL), plus dynamic load allowance (0.35), placed in each lane with multiple lanes loaded reduction factors applied, is not to be greater than 1/600 of the span or 1/300 of the cantilever projection, as applicable (Kirkcaldie 2008).

2.4.6 New Zealand Code

Older version of bridge manual in New Zealand employed limits on L/D and deflection; but in 1994 version, velocity is limited to 2.2 in/sec under two 27 kips axle loads of one HN unit. This limit is only used for bridges with pedestrian traffic or stationary vehicle traffic (Roeder 2002).

2.4.7 International Organization for Standards (ISO)

The International Standards Organization (ISO) recommends vibration limits in terms of peak acceleration via the root-mean-square (RMS) and frequency (Ebrahimpour and Sack 2005). Root-mean-square of the acceleration during time record is defined as:

$$\text{RMS} = \sqrt{\frac{\int_{t_1}^{t_2} \ddot{x}(t)^2 dt}{t_2 - t_1}} \tag{2.4}$$

Where $\ddot{x}(t)$ is the acceleration time history, and t_1 and t_2 define the beginning and end of the time interval considered. As shown in Figure 2.12, a baseline curve is used by ISO and different multipliers are used for different occupancies.

The serviceability for the human body on a walk-way of a highway bridge has not been agreed internationally, but a general criterion on the human sensitivity exists in ISO 2631-2 (1989). Depending on the problem, acceleration or velocity is measured and evaluated through comparison with the criterion. The serviceability on a railway bridge is evaluated by the riding quality of passengers. The riding quality is usually rated using the magnitude of acceleration measured on the floor in car bodies. The vibration induced by the deflection and/or bridge end angular rotations are usually transitional, so the peak value of acceleration is suitable for evaluation. Frequency and acceleration or velocity of the measured response are the parameters to evaluate for the serviceability of pedestrian bridges. Sensitivity criterion for human body exists as allowable level of vibration.

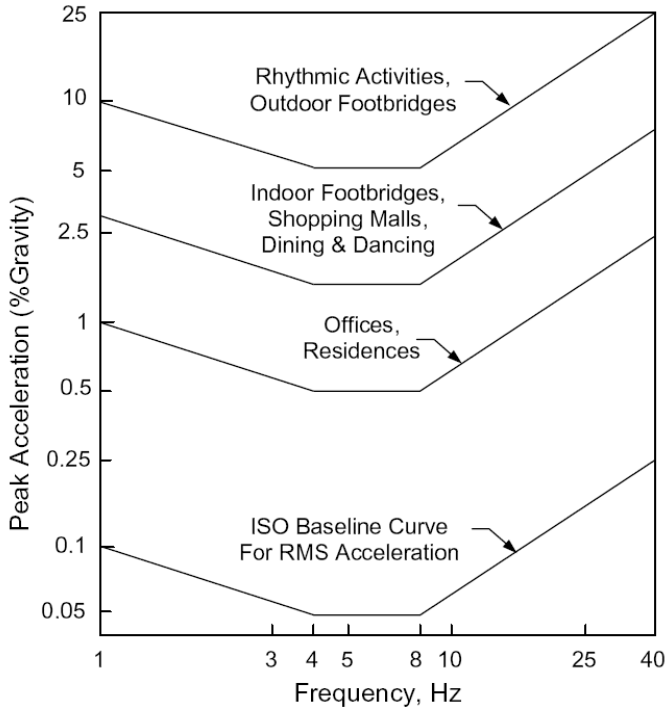

Figure 2.12 Peak acceleration for human comfort for vibrations due to human activity (ISO 1989).

2.4.8 Wright and Walker

In 1971, The American Iron and Steel Institute (AISA) formed a study with the objective of reviewing the current AASHTO deflection limits for multi-stringer steel highway bridges. This study conducted by Wright and Walker. They suggested acceleration limitation rather than using deflection limits and proposed a simple formula for calculating bridge acceleration.

$$\text{Acc.} = \text{DI}\ \delta_{st}\ (2\ \pi\ f)^2 \qquad (2.5)$$

δ_{st} is the static deflection as a result of live-load, with a wheel load distribution factor of 0.7, on one stringer, or beam, acting with its share of the deck. f, Natural

frequency, for both simple span and continuous span is the same and is calculated using Equation 2.6.

$$f = \frac{\pi}{2L^2}\sqrt{\frac{EI}{m_b}} \tag{2.6}$$

L, E, I, and m_b are stringer length, modulus of elasticity, moment of inertia of the steel beam, and mass per unit length of the beam including the concrete slab, respectively. DI is Impact factor and is calculated as speed parameter plus 0.15. The determination of speed parameter is half of the vehicle speed divided by the multiplication of span length and natural frequency.

$$DI = \alpha + 0.15 \tag{2.7}$$

$$\alpha = \frac{V}{2Lf} \tag{2.8}$$

If the acceleration exceeds the limit 100 in/s^2, a redesign is necessary. The acceleration limit was taken the threshold of Unpleasant-to-Few for human response from what was proposed by Wright and Green (1959). Table 2.5 shows the peak acceleration thresholds for the human response to vertical vibrations.

In 1981, Gaunt and Sutton compared Wright and Walker suggestion for simplify the bridge acceleration to a field test and found the results in agreement. Wright and Walker suggested considering additional parameters such as the relative flexural stiffness and torsional stiffness of the cross section in design procedure. They stated that, because reliable evidence on human reaction to bridge motions is so severely limited, the recommended acceleration criterion should receive empirical confirmation prior to any adoption (Machado 2006).

Table 2.5 Peak Acceleration Limit for Human Response to Vertical Vibrations (Wright and Walker 1971)

Human Response	Transient Peak Acceleration in/sec^2	Sustained Peak Acceleration in/sec^2
Imperceptible	5	0.5
Perceptible to Some Perceptible to Most Perceptible	10 20 50	1 2 5
Unpleasant to Few Unpleasent to Some Unpleasant to Most	100 200 500	10 20 50
Intolerable to Some Intolerable to Most	1000 2000	100 200

CHAPTER 3

FINITE ELEMENT MODELING

Existing Finite Element (FE) software provides an ideal platform for parameter study of bridges subjected to moving loads. However, one has to be careful in selecting the modeling parameters as the acceleration and velocity time histories are quite sensitive to such assumptions. As the exact solutions exist for special cases, it can be utilized in this study in order to validate the FE models. For both cases of with and without damping ratio exact solutions for one axle loading were programmed with MATLAB (2012). The results were all investigated at mid span, as at different vehicle velocities it is demonstrated that the maximum dynamic deflection occurs at the vicinity of the bridge mid-span with less than ±3% difference (Esmailzadeh and Jalili 2002).

3.1 Zero Damping Exact Solution

For a simply-supported beam subjected to a constant traveling load P at a constant value, the general exact solution is as follows (Chopra 2007; Fryba 1999):

$$u_{(x,t)} = \sum_{n=1}^{\infty} q_{n(t)} . \phi_{n(x)} \tag{3.1}$$

Where $\boldsymbol{\varphi_n}$ is the mode shape for mode **n** and $\mathbf{q_n}$ is the corresponding modal equation. For the case without damping ratio, the solution is provided in Equation 3.2.

$$q_{n(t)} = \begin{cases} \dfrac{2P_0}{mL}\dfrac{1}{\omega_n{}^2-(n\pi v/L)^2}\left(\sin\dfrac{n\pi vt}{L}-\dfrac{n\pi v}{\omega_n L}\sin\omega_n t\right) & t \le L/v \\ \dfrac{2P_0}{mL}\dfrac{1}{\omega_n{}^2-(n\pi v/L)^2}\dfrac{n\pi v}{\omega_n L}\left[(-1)^n\sin\left(\omega_n(t-L/v)\right)-\sin\omega_n t\right] & t \ge L/v \end{cases} \tag{3.2}$$

Where L is span length, **v** is the velocity of load P_0, and $\boldsymbol{\omega_n}$ is natural circular frequency (2 π f). By differentiating the displacement equation once and twice, velocity and acceleration equations can be derived. These equations have been solved and provided in Equations 3.3 to 3.6 for the case without damping ratio. Natural frequency ($\boldsymbol{\omega_n}$) for simply supported beam can be calculated using Equation 3.7.

$$\dot{u}_{(\frac{L}{2},t)} = \sum_{n=1}^{\infty}\dot{q}_{n(t)}.\phi_{n(L/2)} \tag{3.3}$$

$$\dot{q}_{n(t)} = \begin{cases} \dfrac{2P_0}{mL}\dfrac{1}{\omega_n{}^2-(n\pi v/L)^2}\left(\dfrac{n\pi v}{L}\cos\dfrac{n\pi vt}{L}-\dfrac{n\pi v}{L}\cos\omega_n t\right) & t \le L/v \\ \dfrac{2P_0}{mL}\dfrac{1}{\omega_n{}^2-(n\pi v/L)^2}\dfrac{n\pi v}{\omega_n L}\left[(-1)^n\omega_n\cos\left(\omega_n(t-L/v)\right)-\omega_n\cos\omega_n t\right] & t \ge L/v \end{cases} \tag{3.4}$$

$$\ddot{u}_{(\frac{L}{2},t)} = \sum_{n=1}^{\infty}\ddot{q}_{n(t)}.\phi_{n(L/2)} \tag{3.5}$$

$$\ddot{q}_{n(t)} = \begin{cases} \dfrac{2P_0}{mL}\dfrac{1}{\omega_n{}^2-(n\pi v/L)^2}\left(-\left(\dfrac{n\pi v}{L}\right)^2\sin\dfrac{n\pi vt}{L}+\dfrac{n\pi v\omega_n}{L}\sin\omega_n t\right) & t \le L/v \\ \dfrac{2P_0}{mL}\dfrac{1}{\omega_n{}^2-(n\pi v/L)^2}\dfrac{n\pi v}{\omega_n L}\left[-(-1)^n\omega_n{}^2\sin\left(\omega_n(t-L/v)\right)+\omega_n{}^2\sin\omega_n t\right] & t \ge L/v \end{cases} \tag{3.6}$$

$$\omega_n = \frac{n^2.\pi^2}{L^2}.\sqrt{\frac{E.I}{m}} \tag{3.7}$$

As can be seen in Equation 3.2, n remains in the denominator of the equation. Therefore, higher modes do not contribute to the displacement response while in velocity equations the higher modes contribution is more apparent and in acceleration equations the higher modes contribution is the highest.

3.2 Damped System Analysis

With the consideration of damping ratio (ζ), the modal equation is equal to (Fushun et al. 2007):

$$q_{n(t)} = \frac{2P_0}{mL\omega_n\sqrt{1-\zeta^2}} \int_0^t \sin(\frac{n\pi v\tau}{L}).e^{-\zeta\omega_n(t-\tau)}.\sin(\omega_n\sqrt{1-\zeta^2}(t-\tau)).d\tau \qquad (3.8)$$

The solution for eq. 3.7 is provided in eq. 3.9. By differentiating the displacement equation once and twice, velocity and acceleration equations are derived in Equations 3.11 to 3.14.

for $t \le \frac{L}{V}$, (3.9)

$$u = \frac{2P}{m.L.\omega_D} \sum_1^n \phi_n.\left\{\frac{1}{2(\xi^2.\omega_n{}^2+(\omega_D+\omega)^2)}\left[\omega_n.\xi.\cos(\omega.t) + (\omega_D+\omega).\sin(\omega.t) - e^{-\xi.\omega_n.t}.\omega_n.\xi.\cos(\omega_D.t) + e^{-\xi.\omega_n.t}.(\omega_D+\omega).\sin(\omega_D.t)\right] + \frac{1}{2(\xi^2.\omega_n{}^2+(\omega_D-\omega)^2)}\left[\omega_n.\xi.\cos(\omega.t) + (\omega_D-\omega).\sin(\omega.t) + e^{-\xi.\omega_n.t}.\omega_n.\xi.\cos(\omega_D.t) - e^{-\xi.\omega_n.t}.(\omega_D-\omega).\sin(\omega_D.t)\right]\right\}$$

for $t \geq \frac{L}{V}$, (3.10)

$$u = \frac{2P}{m.L.\omega_D} \sum_1^n \phi_n . \left\{ \frac{1}{2(\xi^2.{\omega_n}^2+(\omega_D+\omega)^2)} \left[e^{\xi.\omega_n.(t_d-t)}.\omega_n.\xi.\cos(\omega_D.(t_d-t)+\omega.t_d) + e^{\xi.\omega_n.(t_d-t)}.(\omega_D+\omega).\sin(\omega_D.(t_d-t)+\omega.t_d) - e^{-\xi.\omega_n.t}.\omega_n.\xi.\cos(\omega_D.t) + e^{-\xi.\omega_n.t}.(\omega_D+\omega).\sin(\omega_D.t) \right] + \frac{1}{2(\xi^2.{\omega_n}^2+(\omega_D-\omega)^2)} \left[-e^{\xi.\omega_n.(t_d-t)}.\omega_n.\xi.\cos(\omega_D.(t_d-t)-\omega.t_d) - e^{\xi.\omega_n.(t_d-t)}.(\omega_D-\omega).\sin(\omega_D.(t_d-t)-\omega.t_d) + e^{-\xi.\omega_n.t}.\omega_n.\xi.\cos(\omega_D.t) - e^{-\xi.\omega_n.t}.(\omega_D-\omega).\sin(\omega_D.t) \right] \right\}$$

for $t \leq \frac{L}{V}$, (3.11)

$$\dot{u} = \frac{2P}{m.L.\omega_D} \sum_1^n \phi_n . \frac{1}{2(\xi^2.{\omega_n}^2+(\omega_D+\omega)^2)} \left[-\xi^2.{\omega_n}^2.e^{\xi.\omega_n.(t_d-t)}.\cos(\omega_D.(t_d-t)+\omega.t_d) + e^{\xi.\omega_n.(t_d-t)}.\omega_n.\xi.\omega_D.\sin(\omega_D.(t_d-t)+\omega.t_d) - \xi.\omega_n.e^{\xi.\omega_n.(t_d-t)}.(\omega_D+\omega).\sin(\omega_D.(t_d-t)+\omega.t_d) - e^{\xi.\omega_n.(t_d-t)}.\omega_D.(\omega_D+\omega).\cos(\omega_D.(t_d-t)+\omega.t_d) + \xi^2.{\omega_n}^2.e^{-\xi.\omega_n.t}.\cos(\omega_D.t) + e^{-\xi.\omega_n.t}.\omega_n.\xi.\omega_D.\sin(\omega_D.t) - \xi.\omega_n.e^{-\xi.\omega_n.t}.(\omega_D+\omega).\sin(\omega_D.t) + e^{-\xi.\omega_n.t}.\omega_D.(\omega_D+\omega).\cos(\omega_D.t) \right] + \frac{1}{2(\xi^2.{\omega_n}^2+(\omega_D-\omega)^2)} \left[\xi^2.{\omega_n}^2.e^{\xi.\omega_n.(t_d-t)}.\cos(\omega_D.(t_d-t)-\omega.t_d) - e^{\xi.\omega_n.(t_d-t)}.\omega_n.\xi.\omega_D.\sin(\omega_D.(t_d-t)-\omega.t_d) + \xi.\omega_n.e^{\xi.\omega_n.(t_d-t)}.(\omega_D-\omega).\sin(\omega_D.(t_d-t)-\omega.t_d) + e^{\xi.\omega_n.(t_d-t)}.\omega_D.(\omega_D-\omega).\cos(\omega_D.(t_d-t)-\omega.t_d) - \xi^2.{\omega_n}^2.e^{-\xi.\omega_n.t}.\cos(\omega_D.t) - e^{-\xi.\omega_n.t}.\omega_n.\xi.\omega_D.\sin(\omega_D.t) + \xi.\omega_n.e^{-\xi.\omega_n.t}.(\omega_D-\omega).\sin(\omega_D.t) - e^{-\xi.\omega_n.t}.\omega_D.(\omega_D-\omega).\cos(\omega_D.t) \right]$$

for $t \geq \frac{L}{V}$, $\ddot{u}$ (3.12)

$$= \frac{2P}{m.L.\omega_D} \sum_1^n \phi_n . \left\{ \frac{1}{2(\xi^2.{\omega_n}^2+(\omega_D+\omega)^2)} \left[-\omega.\omega_n.\xi.\sin(\omega.t) + \omega.(\omega_D+\omega).\cos(\omega.t) + \right.\right.$$

$$\xi^2.{\omega_n}^2.e^{-\xi.\omega_n.t}.\cos(\omega_D.t) + e^{-\xi.\omega_n.t}.\omega_D.\omega_n.\xi.\sin(\omega_D.t) - \xi.\omega_n.e^{-\xi.\omega_n.t}.(\omega_D +$$

$$\omega).\sin(\omega_D.t) + e^{-\xi.\omega_n.t}.\omega_D.(\omega_D+\omega).\cos(\omega_D.t)\Big] +$$

$$\frac{1}{2(\xi^2.{\omega_n}^2+(\omega_D-\omega)^2)} \Big[\omega.\omega_n.\xi.\sin(\omega.t) + \omega.(\omega_D-\omega).\cos(\omega.t) -$$

$$\xi^2.{\omega_n}^2.e^{-\xi.\omega_n.t}.\cos(\omega_D.t) - e^{-\xi.\omega_n.t}.\omega_D.\omega_n.\xi.\sin(\omega_D.t) + \xi.\omega_n.e^{-\xi.\omega_n.t}.(\omega_D -$$

$$\left.\left. \omega).\sin(\omega_D.t) - e^{-\xi.\omega_n.t}.\omega_D.(\omega_D-\omega).\cos(\omega_D.t)\Big] \right\}$$

for $t \leq \frac{L}{V}$, $\ddot{u}$ (3.13)

$$= \frac{2P}{m.L.\omega_D} \sum_1^n \phi_n . \left\{ \frac{1}{2(\xi^2.{\omega_n}^2+(\omega_D+\omega)^2)} \left[-\omega^2.\omega_n.\xi.\cos(\omega.t) - \omega^2.(\omega_D+\omega).\sin(\omega.t) - \right.\right.$$

$$\xi^3.{\omega_n}^3.e^{-\xi.\omega_n.t}.\cos(\omega_D.t) - 2.\xi^2.{\omega_n}^2.\omega_D.e^{-\xi.\omega_n.t}.\sin(\omega_D.t) +$$

$$e^{-\xi.\omega_n.t}.{\omega_D}^2.\omega_n.\xi.\cos(\omega_D.t) + \xi^2.{\omega_n}^2.e^{-\xi.\omega_n.t}.(\omega_D+\omega).\sin(\omega_D.t) -$$

$$2.\xi.\omega_n.\omega_D.e^{-\xi.\omega_n.t}.(\omega_D+\omega).\cos(\omega_D.t) - e^{-\xi.\omega_n.t}.{\omega_D}^2.(\omega_D+\omega).\sin(\omega_D.t)\Big] +$$

$$\frac{1}{2(\xi^2.{\omega_n}^2+(\omega_D-\omega)^2)} \Big[\omega^2.\omega_n.\xi.\cos(\omega.t) - \omega^2.(\omega_D-\omega).\sin(\omega.t) +$$

$$\xi^3.{\omega_n}^3.e^{-\xi.\omega_n.t}.\cos(\omega_D.t) + 2.\xi^2.{\omega_n}^2.e^{-\xi.\omega_n.t}.\omega_D.\sin(\omega_D.t) -$$

$$e^{-\xi.\omega_n.t}.{\omega_D}^2.\omega_n.\xi.\cos(\omega_D.t) - \xi^2.{\omega_n}^2.e^{-\xi.\omega_n.t}.(\omega_D-\omega).\sin(\omega_D.t) +$$

$$\left.\left. 2.\xi.\omega_n.\omega_D.e^{-\xi.\omega_n.t}.(\omega_D-\omega).\cos(\omega_D.t) - e^{-\xi.\omega_n.t}.{\omega_D}^2.(\omega_D-\omega).\sin(\omega_D.t)\Big] \right\}$$

$$\text{for } t \geq \frac{L}{V} \text{ , ü} \tag{3.14}$$

$$= \frac{2P}{m.L.\omega_D} \sum_1^n \phi_n . \left\{ \frac{1}{2(\xi^2.{\omega_n}^2+(\omega_D+\omega)^2)} \left[+\xi^3.{\omega_n}^3.e^{\xi.\omega_n.(t_d-t)}.\cos(\omega_D.(t_d-t)+\omega.t_d) - \right.\right.$$

$$\xi^2.{\omega_n}^2.e^{\xi.\omega_n.(t_d-t)}.\omega_D.\sin(\omega_D.(t_d-t)+\omega.t_d) -$$

$$\xi^2.{\omega_n}^2.e^{\xi.\omega_n.(t_d-t)}.\omega_D.\sin(\omega_D.(t_d-t)+\omega.t_d) -$$

$$e^{\xi.\omega_n.(t_d-t)}.\omega_n.\xi.{\omega_D}^2.\cos(\omega_D.(t_d-t)+\omega.t_d) + \xi^2.{\omega_n}^2.e^{\xi.\omega_n.(t_d-t)}.(\omega_D +$$

$$\omega).\sin(\omega_D.(t_d-t)+\omega.t_d) + \xi.\omega_n.\omega_D.e^{\xi.\omega_n.(t_d-t)}.(\omega_D+\omega).\cos(\omega_D.(t_d -$$

$$t)+\omega.t_d) + \xi.\omega_n.e^{\xi.\omega_n.(t_d-t)}.\omega_D.(\omega_D+\omega).\cos(\omega_D.(t_d-t)+\omega.t_d) -$$

$$e^{\xi.\omega_n.(t_d-t)}.{\omega_D}^2.(\omega_D+\omega).\sin(\omega_D.(t_d-t)+\omega.t_d) -$$

$$\xi^3.{\omega_n}^3.e^{-\xi.\omega_n.t}.\cos(\omega_D.t) - \xi^2.{\omega_n}^2.\omega_D.e^{-\xi.\omega_n.t}.\sin(\omega_D.t) -$$

$$\xi^2.{\omega_n}^2 e^{-\xi.\omega_n.t}.\omega_D.\sin(\omega_D.t) + e^{-\xi.\omega_n.t}.\omega_n.\xi.{\omega_D}^2.\cos(\omega_D.t) +$$

$$\xi^2.{\omega_n}^2.e^{-\xi.\omega_n.t}.(\omega_D+\omega).\sin(\omega_D.t) - \xi.\omega_n.\omega_D.e^{-\xi.\omega_n.t}.(\omega_D+\omega).\cos(\omega_D.t) -$$

$$\left.\xi.\omega_n.e^{-\xi.\omega_n.t}.\omega_D.(\omega_D+\omega).\cos(\omega_D.t) - e^{-\xi.\omega_n.t}.{\omega_D}^2.(\omega_D+\omega).\sin(\omega_D.t)\right] +$$

$$\frac{1}{2(\xi^2.{\omega_n}^2+(\omega_D-\omega)^2)} \left[-\xi^3.{\omega_n}^3.e^{\xi.\omega_n.(t_d-t)}.\cos(\omega_D.(t_d-t)-\omega.t_d) + \right.$$

$$\xi^2.{\omega_n}^2.\omega_D.e^{\xi.\omega_n.(t_d-t)}.\sin(\omega_D.(t_d-t) -$$

$$\omega.t_d) + \xi^2.{\omega_n}^2.e^{\xi.\omega_n.(t_d-t)}.\omega_D.\sin(\omega_D.(t_d-t) -$$

$$\omega.t_d) + e^{\xi.\omega_n.(t_d-t)}.\omega_n.\xi.{\omega_D}^2.\cos(\omega_D.(t_d-t)-\omega.t_d) -$$

$$\xi^2.{\omega_n}^2.e^{\xi.\omega_n.(t_d-t)}.(\omega_D-\omega).\sin(\omega_D.(t_d-t)-\omega.t_d) -$$

$$\xi.\omega_n.\omega_D.e^{\xi.\omega_n.(t_d-t)}.(\omega_D-\omega).\cos(\omega_D.(t_d-t)-\omega.t_d) -$$

$$\xi.\omega_n.e^{\xi.\omega_n.(t_d-t)}.\omega_D.(\omega_D-\omega).\cos(\omega_D.(t_d-t)-\omega.t_d) +$$

$$e^{\xi.\omega_n.(t_d-t)}.{\omega_D}^2.(\omega_D-\omega).\sin(\omega_D.(t_d-t)-\omega.t_d) +$$

$$\xi^3.{\omega_n}^3.e^{-\xi.\omega_n.t}.\cos(\omega_D.t) + \xi^2.{\omega_n}^2.\omega_D.e^{-\xi.\omega_n.t}.\sin(\omega_D.t) +$$

$$\xi^2.\omega_n{}^2.e^{-\xi.\omega_n.t}.\omega_D.\sin(\omega_D.t) - e^{-\xi.\omega_n.t}.\omega_n.\xi.\omega_D{}^2.\cos(\omega_D.t) -$$

$$\xi^2.\omega_n{}^2.e^{-\xi.\omega_n.t}.(\omega_D - \omega).\sin(\omega_D.t) +$$

$$\xi.\omega_n.\omega_D.e^{-\xi.\omega_n.t}.(\omega_D - \omega).\cos(\omega_D.t) +$$

$$\xi.\omega_n.e^{-\xi.\omega_n.t}.\omega_D.(\omega_D - \omega).\cos(\omega_D.t) + e^{-\xi.\omega_n.t}.\omega_D{}^2.(\omega_D - \omega).\sin(\omega_D.t)\Big]\Big\}$$

3.3 Moving Load Model

The validation of FE results was confirmed by comparing the results of FE models with exact solution. The moving load (truck) is modeled by applying the concentrated load at various nodes with the duration equal to element length divided by the moving load velocity (Figure 3.1).

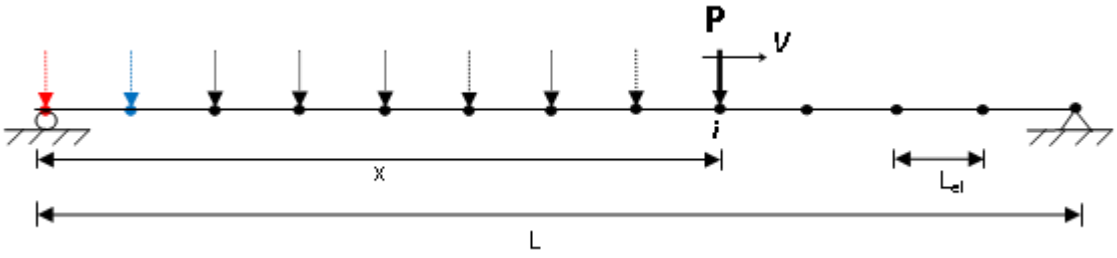

Figure 3.1. Moving load modeling.

Dynamic response determination is sensitive to modeling parameters with acceleration being the most sensitive due to the contribution of higher modes. This has not received much attention in the literature. Parameters that have to be considered in modeling in order to obtain acceptable results for acceleration and velocity are as follows:

- Time step should be taken as the element length divided by load speed.

- Time function should be triangular starting from zero and increasing gradually to reach its maximum value during one time step and decreasing from its maximum value to zero in another time step.

- Loads should be applied exactly on nodes; otherwise, the results for acceleration are significantly different.

- If the concrete deck is not entirely supported at approaches, when the load enters and exits the bridge from some locations other than over girders, it causes local numerical problems in computation.

3.3.1 Time Function

In all the models used in this dissertation, time function is defined as a triangular function as shown in Figure 3.2. Due to the sudden application of rectangular time function (Figure 3.2) to each node, the results of velocity and acceleration can be significantly inaccurate. However, the results for displacement and moment are satisfactory using either time functions. Noting that, the time function duration must be an integer factor of the time step used in integrating the differential equations.

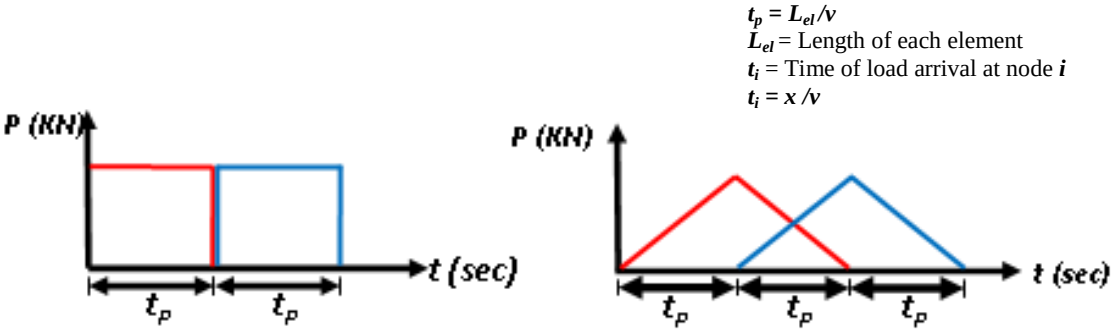

Figure 3.2 Types of time function.

Figure 3.3 shows displacement, velocity and acceleration time histories for both time functions using the direct time integration analysis method with damping ratio (ζ) 0%, time step (dt) of 0.01 second, and load discretization (t_p) 0.01 sec. The results were compared to the exact solution, modal analysis using 80 modes.

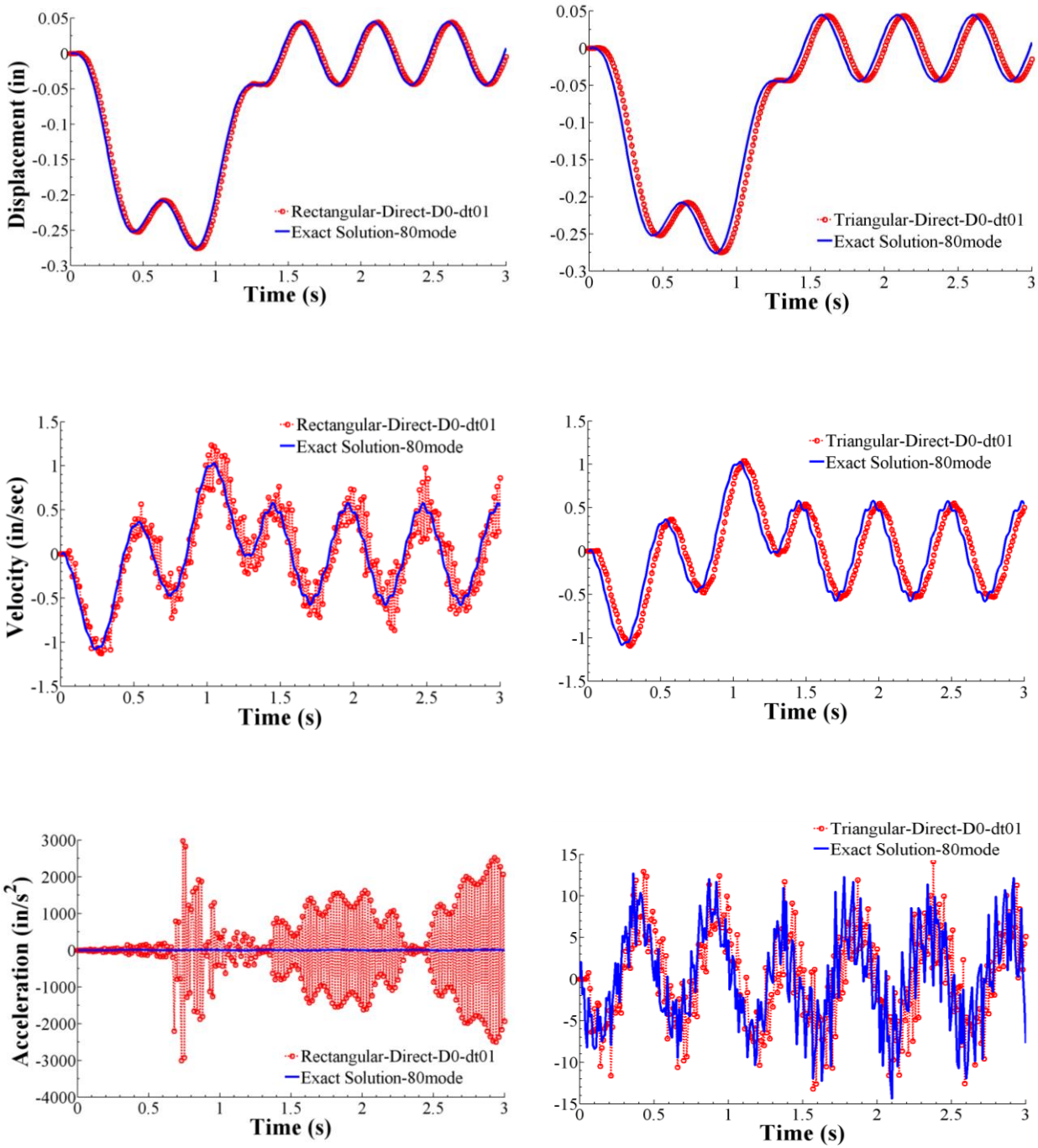

(a) (b)

Figure 3.3 Effect of rectangular (a) and triangular (b) time function on bridge response.

As can be seen the displacement results are very accurate regardless of the type of time function used to model the moving load. However, acceleration has significant error when the rectangular time function is used. Velocity results inaccuracy is not as inaccurate as the acceleration results although unlike displacement they are affected by the type of time function. This proves the fact that higher modes significantly affect acceleration results. Therefore, a small inaccuracy in choosing the model parameters can result in a significantly large error in acceleration response.

3.3.2 Time Step

Time step is also important for accurate modeling of the problem and affect all three dynamic responses (displacement, velocity and acceleration). In order to investigate the influence of time step on response results, two time steps of 0.01 sec and 0.04 sec were used. As it can be seen in Figure 3.4, the error is more significant in acceleration response although displacement and velocity contain small errors.

The results presented here highlight the importance of correctly selecting the finite element model parameters. This determination was made through a significant number of analyses and once the confidence was established in the accuracy of the model, it was used for parameter study, the results of which are discussed in the following chapter.

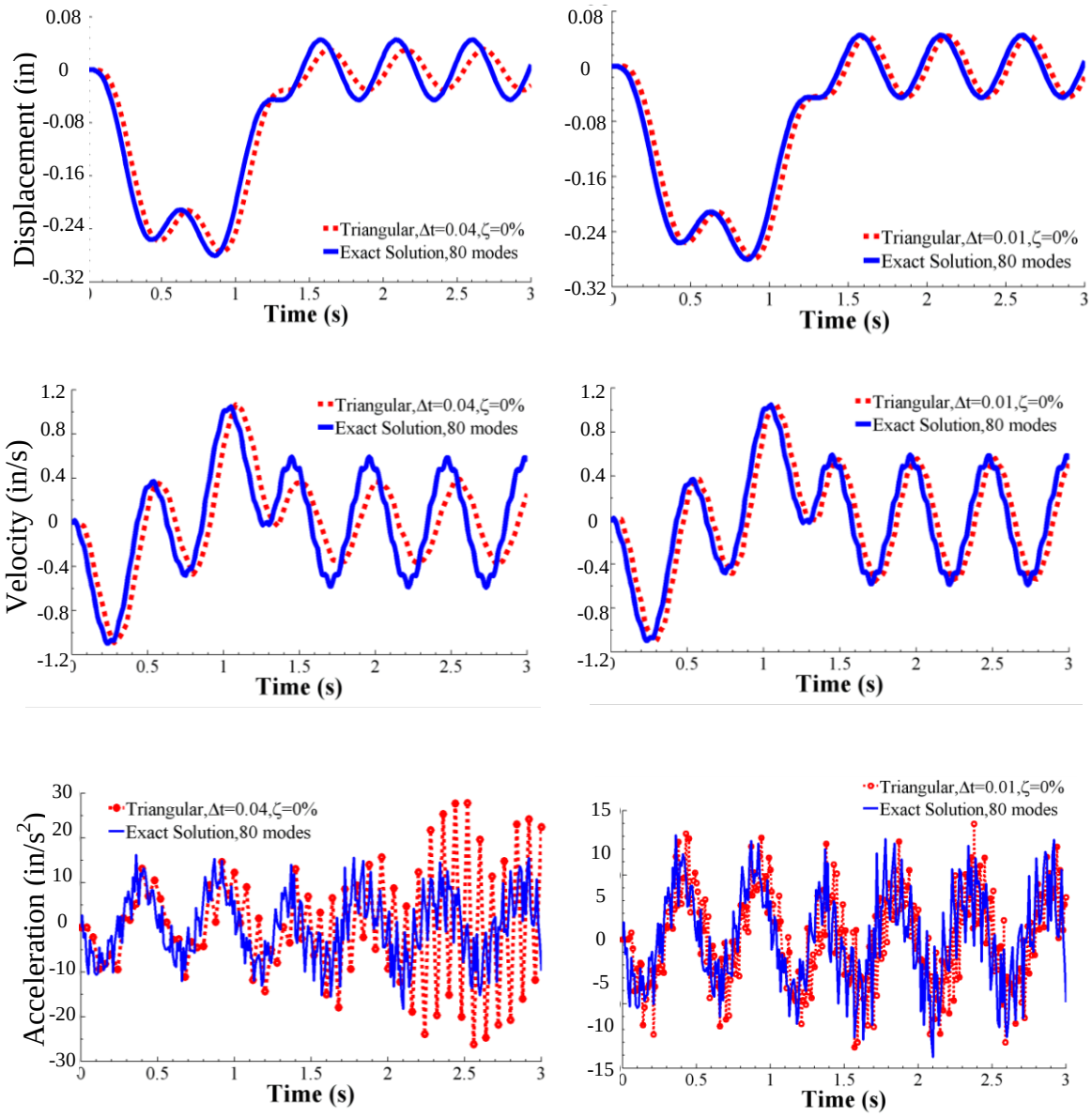

(a) (b)

Figure 3.4 Effect of 0.04 sec (a) and 0.01 sec (b) time Step on bridge response.

CHAPTER 4

PARAMETRIC STUDY

In this chapter, the effect of various vehicle and bridge parameters on bridge dynamic response was investigated. These parameters include vehicle velocity, span length, bridge natural frequency, speed parameter, damping ratio (ζ), load sequence, number of spans, spatial effects, and boundary conditions. Vehicle velocity (V), span length (L), and bridge frequency (f) have the most influence on bridge dynamic response. These three parameters have been investigated in a combined parameter called speed parameter (α) by several researchers (Majka and Hartnett 2008; Fryba 1999; Wright & Walker 1972) prior to this study. Speed parameter is traditionally defined as $\alpha=V/2Lf$. However, in this study it is shown that bridge k-parameter (k_b), which is equal to Lf/V and defined under this study, better explains the structure response characteristic due to a moving load. After introducing k_b in this chapter, it will be used for the rest of the study for comparison; note that k_b is equal to half of the inverse speed parameter.

4.1 Speed Parameter and k-Parameter

Using the exact solution equations (see Chapter 3), the bridge responses are graphed for different speed parameters in Figure 4.1. Many cases are analyzed by varying V, L, and f while holding α constant. It is determined that bridge dynamic responses are not affected by these variations and are equivalent for the same α (Figure 4.1). The results are presented in dimensionless units and the displacement graph is compared with the results of another study by Saadeghvaziri (1993). Dimensionless displacement or dynamic load

amplification, impact factor (IM) plus one is calculated by dividing dynamic displacement by static deflection (δ_{st}). Dimensionless velocity and acceleration is defined by dividing the maximum velocity and acceleration by the product of static deflection and natural frequency ($\omega.\delta_{st}$), or the squared natural frequency ($\omega^2.\delta_{st}$), respectively.

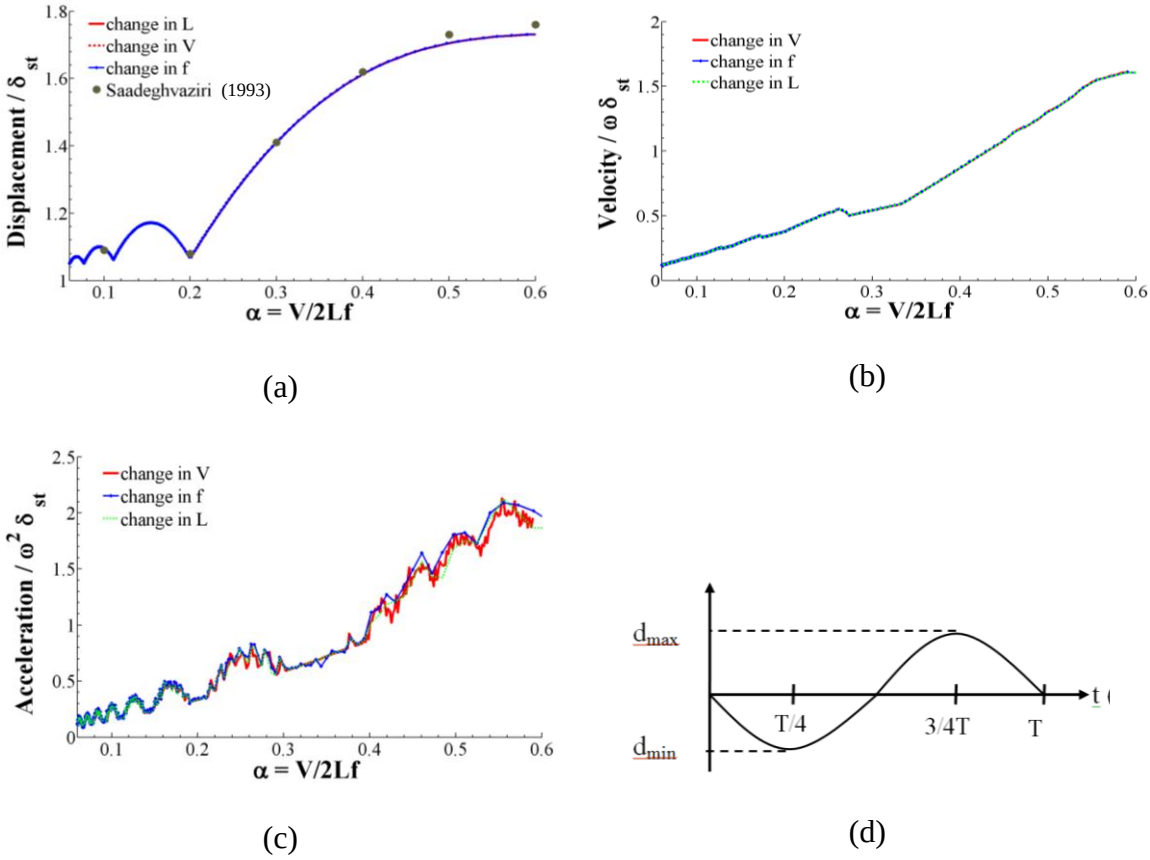

Figure 4.1 Dimensionless displacement (a), velocity (b), acceleration (c) for single moving load and 0% damping for different velocity (V), span length (L), and bridge natural frequency (f), and (d) Typical displacement response time history.

The peaks in displacement and acceleration graphs can be explained in light of the time it takes for a moving load to travel over the bridge. Harmonic motion displacement is at the extreme at 0.25T and 0.75T (Figure 4.1d). Therefore, if the maximum/minimum

dynamic displacement occurs at the same time that the maximum static displacement occurs, the total bridge displacement would be at its highest/lowest values.

The time taken for the load to traverse the span is t_d (duration) and it is equal to L/V. Thus, at L/2V the load is at the middle of the span causing the maximum static displacement at that point. If at that moment, bridge dynamic displacement is in the (i±0.25) T, the minimum and the maximum displacement occurs.

$$\frac{L/2}{V} = (i \pm 0.25).T_b \quad , \quad \frac{Lf_b}{V} = \begin{cases} 2(i-0.25) & \text{Max response} \\ 2(i+0.25) & \text{Min response} \end{cases} \tag{4.1}$$

When a bridge k-parameter (k_b), defined as Lf_b/V, is equal to 1.5, 3.5, 5.5, etc., the maximum dynamic displacement occurs; and when this value is equal to 2.5, 4.5, 6.5, etc., the minimum displacement response occurs. Figure 4.2 represents the dynamic response for bridges with different k_b. As can be seen, acceleration is at its peak values when k_b is equal to an integer number; and at its minimum values when k_b is equal to i+0.5, considering i as an integer number. The maximum bridge acceleration occurs when the load enters or leaves the bridge. If the time for the moving load to traverse the bridge is an integer factor of the bridge period, then acceleration will be further amplified.

As t_d is the loading duration on the span and $t_d = L/V$, k_b can be written as:

$$k_b = \frac{Lf}{V} = \frac{L}{VT} = \frac{L/V}{T} = \frac{t_d}{T} \tag{4.2}$$

As $\alpha = V/2Lf$, k_b is equal to half of the reversed speed parameter.

$$k_b = \frac{Lf}{V} = 0.5\frac{2Lf}{V} = 0.5\frac{1}{V/2Lf} = 0.5\,\frac{1}{\alpha} \tag{4.3}$$

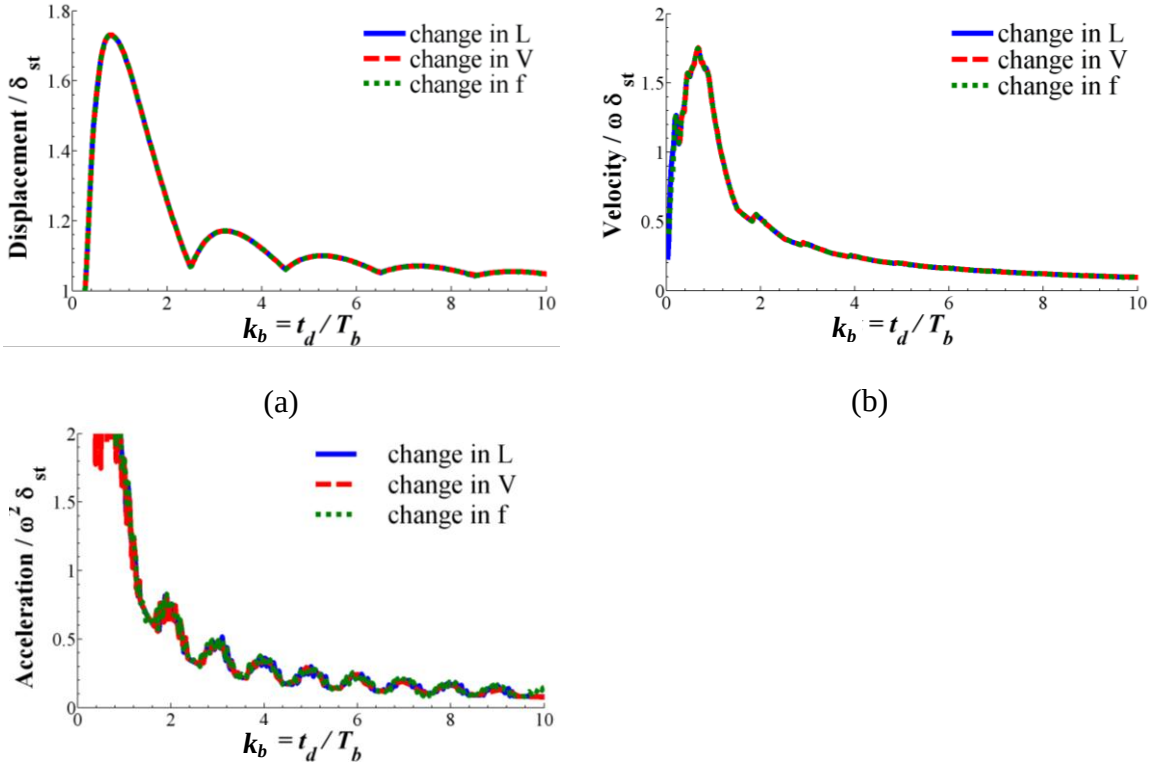

Figure 4.2 Dimensionless displacement (a), velocity (b), and acceleration (c) for single moving load and 0% damping for different moving load velocity (V), span length (L), and bridge frequency (f) versus the parameter $k_b = t_d / T_b$.

In a study by Manning (1981), it was concluded that the maximum dynamic response occurs when the time to travel the span (t_d) is equal to the fundamental period (T_b) of the bridge. In such a situation, k_b would be equal to 1 and the speed parameter, α, would be equal to 0.5, supporting the results of this study. However, a bridge k-parameter can never be equal to 1. In such case, the product of bridge frequency and span length should be equal to vehicle speed. For vehicle speed equal to 65 mph and bridge frequency between 2 and 6, the span length should be less than the values stated in Table 4.1 so that k_b is less than or equal to 1. This only occurs in short span bridges with low frequencies.

Table 4.1 Bridge Natural Frequency and Span Length Corresponding to $k_b = 1$

Span Length (in.)	570	378	276	228
Frequency (Hz)	2	3	4	5

To investigate the common range for k_b among existing composite bridges, the results of a survey (Saadeghvaziri and Hadidi 2002) are used to calculate the practical range of k_b. k_b ranges from 2 to 5 for most bridges (Table 4.2).

Table 4.2 Calculated Bridge k-Parameters (k_b) for Some Bridges in New Jersey

Bridge ID	span length (in)	frequency	k-parameter
0206-165	1082	3.32	2.5
1013-151	1498	2.81	2.9
1103-158	1143	3.57	2.9
1149-176	1575	2.63	2.9
1149-176	1488	2.95	3.1
1312-154	1361	3.55	3.3
1143-168	1320	3.75	3.6
1143-170	966	5.4	3.8
1143-166	1103	5.34	4.2

4.2 Damping Ratio

The effect of damping ratio on dynamic response of the bridge is investigated with respect to speed parameter. Figure 4.3 shows the results for 0 to 5% damping ratio for displacement, velocity and acceleration. Every 1% change in damping ratio influences displacement and acceleration by approximately 1.2% and 10%, respectively. Velocity is not much influenced by damping ratio. In this study, the minimum damping ratio of 1% has been used for simulations so that the maximum possible dynamic response will be obtained.

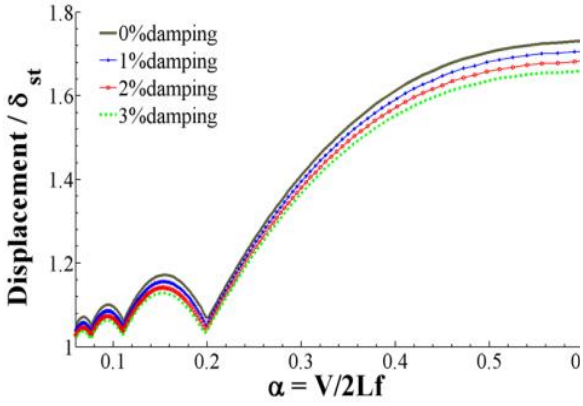

(a)

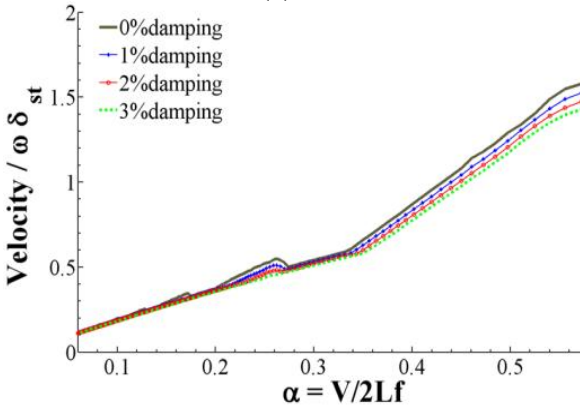

(b)

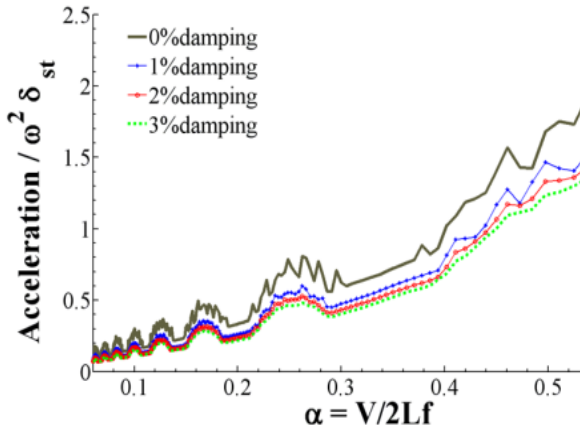

(c)

Figure 4.3 The effect of damping ratio on bridge dynamic response (a) displacement, (b) velocity, and (c) acceleration.

4.3 Load Sequence

The results shown in the previous sections are for a condition in which the bridge is at rest before the excitation begins. The pre-existing vibration can be investigated in two different ways; single-axle loading, in which only one load is on the bridge at any time and the 2nd load enters the bridge after the 1st load exits the bridge; and multi-axle loading, in which two or more loads move over the bridge simultaneously. Static deflection in single-axle loading can be computed using simple structural analysis equations such as $PL^3/48EI$ for simply supported bridges. However, static deflection for multi-axle loading is not as simple as single-axle loading.

Due to the large variety of trucks in terms of axle weight, axle distances and number of axles, a 24-hour set of truck weight data in a random highway in New Jersey is considered in this study, and an average type of truck was chosen for further investigation. In order to have a general idea about bridge dynamic response due to a truck load, bridge dynamic response is first considered for consecutive one-axle loads, two-axle loads with identical axle weights, and two-axle loads with various axle weights. Then, the bridge response is considered under a multi axle truck.

4.3.1 Consecutive One-Axle Loads

In the case of consecutive one-axle loading (Figures 4.4a and 4.4b), once the 2nd load enters the bridge, the 1st axle has already exited the bridge. Hence, there is only one axle load over the bridge at any time. The time that the 2nd load enters the bridge could be varied and is measured with respect to the time that the 1st axle exits the bridge. This arrival time can be investigated relative to the bridge's natural frequency/period.

Analytical studies show that when this arrival time (A_t) is equal to 0 or T, the maximum response occurs; minimum response occurs when A_t is equal to 0.5T.

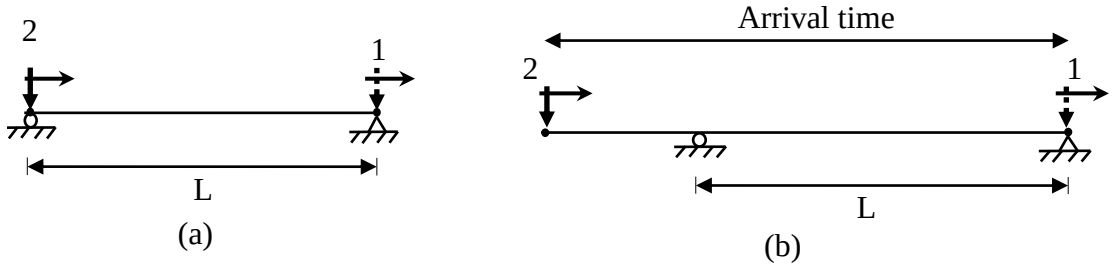

Figure 4.4 The schematic of one axle load over the bridge at a time with (a) zero arrival time and (b) with non-zero arrival time.

Figure 4.5 shows the results for k_b equal to 2, 2.5 and 3. The steady state part of the vibration refers to the bridge dynamic response while the load is over the bridge, and the transient part of the vibration refers to the bridge dynamic response once the load has cleared the bridge. As can be seen, for k_b equal to 2.5 the response is nearly constant and it is not influenced by different arrival times. As it was mentioned before, the transient vibration is nearly equal to zero when k_b is equal to an integer number plus 0.5 (i+0.5). Bridges with k_b equal to i+0.5 have this advantage; there is no vibration once the load has left the bridge.

If the same investigation is performed for three single loads passing through a bridge with identical arrival times, the response increases further. Figure 4.6 shows the results of 2-axle and 3-axle loads (one axle over the bridge at a time) for displacement, velocity and acceleration responses. The result of one axle loading with respect to k_b is also shown in Figure 4.6 for comparison. As can be seen, bridge dynamic response is increased by a higher number of axles.

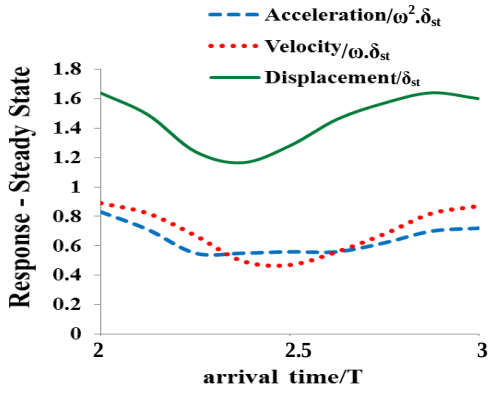

(a1)k_b = 2

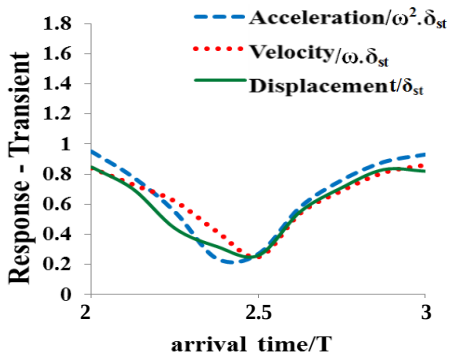

(b1) k_b = 2

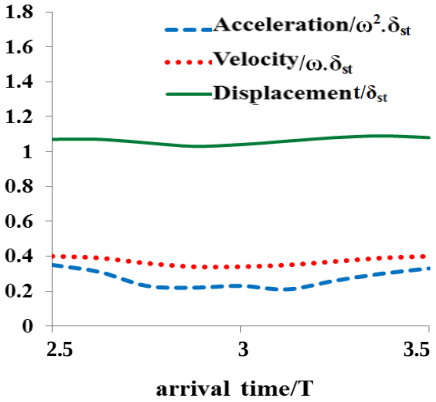

(a2) k_b = 2.5

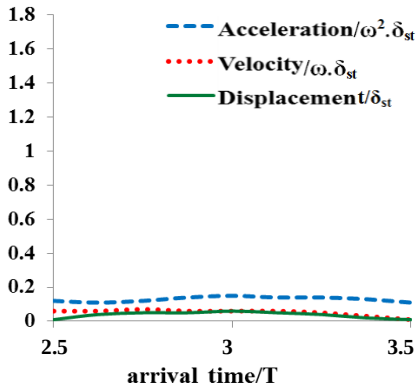

(b2) k_b = 2.5

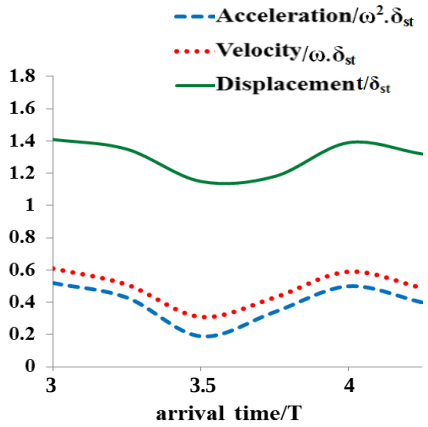

(a3) k_b = 3

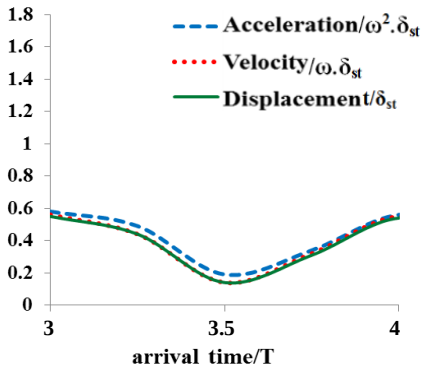

(b3) k_b = 3

Figure 4.5 The maximum (a) steady state and (b) transient part of the bridge dynamic response under one-axle load at a time for (1) k_b = 2, (2) k_b = 2.5, and (3) k_b = 3.

Considering k_b in the range of 2 to 5, the steady state part of the vibration can be twice as much as the response for one axle loading. Note that for short span bridges, in calculating static deflection, some axle weights are not considered. Using AASHTO static deflection criteria, the excessive vibration on short span bridges cannot be predicted. In fact, deflection/fatigue criteria for bridges shorter than 40 ft cannot provide a good estimation of bridge dynamic response.

AASHTO LRFD (2007) specifies that live load deflection should be taken as the larger of "that resulting from the design truck alone" or "that resulting from 25 percent of the design truck taken together with the design lane load". The design truck used in deflection control is identical to a HL-93 truck. The design lane load is equal to 0.64 kip/ft and is uniformly distributed in a longitudinal direction. Impact Factor only applies to the design truck and shall be taken as 33% of the static load.

Distribution factor is used to apply the appropriate amount of live load to a single stringer from the standard HL-93 loading. AASHTO assumes all stringers deflect equally when calculating live load deflection.

$$\text{Distribution Factor} = \frac{\text{Number of Lanes}}{\text{Number of Stringers}} \tag{4.4}$$

The multiple presence factor (m) is applied to reduce the total deflection when there are more than two lanes, assuming not all the lanes are fully loaded. This factor (m) is equal to 1.2, 1, 0.85, and 0.65, for one, two, three, and more than three lanes, respectively.

For short span bridges, where a HL-93 truck cannot be completely located on the bridge to compute static deflection, the static deflection is computed only by a 1-axle

load of 32 kip. This way, dynamic response may be underestimated by 50% and 20% for bridges with k_b equal to 2 and 3, respectively.

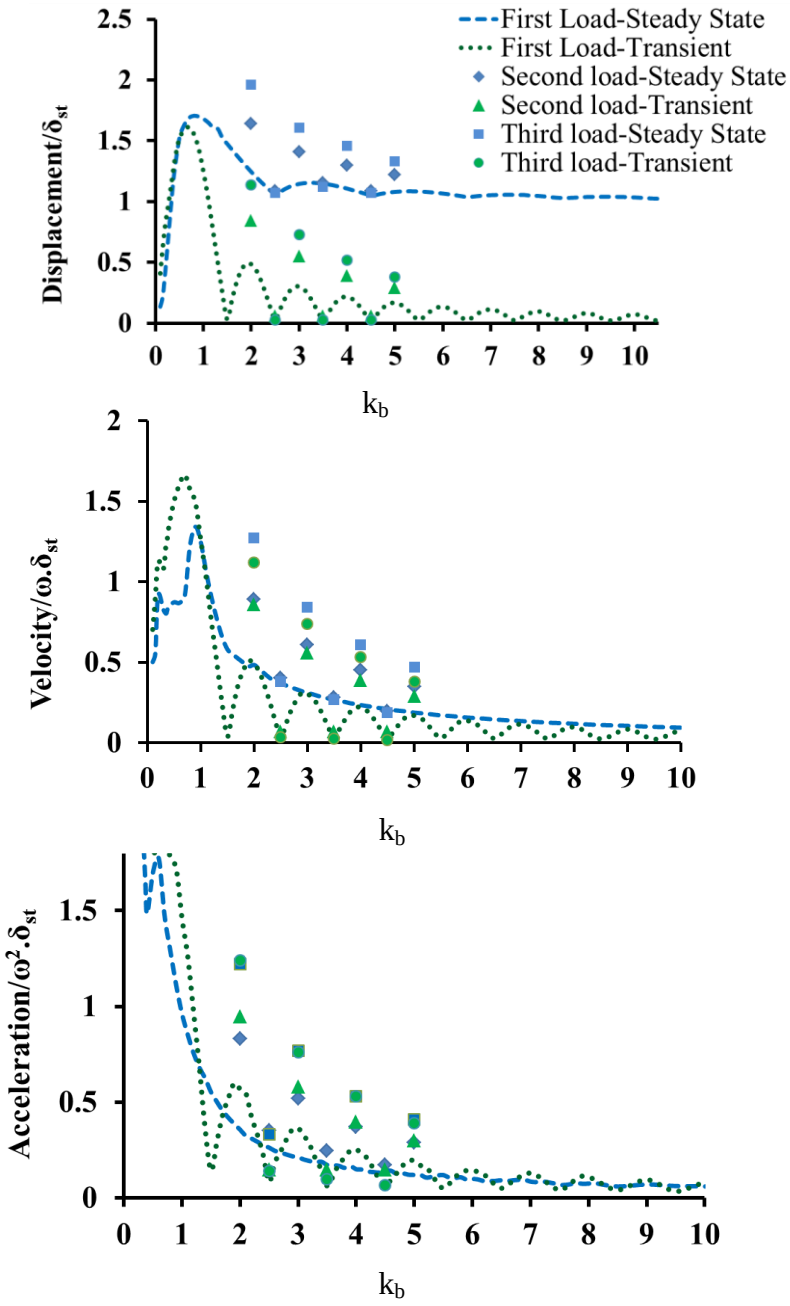

Figure 4.6 Vibration due to two and three consecutive loads, one axle over the bridge at a time.

4.3.2 Two-Axle Loads

Under the condition that there are more than one axle loads over a bridge, simultaneously, investigating the bridge dynamic response becomes very complicated. The parameters affecting dynamic response are: the numbers of axles, axle arrangements, distances, and weights have to be considered. Moreover, static deflection varies from case to case, depending on the distance between axles. Figure 4.7 shows how the definition of arrival time (A_t) differs from two-axle loading to one-axle loading. The arrival time for two axle loading is considered as the time difference between the 1st and the 2nd axles.

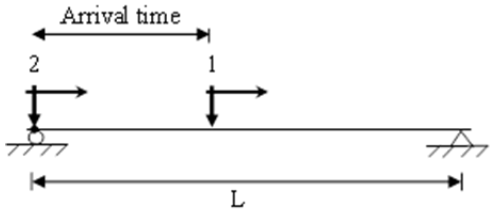

Figure 4.7 Two-axle load over a bridge.

The ratio of arrival time (A_t) to bridge natural period (A_t /T_b) is equal to the axles distance (L_v) multiplied by the bridge frequency (f) divided by vehicle velocity (V), as seen in Equation 4.4. The value of A_t /T_b is called vehicle k-parameter (k_v). The only difference between bridge and vehicle k-parameters is length term. In the bridge k-parameter (k_b) the term L represents span length while the term L_v in Equation 4.5 is the vehicle length or the distance between the heaviest axles.

$$k_v = \frac{A_t}{T} = \frac{L_v}{V} f \qquad (4.5)$$

In this section, three bridges with different k_b of 2, 2.5, and 3 are subjected to a two-axle truck with different axle distances, which results in various k_v. Both axles are considered to have identical weights. The case with different axle weight is investigated in the next section. The results are normalized with respect to static deflection and bridge natural frequency. For simplicity, static deflection is considered as the value resulting from one axle load. All of the results are normalized with respect to one-axle static deflection. Figure 4.8 shows the dimensionless dynamic displacement, velocity, and acceleration responses for two-axle loading.

As can be seen, when $k_v = A_t / T_b$ is equal to 0.5, 1.5, and 2.5, the minimum dynamic response occurs; and once it is equal to an integer number, 0 or 1 or 2, the maximum response occurs. For k_b equal to 2.5, the transient part of the vibration is nearly equal to zero. This means that for bridges with k_b equal to i+0.5, the vibration in the transient part is negligible even for two axle trucks.

The steady state response of the displacement is at its maximum when the axles are closer to each other. This is because the dynamic response is normalized with respect to only one-axle static deflection. In all other responses in both transient and steady state parts of vibration, the maximum response occurs when both k_b and k_v are integer numbers.

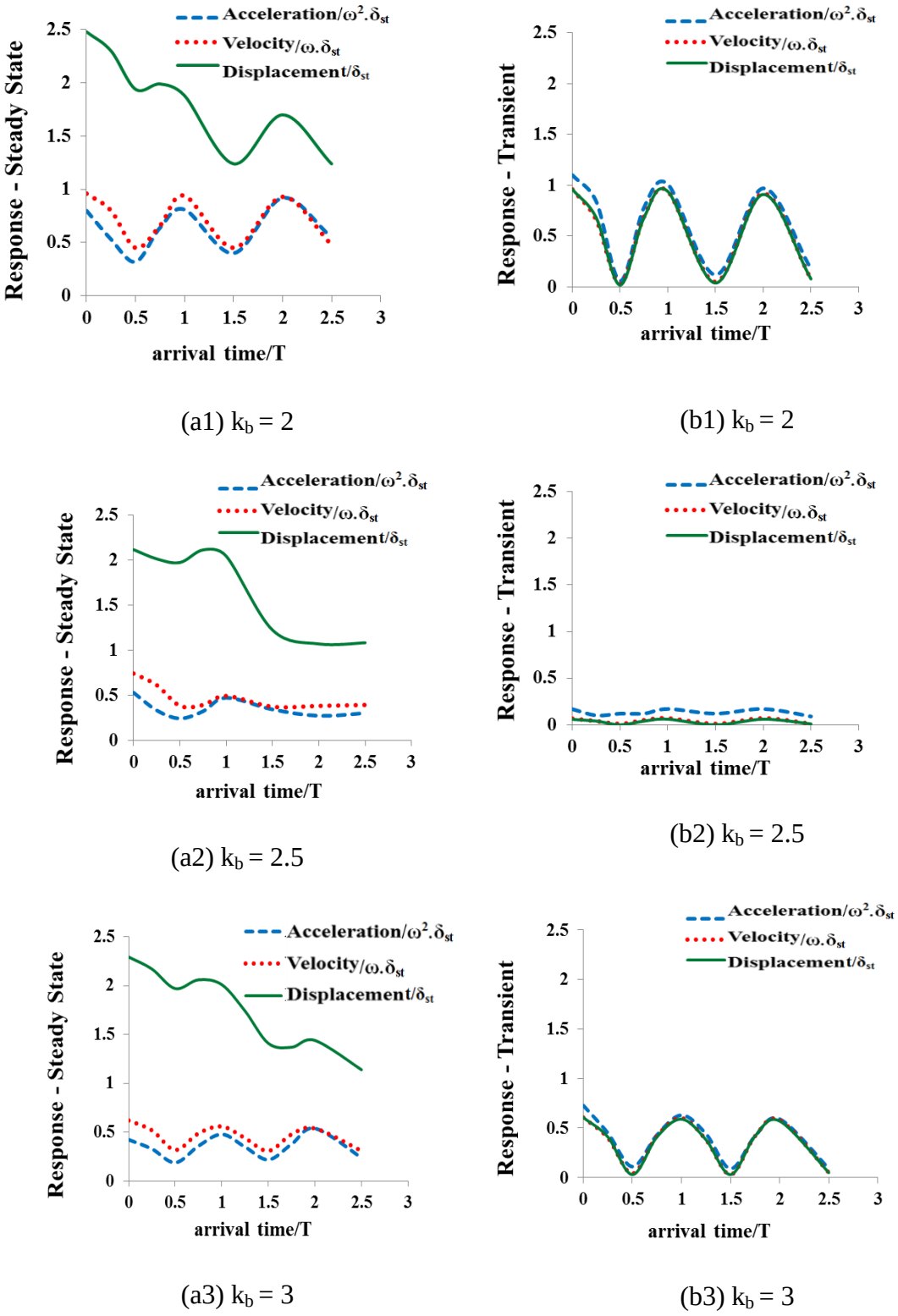

Figure 4.8 The maximum (a) steady state and (b) transient part of a bridge dynamic response under two-axle loading for different arrival time.

Note that the dimensionless displacement, velocity and acceleration responses are equal to each other in the transient part of the vibration; while only velocity and acceleration responses are equal to each other in the steady state part of the vibration. This is due to the change in static deflection with respect to the truck position, static equilibrium. Clearly, the value of dimensionless velocity and acceleration indicates the value of the impact factor in dynamic displacement.

If the bridge is only subjected to a one-axle load, the transient response is solely influenced by k_b. However, by the participation of the 2nd load, the transient response may increase or decrease depending on the 2nd axle arrival time. The participation of the 2nd axle can be defined by a participation factor which may vary from -1 to 1; this can decrease or increase the dynamic response caused by the 1st axle load. When k_v is equal to an integer number, the participation factor is equal to 1. When k_v is equal to i+0.5, the participation factor is equal to -1. Therefore, all the transient responses caused by the 1st load are canceled out when the 2nd load enters the bridge with an arrival time equal to $(i+0.5)T_b$.

4.3.3 Different Axle Weights

Considering the discussion in the previous section, bridge dynamic response under a truck load with two axles can be computed using the load superposition in which a participation factor is applied to the 2nd load's dynamic response. The value of the participation factor for the dynamic response of the 2nd axle depends on its arrival time.

In this section, bridge dynamic response under a two-axle load with different axle weights is investigated. The 1st load weight is kept constant and the 2nd load weight is

varied. The 2nd load participation factor is graphed in Figure 4.9 for various arrival time and axle weights.

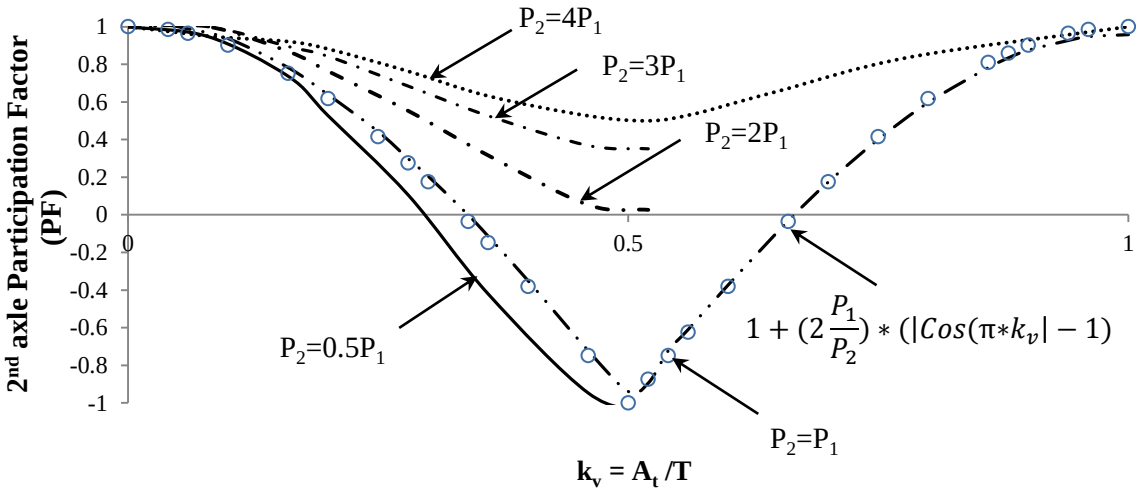

Figure 4.9 2nd axle participation factor with respect to its arrival time.

As can be seen, the 2nd load participation factor (PF) increases when the ratio of the 2nd axle weight (P_2) to the 1st axle weight (P_1) increases. The 2nd load participation can be computed using the cosine function of:

$$PF = 1 + 2\frac{P_1}{P_2}\left(|\mathrm{Cos}(\pi . k_v)| - 1\right) \tag{4.6}$$

The participation factor is only accurate to obtain the bridge response due to two-axle truck loads which can be estimated as:

$$\text{Bridge Response} = \left[1 + \frac{P_2}{P_1} + 2\left(|\mathrm{Cos}(\pi . k_v)| - 1\right)\right] . R_1 \tag{4.7}$$

Where, P_1 and P_2 are the 1st and 2nd axle weights, respectively; k_v is the vehicle k-parameter and it can be computed using Equation 4.5. R_1 is the bridge response under the

1st axle load and can be estimated using the graphs in section 4.1 depending on the bridge k-parameter (k_b).

In reality, truck axle weights are nearly similar to each other. The AASHTO design truck, which is simplified by one axle of 8 kip and two axles of 32 kip, corresponds to an actual truck with five axles. This truck includes one axle of 8 kip in front, two axles of 16 kip at the middle and two axles of 16 kip at the rear of the truck.

4.3.4 Three-Axle Trucks

In this section, bridge dynamic response is investigated under a three-axle truck load. As was mentioned, k_b represents the number of cycles that a bridge vibrates while the load is over the bridge. For instance, for a bridge with k_b equal to 2, the bridge vibrates for two cycles while the load is on the bridge. In order to have all three axles over the bridge at the same time, the arrival time for the 3rd axle (A_{t3}) should be less than twice of the bridge period (T_b), Figure 4.10. For k_b equal to 2.5, the ratio of (A_{t3}/T) should be less than 2.5; and when k_b is equal to 3, that ratio cannot be larger than 3; otherwise, the circumstances of a two-axle loading exists.

The effect of the 3rd axle arrival time, A_{t3}, on the bridge dynamic response is here studied for various conditions, where the 2nd axle arrival time, A_{t2}, is considered as 0.25T, 0.5T, 0.75T, and T. The dimensionless results are shown in Figure 4.11 for different arrival times. The second axle arrival time (A_{t2}) and the third axle arrival time (A_{t3}) are both considered as the arrival time with respect to the front axle. Note that, the axle weights are identical, bridge k parameter, k_b, is equal to 2, and the results have been normalized with respect to the bridge static deformation under a one- axle load.

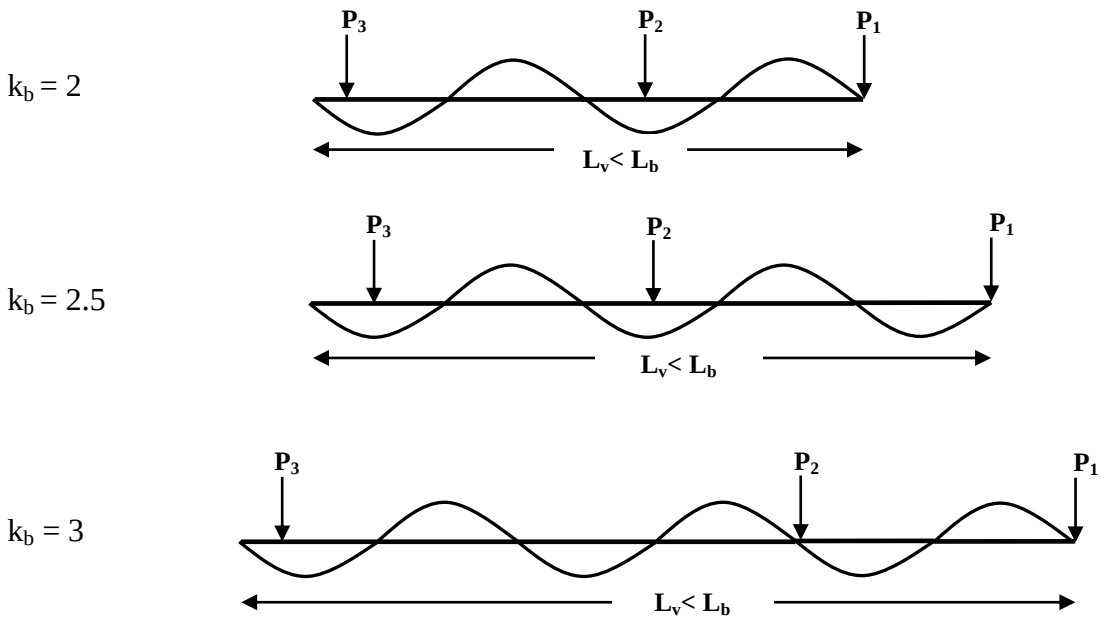

Figure 4.10 Illustration of bridges with different k_b.

The maximum response occurs when the 2nd and the 3rd axles enter the bridge at an integer order of the bridge period. The minimum response occurs when the time difference between the 1st and the 3rd axles is equal to 0.5 or 1.5 of a bridge period. Therefore, when the bridge excitation (entering or exiting loads) occurs at an integer (i) order of the bridge natural period, the maximum response occurs and when the excitation occurs at (i+0.5), the minimum response occurs.

As can be seen, the total dynamic response varies from 0.3 to 1.3 of the response for a one-axle load. This range equals 60% to 260% of the response, corresponding to one-axle loading, which is equal to 0.5 for $k_b = 2$, Figure 4.6. For short-span bridges where the computed static deflection does not reflect the influence of all axle weights, estimation of dynamic response only by considering AASHTO impact factor cannot be a good solution.

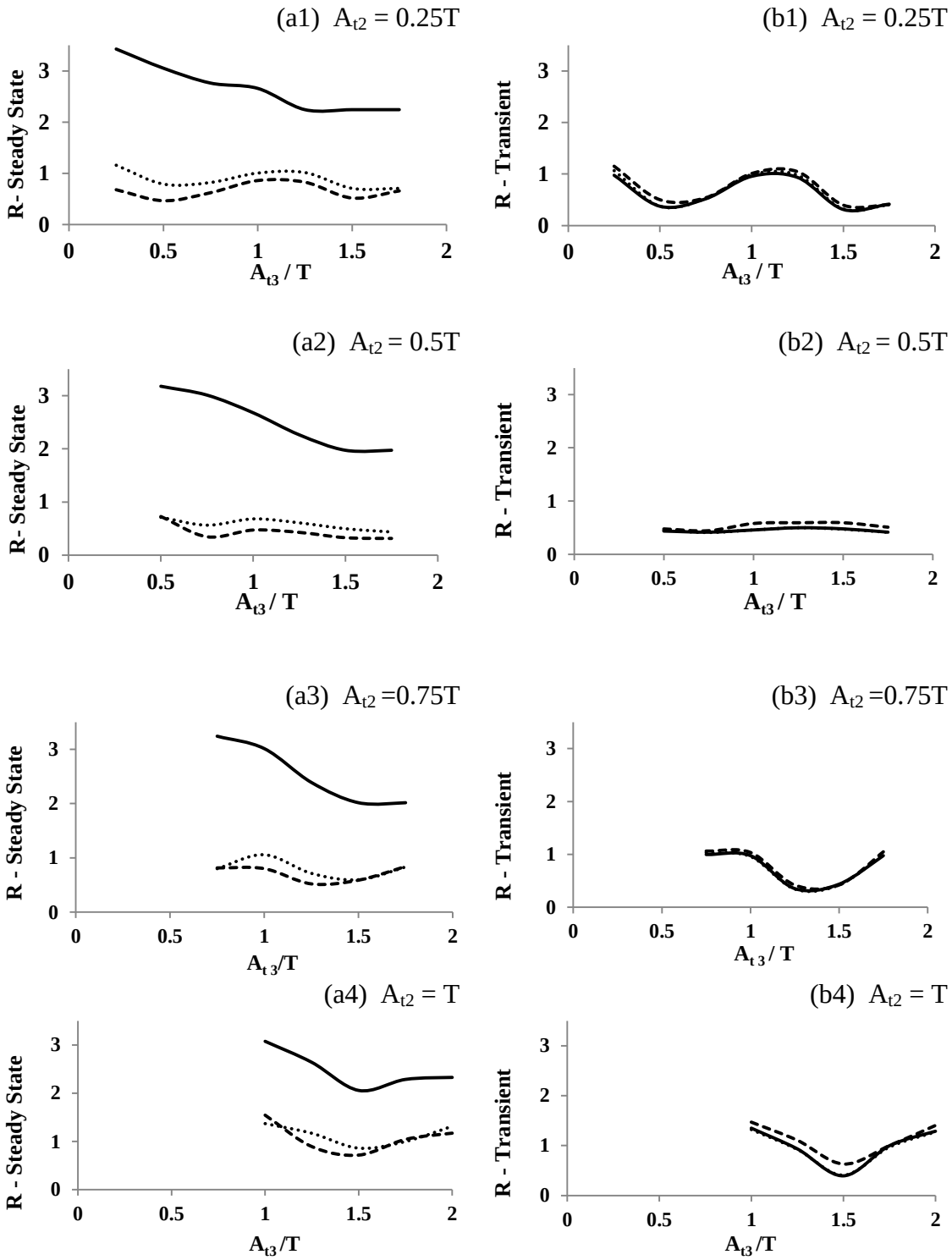

Figure 4.11 The maximum (a) steady state Response (R) and (b) transient R of a bridge dynamic displacement ——— velocity ····· and acceleration --------- responses under a three-axle truck for different A_{t2} and A_{t3}.

Knowing the fact that only the axle's arrival time and weight ratio (P_2/P_1) affect the maximum dynamic response, a bridge dynamic response can be estimated using the weights and the arrangement of the most common truck.

4.3.5 Bridge Response Due to Truck Loads

The investigation for one, two, and three axle loads with various bridge parameters and arrival times illustrates the important factors that affect bridge dynamic response. In this study, it was shown that a bridge response is directly influenced by the arrangement of loads and the axles' weight ratio.

To utilize the most common truck for analysis, the weight chart from one of the New Jersey weight control stations (station ID 00080C) in Rt. 80 close to Rt. 287 has been used. The weight data was obtained during 24 hours of October 8th, 2010. Figure 4.12 shows the percentage of the most common truck types.

As can be seen, 48% of the trucks in that random sampling on a highway in New Jersey are nearly identical to AASHTO fatigue truck. However, AASHTO utilizes three axles for the whole truck with 8-32-32 kip axle weights and 14-30 feet axle distances while the observed most common truck has five axles of average 12 kip weight. The percentage of an actual 3-axle truck is also shown in Figure 4.12, which is equal to 1% of the truck population in New Jersey.

The most common truck in New Jersey is noted as NJ122. NJ122 has five axles with the average axle weights and distances of 12 kip and 16-4-32-4 feet, respectively. The numbers following the NJ designation represent1 the arrangement of the truck axles; one axle leading two very close axles (4 ft apart from each other) followed by another

two close axles (4 ft apart). Depending on the bridge frequency, the arrangement of this type of truck varies on different bridges, thus the dynamic response varies.

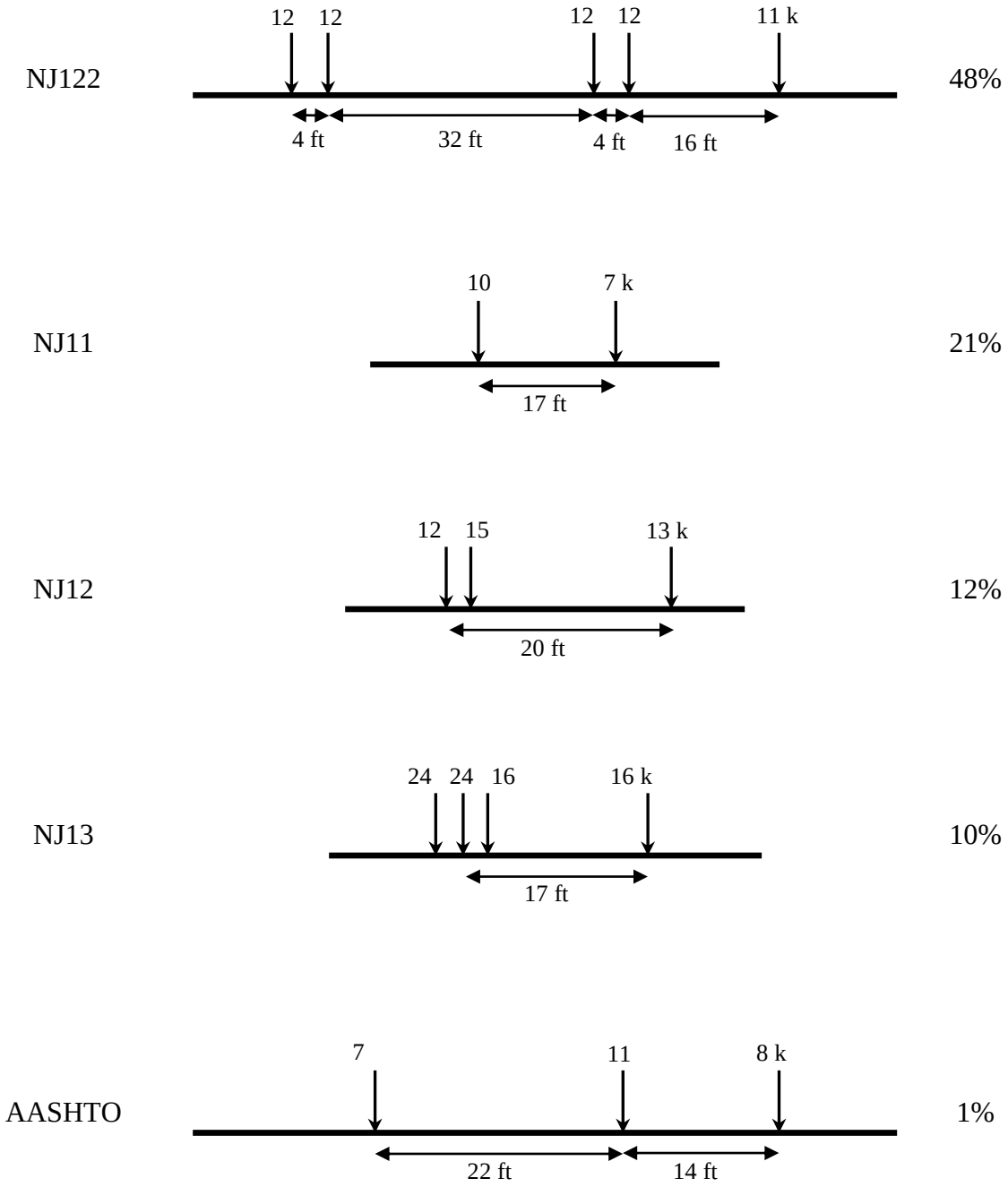

Figure 4.12 The most common truck types in a randomly selected highway in New Jersey.

In this study, several bridges with different kb are investigated and the dynamic response under this type of truck is obtained. Figures 4.13 to 4.15 show the dynamic response of three bridges with k_b equal to 2, 3, and 6. Since the rear and the middle axles for truck NJ122 are much heavier than the front axle, the participation of these two axles is much higher than the participation of the front axle. Therefore, vehicle k-parameter, k_v, is computed using the distance between middle and rear axles.

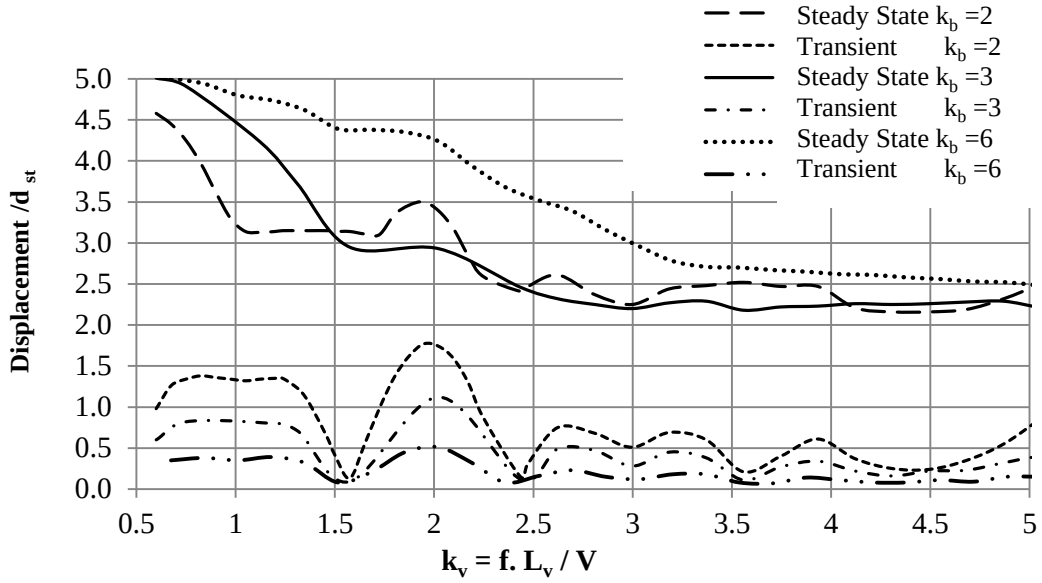

Figure 4.13 Dimensionless displacement for three bridges of k_b =2, k_b =3 and k_b =6.

It is observed that when the time distance between these two axles is equal to an integer order of the bridge period (k_v = 1, 2, 3, 4), the maximum response occurs. Since the distance between the 1st and the 2nd axles is equal to half of the distance between the 2nd and the 3rd axles, the maximum response occurs when the truck length is such that the time difference between the first and the last axles is equal to 1.5i T_b (i as an integer number). At this truck length, the time difference between the middle and rear axles

would be in an integer order to bridge period; because the distance between the middle and rear axles is twice as much as the distance between the front and middle axles.

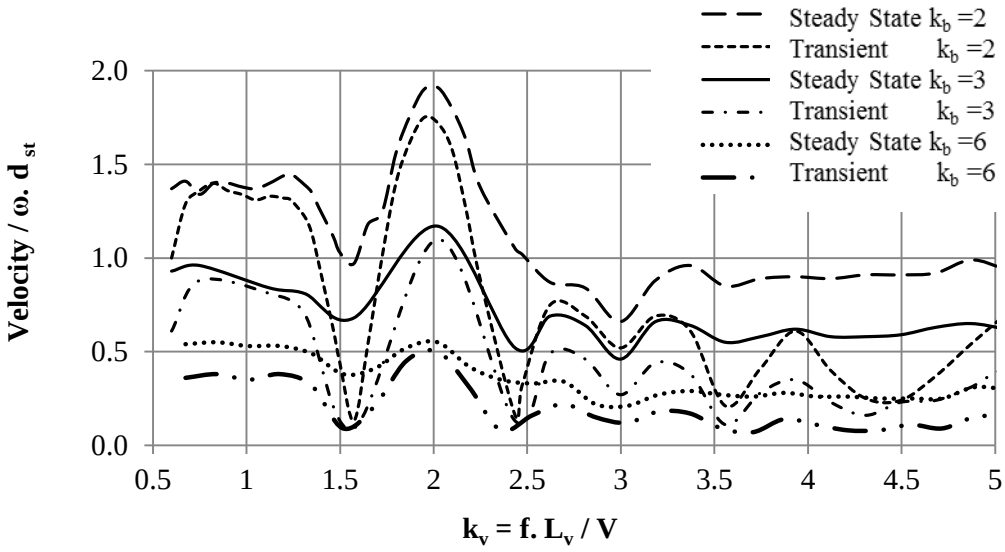

Figure 4.14 Dimensionless velocity for three bridges of k_b =2, k_b =3 and k_b =6.

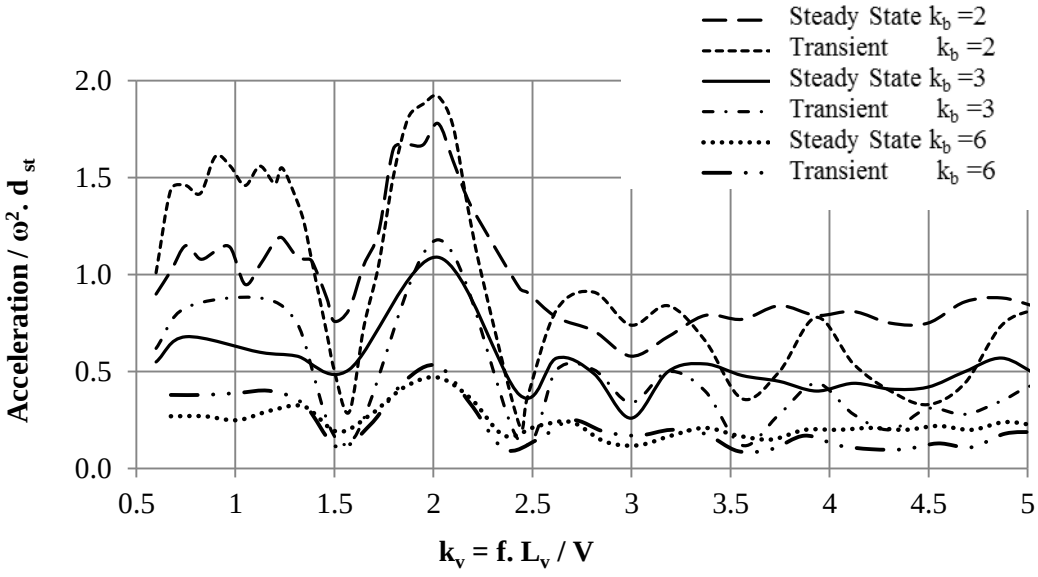

Figure 4.15 Dimensionless acceleration for three bridges of k_b =2, k_b =3 and k_b =6.

To estimate the bridge maximum dynamic response due to moving trucks, computing both k_b and k_v is required. If either of k_b or k_v is equal to an integer number plus 0.5 (i+0.5), the bridge dynamic response is negligible. However, since vehicle velocity is not an exact value, the values of k_b or k_v are not exact either. Thus, the dynamic response may be higher than the anticipated values. For this, the dynamic response of a bridge can be computed using Equations 4.8 and 4.9. Note that δ_{st} is as a result of bridge deflection due to the heaviest axle, P_{max}.

$$k_v \leq 2 \begin{cases} \delta_{Transient} = \dfrac{2}{k_b}(0.3k_v + 1.2).\delta_{st} \\ Vel = \omega\delta_{Transient} \\ Acc = (1+5\%)\omega^2\delta_{Transient} \end{cases} \tag{4.8}$$

$$k_v > 2 \begin{cases} \delta_{Transient} = \dfrac{2}{k_b}\left(0.2{k_v}^2 - 1.75k_v + 4.5\right).\delta_{st} \\ Vel = \omega\delta_{Transient} \\ Acc = (1+5\%)\omega^2\delta_{Transient} \end{cases} \tag{4.9}$$

Equations 4.8 and 4.9 are graphed in figures 4.16 to 4.18 with respect to both k_b and k_v. A bridge frequency is usually between 2 to 12 Hz, which corresponds to the value of k_v between 0.5 to 5. Using these graphs and equations, one can estimate bridge dynamic transient response due to the most common trucks. k_v is computed using the average vehicle speed, bridge frequency, and the distance between the heaviest axles. Static deflection is computed using one axle load which is the average weight of the heaviest axles; and bridge frequency is computed using Equation 2.6. Equation 2.6 is only utilized for simply supported bridges. If the bridge is a multi-span bridge with identical span length, Equation 2.6 is still applicable. Otherwise, the bridge frequency

should be computed using different methods, such as modal finite element analysis for a simplified bridge model.

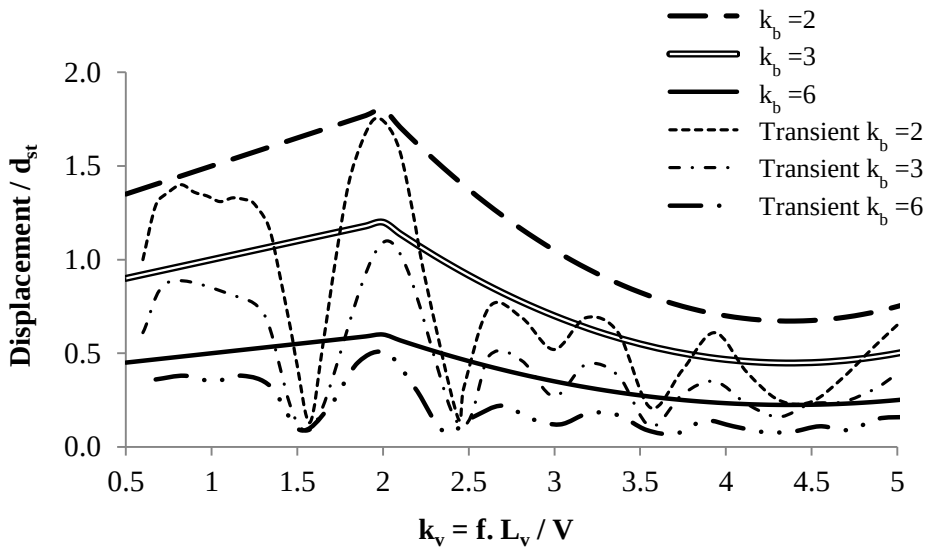

Figure 4.16 Transient displacement for three bridges of $k_b = 2$, $k_b = 3$ and $k_b = 6$.

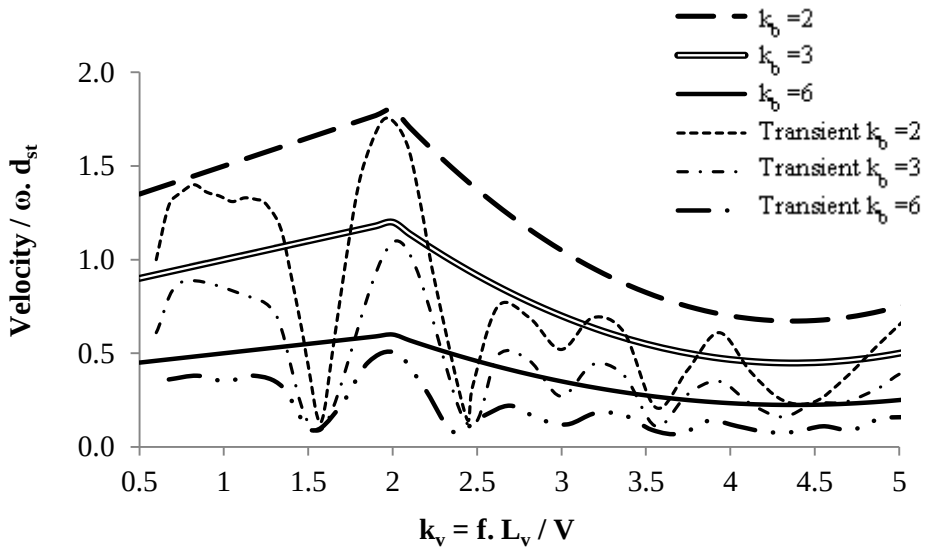

Figure 4.17 Transient velocity for three bridges of $k_b = 2$, $k_b = 3$ and $k_b = 6$.

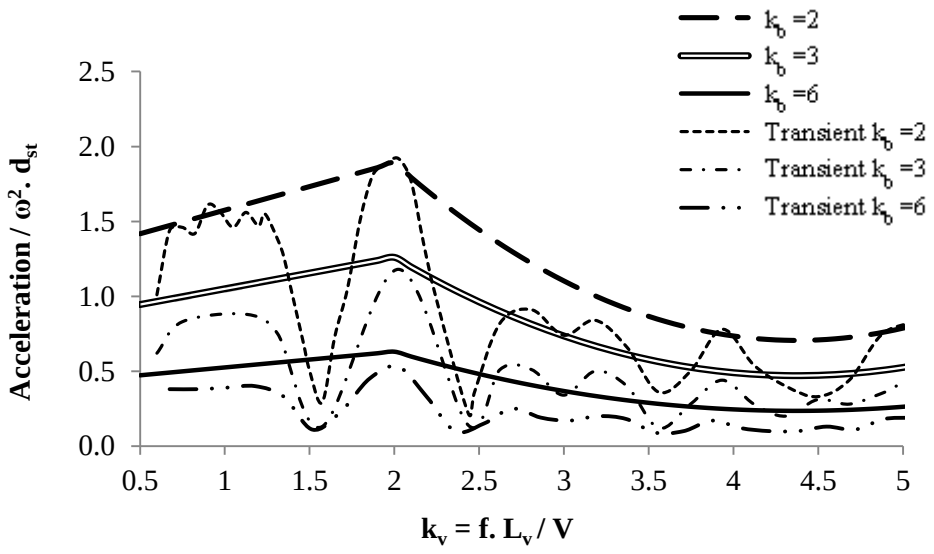

Figure 4.18 Transient acceleration for three bridges of $k_b = 2$, $k_b = 3$ and $k_b = 6$.

As for bridges with a frequency between 2 and 8 Hz, the value of k_v is less than 4; the critical frequencies for the response due to 48% of the trucks are 2.7 and 5.4 Hz for 65 mph vehicle speed. These two values were reported by other researchers based on experimental data. Bartos (1979) and Tilly et al. (1984) claimed that the bridge natural frequency should be out of the range of 1.5 to 5 Hz, otherwise, unacceptable dynamic effect is unavoidable. Moreover, the maximum deflection in the Ontario code was reduced to L/450 to reduce the natural frequency of the medium span bridges to 1.5 Hz, which is out of the range of the natural frequencies for trucks. Bartos (1979) stated that AASHTO deflection limitation leads most medium span steel bridges to have the natural frequency of 2.5 Hz which coincides with the typical truck frequency. Blanchard et al. (1977) recommended using dampers or other means to reduce the response for the bridges with natural frequencies between 4-5 Hz.

Also, Ontario Code specified raising the impact value if natural frequency of the bridge was in the range of 1.0 to 6.0 Hz. Note that, highway speed limit in Canada is 80

km/hr which equals to 50 mph. Figure 4.19 is the adjusted graph for various frequencies and k_b compared with the impact factor in Ontario code. This graph represents Figure 2.12 combined with the ratio of transient response to steady state response in Figure 4.13. As can be seen, for the bridge frequency between 1-6, the bridge response is at its maximum because k_v is between 0.5 to 2.5 for this range of frequencies, Figures 4.13 to 4.18.

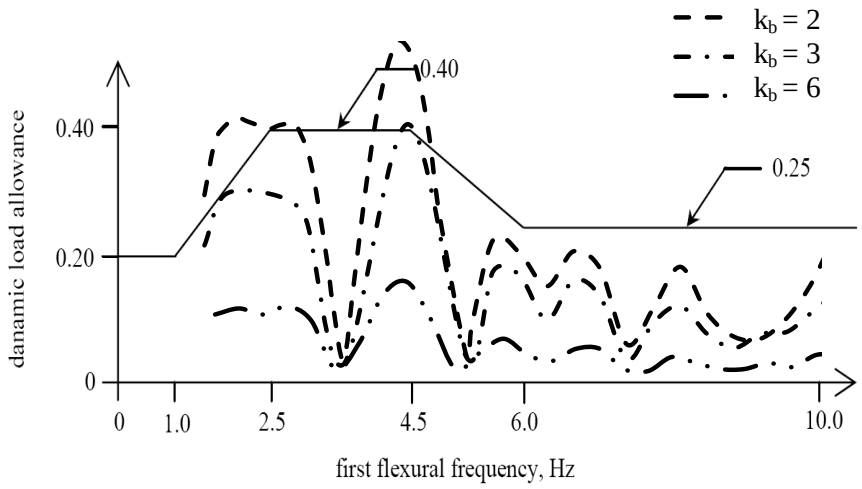

Figure 4.19 Dynamic load allowance compared with impact factor suggested by Canadian code.

4.4 Number of Spans

In this study, the effect of the number of spans on bridge dynamic response is considered only under one-axle loading. Otherwise, the orientation of load axles on different spans may influence the results significantly.

Bridge dynamic response is investigated under a one-axle moving load and k_b equal to 2.75 for 2, 3, 4, 5, and 6-span bridges with identical span lengths. The results for 1, 2, 3, 4, 5, and 6-span bridges are shown in Figures 4.20 through 4.25 for the steady

state and transient dimensionless responses. As can be seen, in most of the cases a higher number of spans would decrease the response. Therefore, response estimation using a single-span bridge overestimates the multi-span dynamic response. Note that, if there are several axles acting on two adjacent spans the bridge response would be reduced due to the stiffer support conditions.

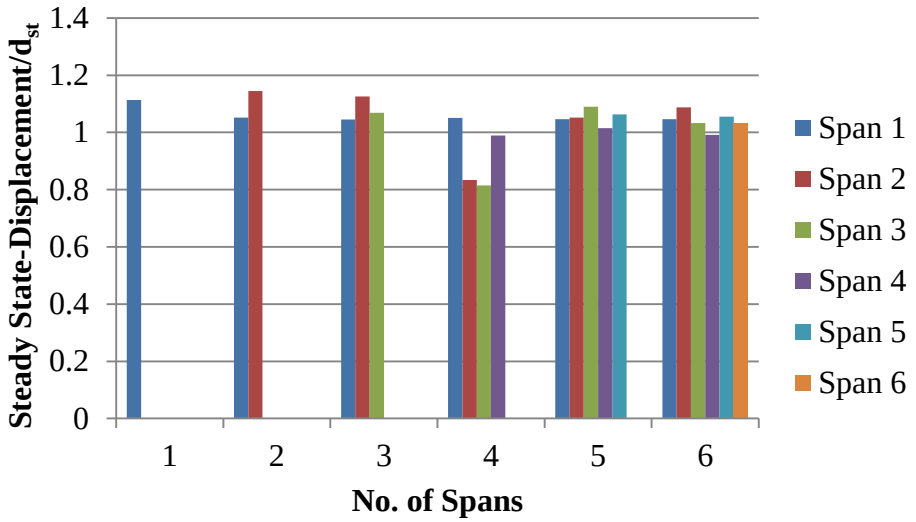

Figure 4.20 Steady state dimensionless displacement for 1, 2, 3, 4, 5, and 6-span bridges.

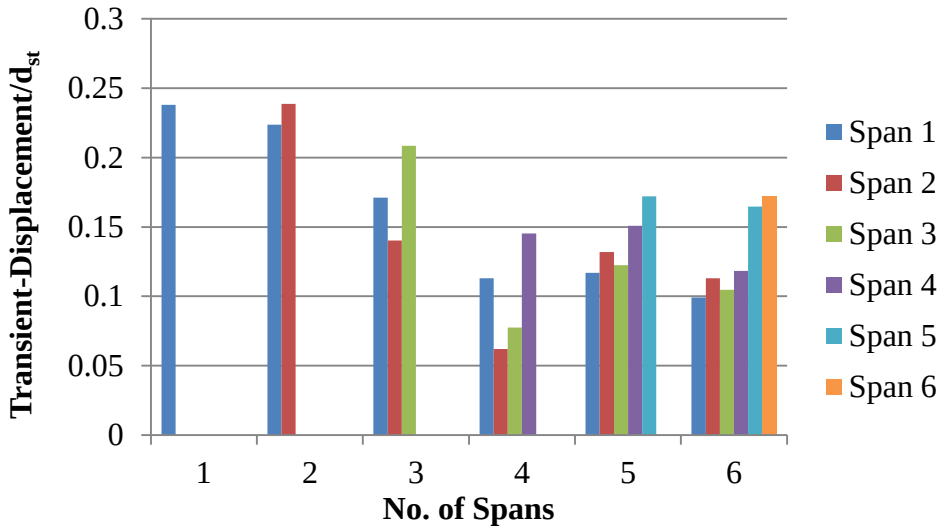

Figure 4.21 Transient dimensionless displacement for 1, 2, 3, 4, 5, and 6-span bridges.

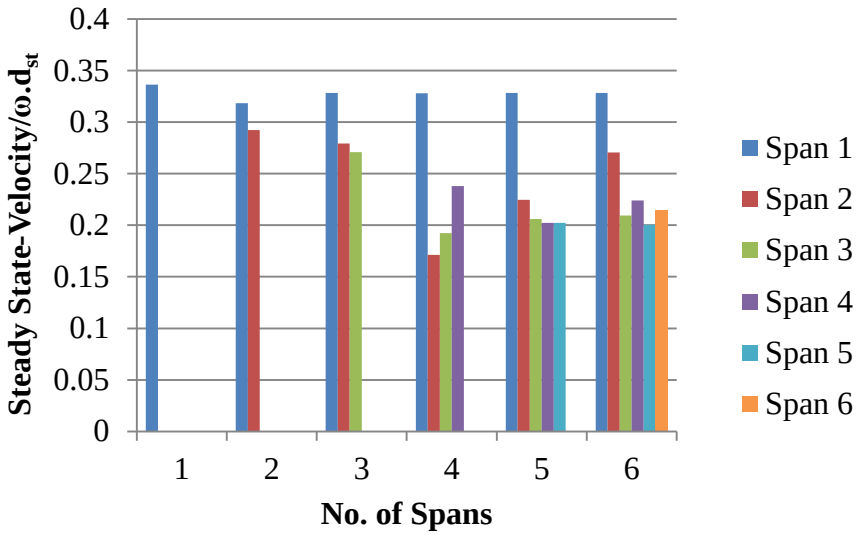

Figure 4.22 Steady state dimensionless velocity for 1, 2, 3, 4, 5, and 6-span bridges.

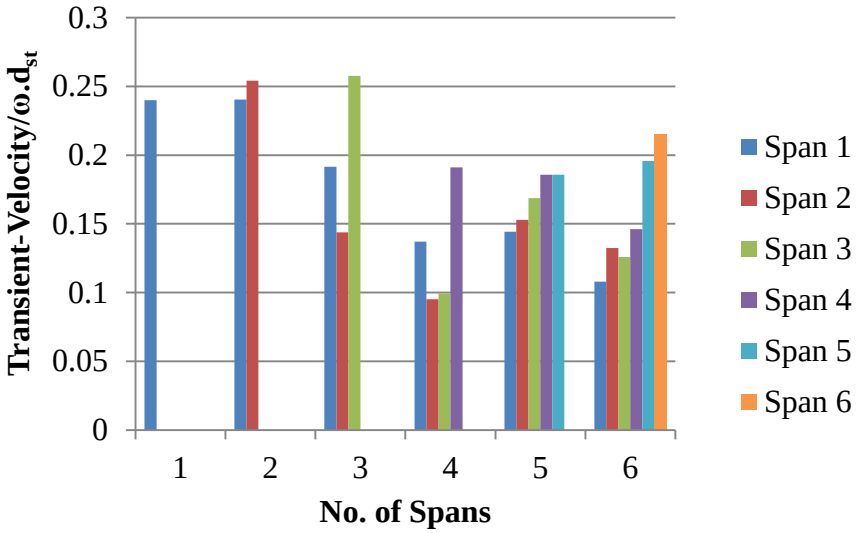

Figure 4.23 Transient dimensionless velocity for 1, 2, 3, 4, 5, and 6-span bridges.

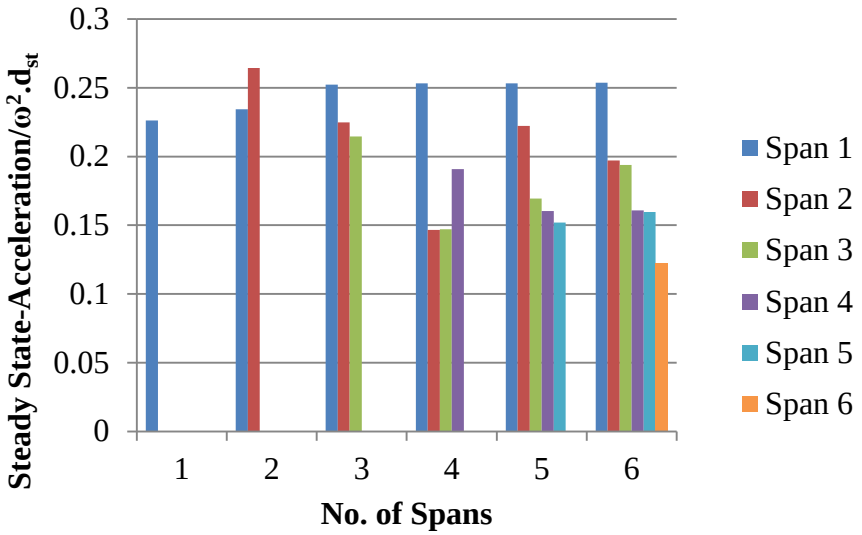

Figure 4.24 Steady state dimensionless acceleration for 1, 2, 3, 4, 5, and 6-span bridges.

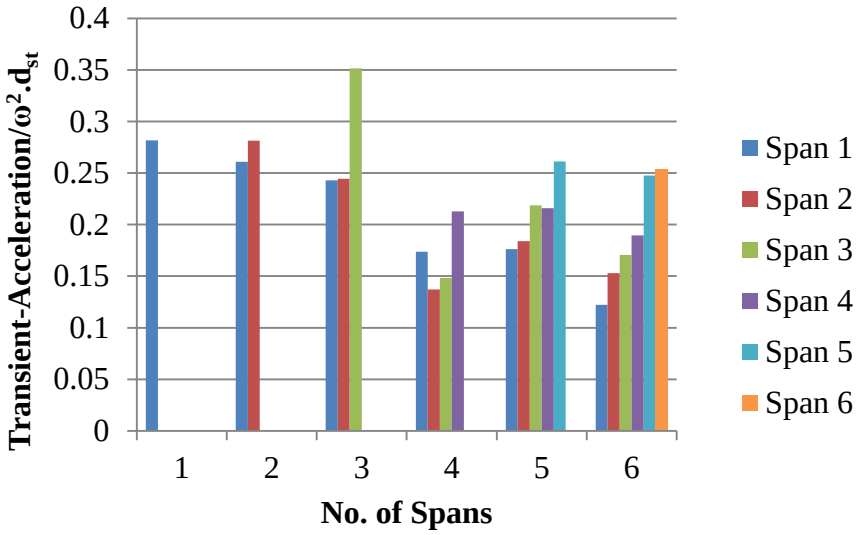

Figure 4.25 Transient dimensionless acceleration for 1, 2, 3, 4, 5, and 6-span bridges.

4.5 2-Dimensional vs. 3-Dimensional Models

Two-dimensional models are accurate to investigate the effect of those parameters that are not affected by the third dimension. Parameters such as stringer distances and bracing effect only can be investigated in three-dimensional models. Moreover, the effect of

elastomeric bearings on bridge dynamic response is investigated and compared with the results obtained by the equivalent spring supports in 2-D.

A sample bridge is investigated in both 2-D and 3-D. The bridge is similar to the actual existing bridge on Rt. 130 over Rt. 73 in New Jersey. However, some modifications have been made for finite element analysis. For example, the length was modified marginally in order to fit the considered element size. The length of the bridge is equal to 1590 inches total; 1577.28 inches center to center of the elastomeric bearings. The superstructure includes 5 stringers and 8 inches of concrete deck, on simply supported bearings (pin/roller). The stringers' dimensions and 3-D hexahedron solid elements are shown in Figure 4.26.

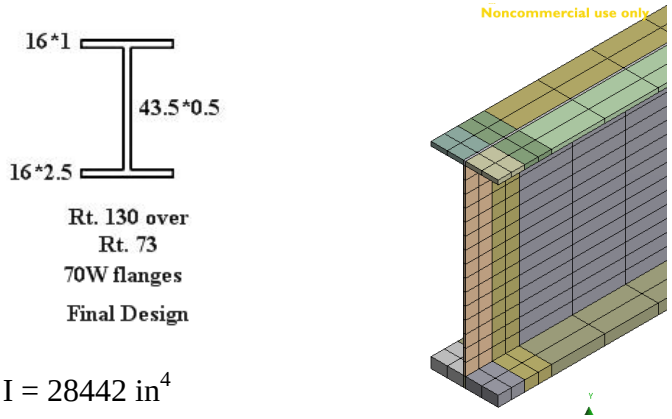

Figure 4.26 Stringers dimensions for the bridge on Rt. 130 over Rt. 73.

Mesh size, number of modes, time step, and time function have been selected so that accuracy of dynamic response is ensured. The element size and the load velocity are considered as 12.72 inches and 1272 in/sec. This consideration provides a time step of 0.01 seconds. The time function is triangular in which the load increases from zero to 40

kip in 0.01 seconds and then decreases from 40 kip to zero in another 0.01 seconds. This provides a smooth loading and unloading on each node/element. 3-D models were simulated by using solid elements for both the concrete deck and stringers. In 2-D models, only beam elements were used and the beam parameters such as moment of inertia, cross section area and weight were computed by considering one stringer with its proportional deck.

Only one axle load was considered in both 2-D and 3-D models. The dynamic response for 2-D model, using CsiBridge (SAP2000) software program, was compared to the 3-D model, using ANSYS software program. In order to validate the model, first a 3-D model with only one stringer was compared with the corresponding 2-D model. The loading on the 3-D model was defined as surface pressure and the tire contact area with the bridge is considered as a value close to the value provided by AASHTO LRFD (2007). As is mentioned in article 3.6.1.2.5 in AASHTO, "the tire contact area of a wheel consisting of one or two tires shall be assumed to be a single rectangle, whose width is 20.0 in. and whose length is 10.0 in". The contact area was considered as 16 inches wide and 12.72 inches long with the consideration of finite element modeling. The results for both static and dynamic loads in 2-D and 3-D are in agreement with each other. The results are shown in Table 4.3.

Table 4.3 One Stringer 3-D Model (Solid Element) vs. 2-D Model

	Theoretical	SAP 2-D	ANSYS 3-D
Frequency (Hz)	2.40	2.40	2.38
Static deflection (in)	3.96	3.98	4.03
Dynamic displacement (in)	–	4.57	4.60
Velocity (in/s)	–	18.93	18.94
Acceleration (in/s^2)	–	296.6	295

As can be seen, the type of loading in the 3-D model (surface moving pressure) seems reasonable and matches with the 2-D model. Therefore, it can be used for further investigation.

4.5.1 Stringer Spacing

To investigate the effect of stringer spacing, five stringers are considered with three different spacing values of 8, 10, and 12 ft. The results are compared with the 2-D model and shown in Table 4.4.

As can be seen, the natural frequency of 3-D models is 3-5% smaller than the corresponding theoretical value and 2D models. Static deflection is 25-35% greater than the corresponding 2-D and theoretical values. These are both due to the bridge flexibility in transverse direction, which is considered by AASHTO LRFD under distribution factor. However, the dimensionless dynamic responses in 2-D and 3-D models are nearly identical and the results obtained from the 2D model correspond to the expected dynamic response in 3D.

Table 4.4 Frequency and Static Deflection of 2D and 3D Models

	Theoretical	SAP 2-D	ANSYS 3-D
5 stringers with 8 ft distance	2.12 Hz 0.30 in	2.13 Hz 0.30 in	2.07 Hz 0.38 in
5 stringers with 10 ft distance	2.02 Hz 0.28 in	2.03 Hz 0.28 in	1.93 Hz 0.35 in
5 stringers with 12 ft distance	1.93 Hz 0.27 in	1.93 Hz 0.27 in	1.83 Hz 0.37 in

Figure 4.27 shows the time history displacement for three adjacent stringers in the 3-D model, including the loaded stringer. The loaded stringer is the one located under

wheel load, stringer 1 is the closest adjacent stringer to the loaded stringer and stringer 2 is the one adjacent to stringer 1.

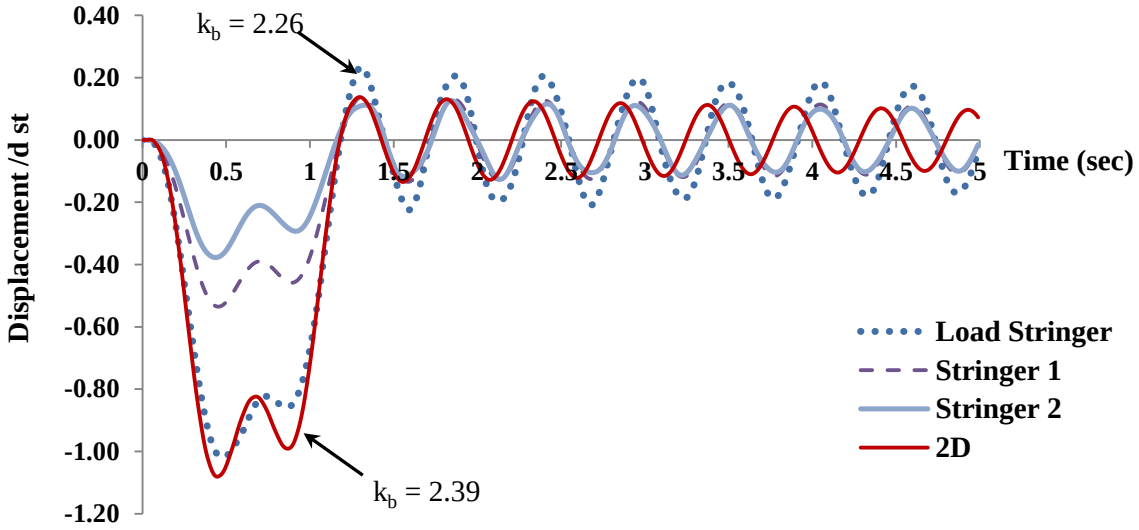

Figure 4.27 Dimensionless displacement response for the sample bridge with 5 stringers spacing at 12 ft.

As can be seen, the loaded stringer exhibits the maximum deflection and the response in 2-D is marginally more than 3-D in the steady state part of the vibration. As the bridge natural frequency is not identical in 2-D and 3-D due to the flexibility in transverse direction, the transient response varies, which is attributed to the change in k-parameter (k_b) from 2.39 in 2-D to 2.26 in 3-D. As it was mentioned before, the closer k_b is to an integer number, the higher the transient response is.

4.5.2 Effect of Bracing

Cross frames/bracing, which are primarily used to provide lateral stiffness on bridges, are also used to maintain stability of the bridge girders/stringers during construction and

pouring of deck slab. Diaphragms, comprised of either steel angles, channels or wide flange I-beams, serve the following important functions:

1. During construction, they serve as temporary members for bracing adjacent girders while maintaining the stability of girder flanges in compression during deck construction
2. Supporting utility pipes under the deck between girders
3. Resisting lateral wind/earthquake forces acting on superstructure
4. Prevent twisting of girder web and torsion under live load
5. Distribute dead loads and truck loads both to near and far girders

End diaphragms are located at the ends of girders to support the slab edge at bearing stiffeners. They are heavier than intermediate girders, due to greater shear force and reaction. To investigate the effect of bracing on bridge vibration, an actual bridge (Magnolia Bridge over Rt. 1 & 9) is simulated using 3-D models with bracing (Figure 4.28) and without bracing.

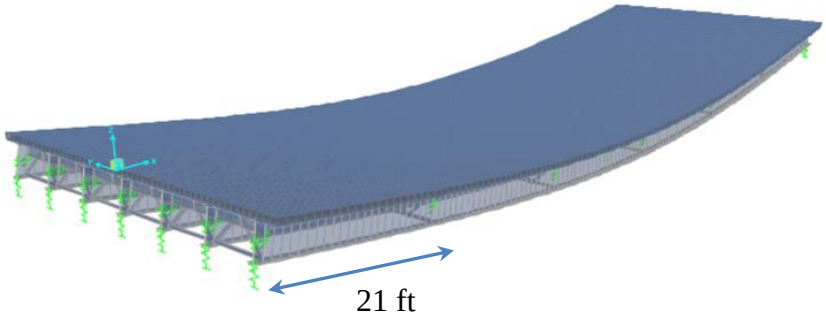

Figure 4.28 Three dimensional model for a sample bridge.

The number of stringers and stringer distances are varied from 4 to 7, and 6.5 ft to 12 ft, respectively. The bridge was subjected to the HL93 AASHTO truck load on one lane and modal dynamic analysis was performed in CsiBridge (SAP2000). Table 4.5 shows the results for this investigation. As can be seen, dynamic responses are nearly

identical for all cases with or without bracing, regardless of the distance between stringers. Therefore, transverse bracing does not affect bridge dynamic response.

Table 4.5 The Effect of Bracings on Bridge Dynamic Response

Magnolia bridge							
stringer distance	number of stringers	Cross frames	k	f (Hz)	displacement (in)	Velocity (in/sec)	Acceleration (in/sec^2)
6.5 ft	7	with bracing	2.72	1.996	0.855	2.14	20.45
		No bracing	2.73	2.004	0.893	2.24	20.174
7.8 ft	6	with bracing	2.62	1.928	0.901	2.32	14
		No bracing	2.63	1.936	0.935	2.41	15.79
9.75 ft	5	with bracing	2.51	1.842	0.946	2.57	18.83
		No bracing	2.52	1.849	0.972	2.63	19.285
12 ft	4	with bracing	2.36	1.731	0.989	2.93	22.3
		No bracing	2.36	1.737	0.999	2.95	24.27

4.6 Effect of Elastomeric Bearing

Elastomeric bridge bearings are either made of natural rubber (NR) or neoprene (polychloroprene). The differences between the two are usually not very significant. The shear modulus for these two materials is in the range of 80 to 180 psi. The shear stiffness of the bearing is the most important property of elastomeric bridge bearings, as it affects the forces transmitted between the superstructure and substructure. Elastomer compounds are designed, manufactured and tested in accordance to requirements with AASHTO M 251 which requires the minimum tensile strength to be 2250 psi (15.5 MPa) and the minimum ultimate elongation is 400%. The test results are with accordance with ASTM D 2240 and D 412.

4.6.1 Test Data

The purpose of this simulation is to find the effect of a typical elastomeric bearing on bridge dynamic response due to moving load. In this study, four sets of test data are considered for Natural Rubber (NR), namely: uniaxial tensile, biaxial, shear, and volumetric tests. These tests data were obtained from experimental studies by Yoshida et al. (2004), Amin et al. (2006) and Matsuda (2004) for Natural Rubber. Figures 4.29 to 4.31 show the results of these studies. The results of these three studies can be used to model the natural rubber elastomers in ANSYS software program. In order to model a nonlinear material and use its characteristics for dynamic analysis, a set of material stress strain curve is required. Based on this set of data, strain energy function can be developed and utilized in dynamic analysis.

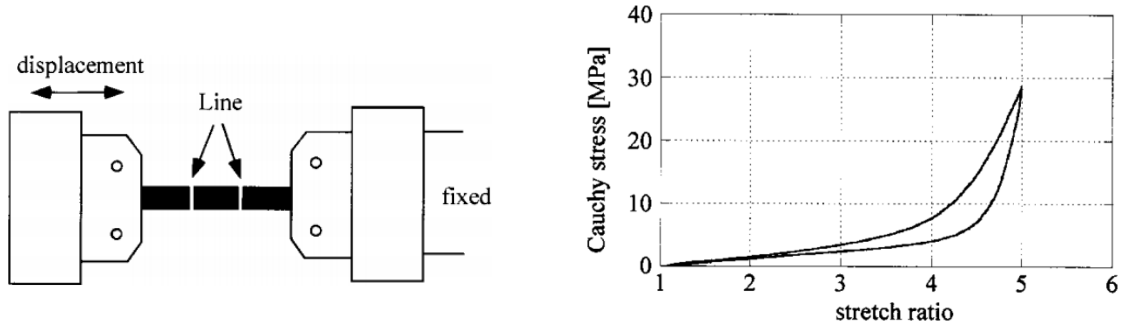

Figure 4.29 Uniaxial tensile test data (Yoshida et al. 2004), loading velocity 69.5 mm/min.

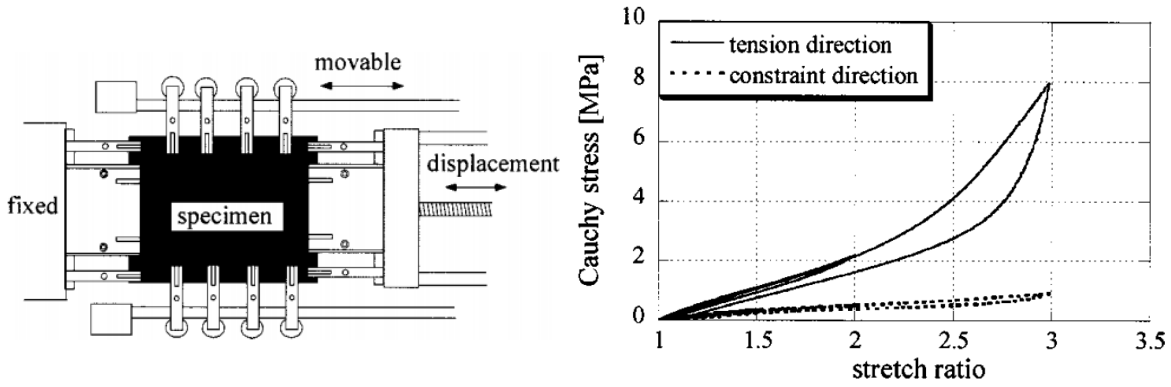

Figure 4.30 Biaxial tension test equipment and experimental data for NR (Yoshida et al. 2004).

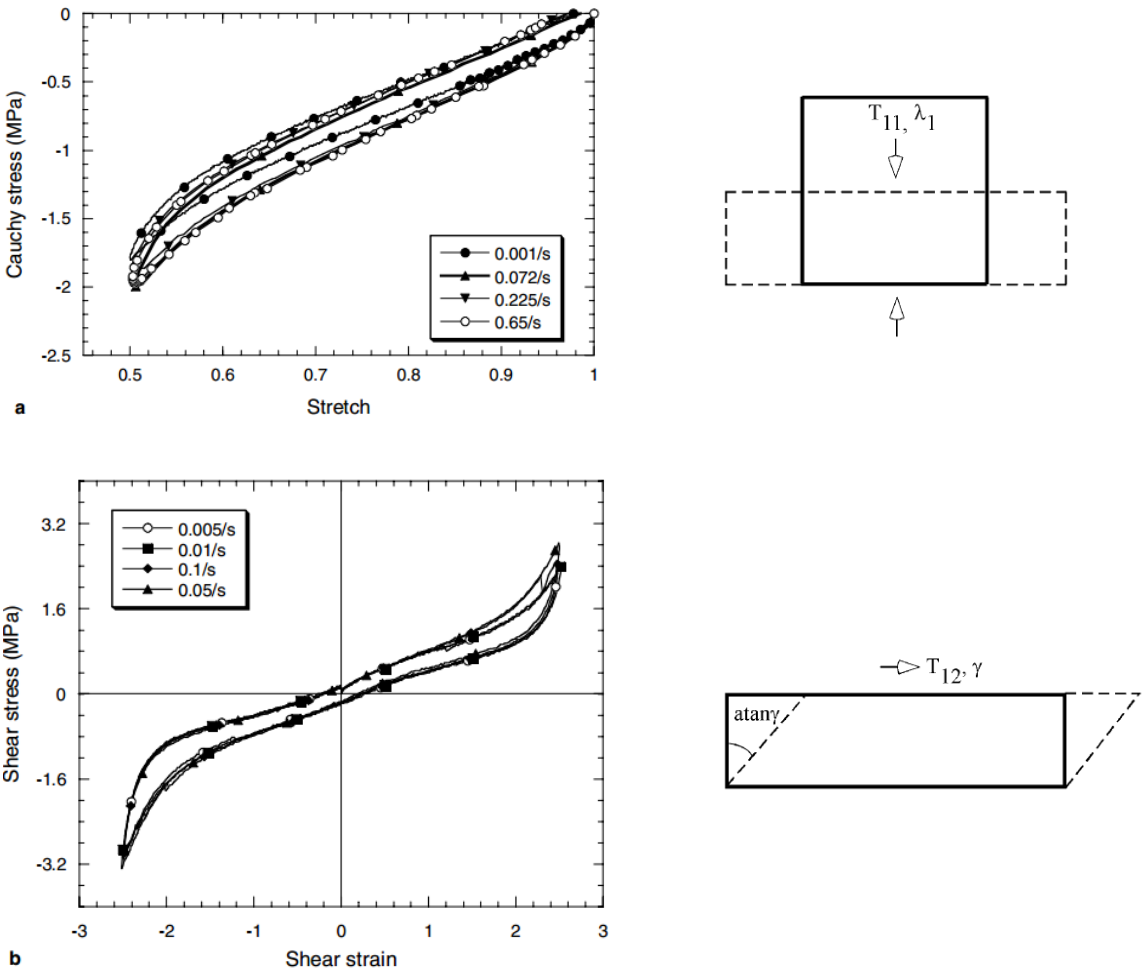

Figure 4.31 Compression test data (a) and simple shear test data (b) for NR and different strain rates (Amin et al. 2006).

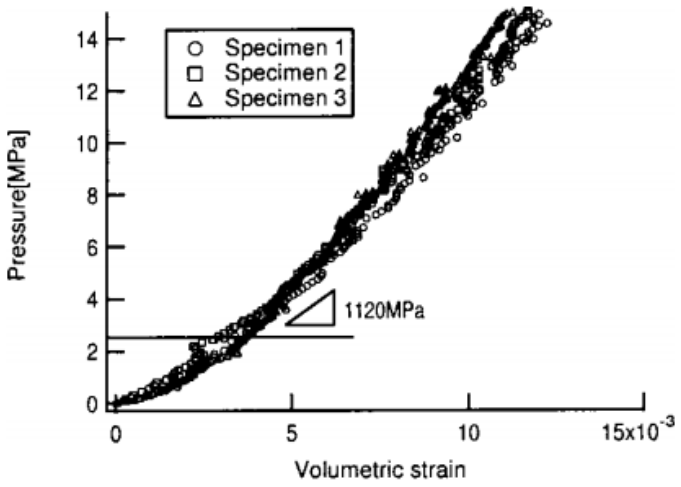

Figure 4.32 Volumetric test data for NR (Matsuda 2004).

Literature shows that energy dissipation in NR is negligible for low ranges of strain. It is reported that actual rubber materials are slightly compressible, and this property greatly affects the behavior of laminated rubber bearings (Takayama et al. 1992; Matsuda 2004). It is reported by Yoshida et al. (2004) that hysteretic energy loss only occurs in the high strain range, where the hardening is observed. Furthermore, NR is seen to almost recover its original shape even after a large deformation (Yoshida et al. 2004). However, in this study, a hyperplastic material model with both elastic and viscous parameters was selected to provide enough accuracy for dynamic analysis. For that, the visco-elastic characteristic of NR is considered in the material model, which requires test data from NR viscous behavior. Stress relaxation test data shows the change in shear modulus in the time domain.

The input data for modeling the viscoelasticity behavior of a material in the ANSYS software program is the relaxation time versus shear modulus. In the ANSYS software program, shear modulus is specified in the Prony series. In this study, only one

mode of the Maxwell model is used, since the experimental relaxation test data for Natural Rubber or Neoprene is not available in literature with more accuracy.

The test results corresponding to Natural Rubber relaxation data are provided by Amin et al. (2006). Shear relaxation of natural rubber is provided for various strain/stretch ranges (Figures 4.33 and 4.34).

Using the graph shown in Figures 4.33 and 4.34, the initial and final shear modulus from shear test data has been computed. The results show that the shear modulus decreased to 10% - 25% of the initial shear modulus after 500 seconds. Due to the lack of accuracy in relaxation measurement during a short time period (less than 5 seconds), the relaxation time for dynamic analysis is estimated as 5 seconds. This time refers to the time in which the material lost 63% of its total stiffness loss. Therefore, 25% shear modulus loss at 5 seconds relaxation time is considered for analysis.

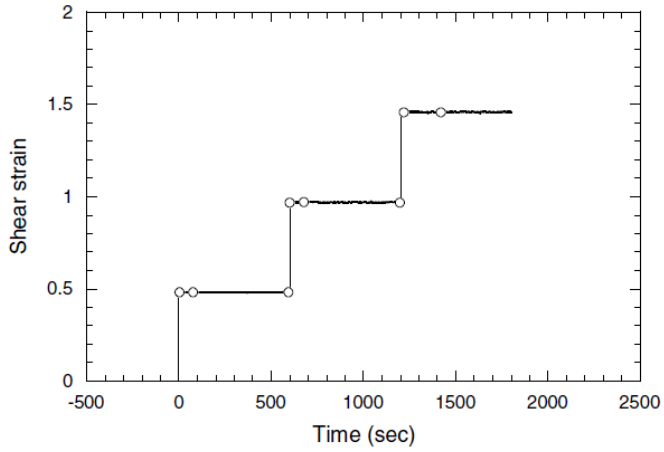

Figure 4.33 Applied strain (stretch) histories in multi-step relaxation tests for simple shear (Amin et al. 2006).

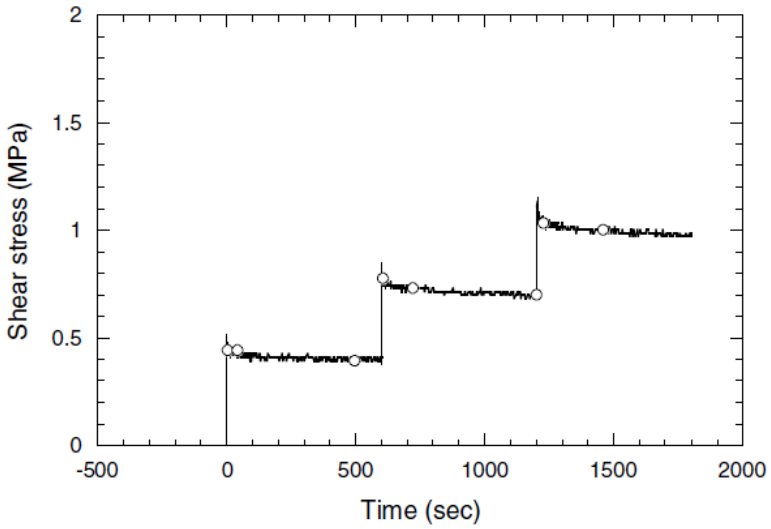

Figure 4.34 Stress history recorded in multi-step relaxation tests on Natural Rubber for simple shear (Amin et al. 2006).

4.6.2 Material Model

The material model used in the ANSYS software program is verified with test data provided by other studies. The specimens used for shear, tension and compression tests are modeled and finite element analysis is performed. The simple shear specimens (25 mm x 25 mm x 5 mm) have a net shear area of 25 mm x 25 mm (Amin 2006). For compression tests cylindrical specimens with 41 mm in height and 49 mm in diameter were used (Amin 2006). Uniaxial test specimens have the length, width, and thickness of 20 mm, 5 mm, and 2 mm, respectively. The tensile stress is applied on a 5 mm * 2 mm surface and the strain is measured through 20 mm length (Yoshida et al. 2004).

The material properties and the test data that are used for natural rubber matched AASHTO requirements, minimum ultimate stress of 2500 psi (17 MPa) and elongation at break of 400%. Yeoh strain energy function's parameters, C_{10}, C_{20}, C_{30} and D_n, are obtained through trial and error and the best curve is fit into the experimental data, Figure 4.35. The constants for this function are shown in Table 4.6.

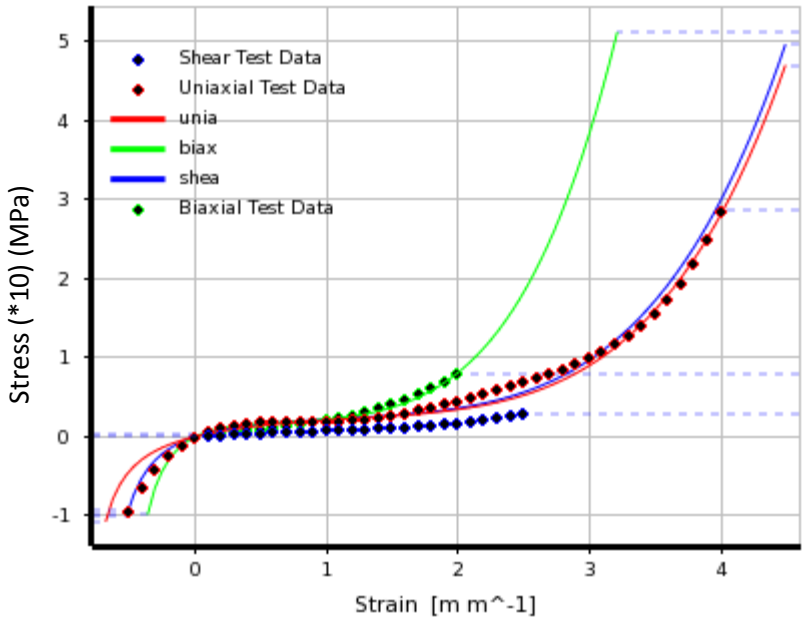

Figure 4.35 Yeoh strain energy function and test data.

Figures 4.36 to 4.38 show the compared FE results with test results. As can be seen, the FE material model is stiffer in tension and compression while it is softer in shear. The difference between test and FE results in uniaxial tension may be because of the dumbbell shape test specimens, while in FE models a rectangular box was used to model the specimen. However, tensile test results match with experiment for small ranges of tensile stress. Note that, an elastomeric bearing is only subjected to pressure and shear stresses when a bridge is loaded only by dead and live loads. In special cases where an earthquake or other specific loading types occur, the tensile behavior of elastomeric bearings may be of the interest.

Table 4.6 Material Constants for Yeoh Strain Energy Function

Material Constant			Incompressibility Parameter		
C_{10} (MPa)	C_{20} (MPa)	C_{30} (MPa)	D_1 (1/MPa)	D_2 (1/MPa)	D_3 (1/MPa)
0.392	-0.0224	0.0023	0.002669	6.12E-07	-5.92E-10

Considering compression and shear behavior of this hyperelastic model, the material model is reliable enough to continue the investigation for the effect of elastomeric bearings on bridge dynamic behavior under a moving truck.

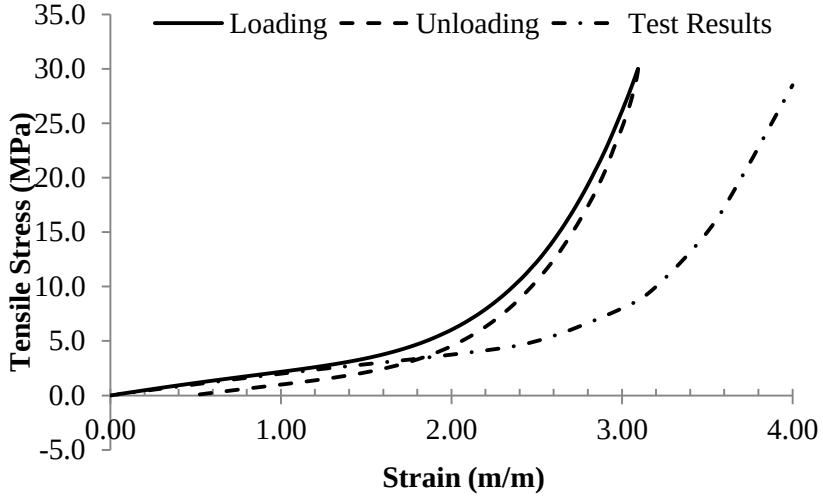

Figure 4.36 Uniaxial tensile FE model and test data.

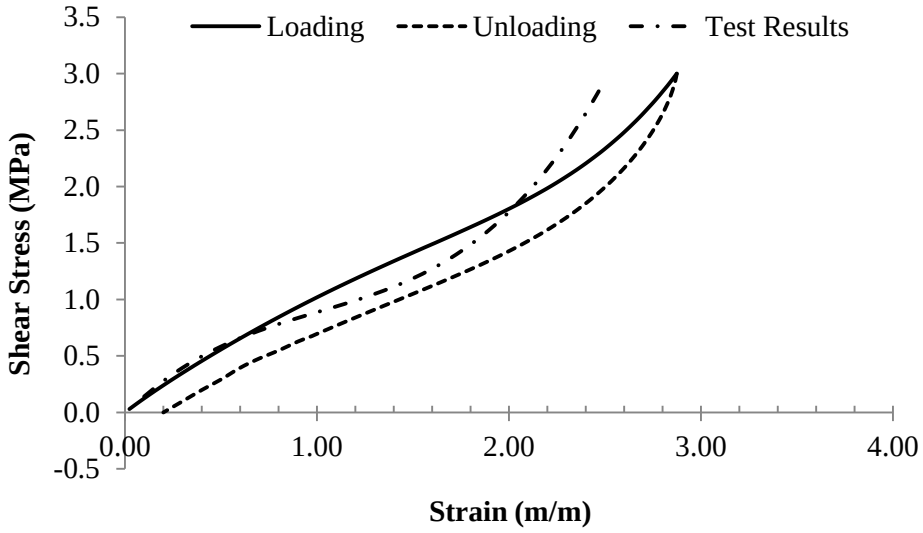

Figure 4.37 Simple shear test results.

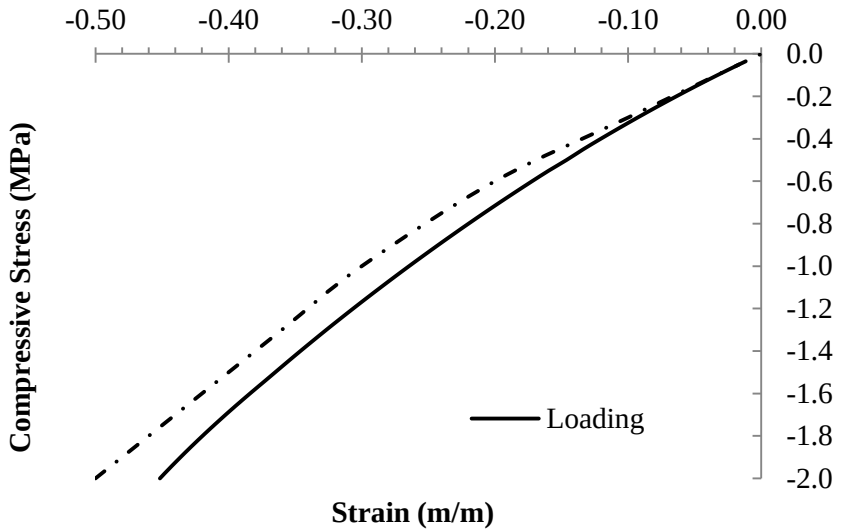

Figure 4.38 Compression test results.

4.6.3 Dynamic Response Due to Elastomeric Bearings

In this section, the effect of elastomeric bearing on bridge vibration is considered in 3-D models. Two bearing types were investigated in this dissertation. Bearing B1 is the actual designed bearing for Rt. 130 over Rt. 73 bridge with 9 layers 0.5 inch elastomer and the surface area of 12.72*16. Bearing B2 is assumed to have the same surface area but with 1 inch elastomer thickness. Bearings are subjected to a static pressure of 196.54 psi, which represents a 40 kip axle load acting on 12.72 in * 16 in stringer area. The tire contact area matches the contact area suggested by AASHTO. AASHTO suggests an area of 200 squared inches for tire contact surface with the bridge.

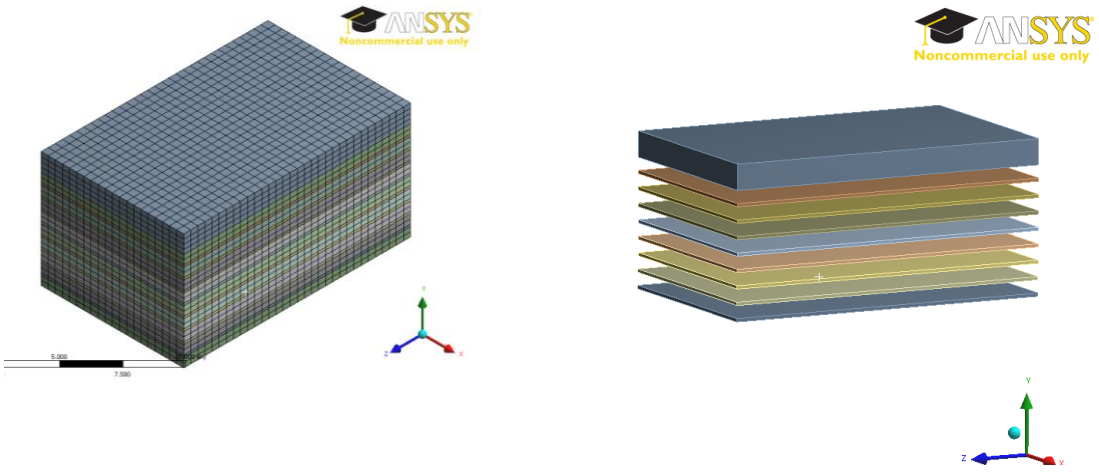

Figure 4.39 Model of elastomeric bearing B1.

Static analysis is performed to obtain the bearing deformation under various pressures. Compressive modulus (E_c) is computed and compared with the value suggested by AASHTO LRFD (2007), which is mentioned in article C14.6.3.2-1 and shown in Equation 4.34.

$$E_c = 6GS^2 \tag{4.34}$$

Where S is the shape factor of the thickest layer of an elastomeric bearing, and G is the shear modulus of the elastomer.

Shape factor is defined as the ratio of the surface area or plane area of one loaded face to the area free to bulge around the perimeter of one internal elastomeric layer of the pad.

$$S = \frac{L_s \times W_s}{2h_{ri}(L_s + W_s)} \tag{4.33}$$

In Equation 4.33, L_s and W_s are the length and width of the bearing, respectively and h_{ri} is the thickness of elastomer number i.

By considering shear modulus values in the range of 80 to 180 psi, E_c can be computed as:

$$S_1 = \frac{12.72 * 16}{2 * 0.5 * (16 + 12.72)} = 7.17 \quad (4.35)$$

$$E_c = 6 * G * (7.17)^2 = 301.3\, G = 24{,}104 \ \ to\ 54{,}234\, psi \quad (4.36)$$

The compressive stiffness can be also obtained from FE analysis for compressive pressure. Figure 4.40 shows the stress-strain graph. E_c can be obtained from the secant tangent of this graph. This value is equal to 24,117 psi which is within the range of the values predicted by AASHTO.

For elastomeric bearing B_2, the corresponding shape factor and E_c using AASHTO equation can be obtained as follows:

$$S_2 = \frac{12.72 * 16}{2 * 1 * (16 + 12.72)} = 3.54 \quad (4.37)$$

$$E_c = 6 * G * (3.54)^2 = 75.2\, G = 6{,}016 \ \ to\ 13{,}536\, psi \quad (4.38)$$

The value of E_c from finite element model (Figure 4.40) is equal to 10,335 psi, which falls into the range suggested by AASHTO in Equation 4.38.

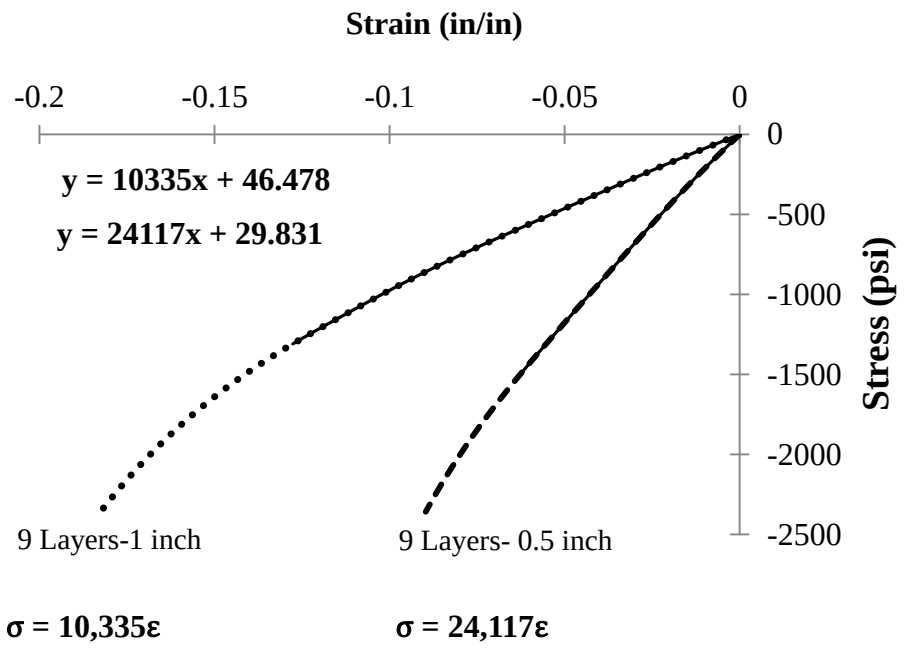

Figure 4.40 Compressive stiffness of elastomeric bearing B1.

The actual bridge investigated earlier, Rt. 130 over Rt. 73 (Figure 4.26), is studied for the effect of both elastomeric bearings B_1 and B_2. The stringer is subjected to a single axle moving load of 40 kip and the dynamic response for 1% damping ratio is examined. The results are compared to 2-D models with rigid supports, flexible 1 DOF spring supports, and linear spring supports distributed within 12.72 in (Figure 4.41).

For B1, the computed values for linear spring stiffness and single spring are shown in Equations 4.39 and 4.40.

1 DOF: $K_s = E_c . A_s / L_s = 24{,}117 * (12.72*16)/(9*0.5) = 1090$ kip/in (4.39)

Linear Spring Supports: $K_{ls} = K_s / L_s = 1090/12.72 = 85.70$ kip/in/in (4.40)

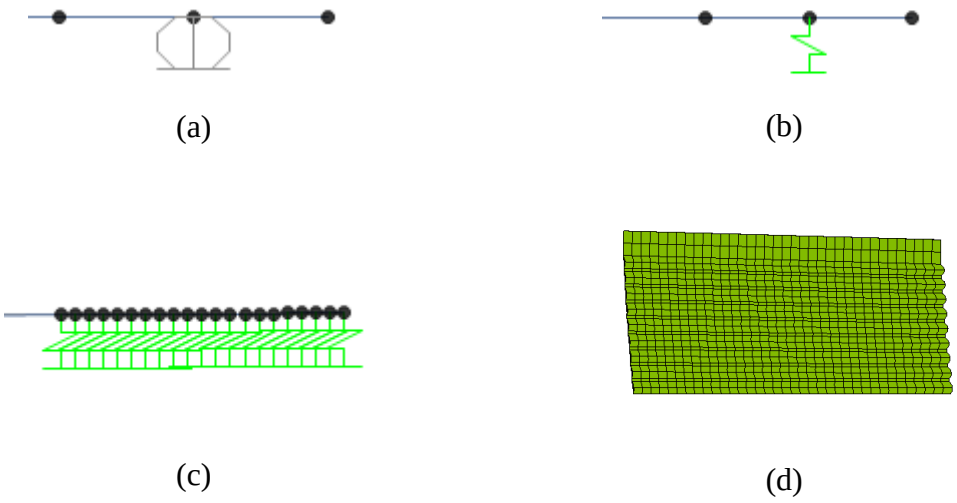

Figure 4.41 Different types of support conditions (a) rigid support, (b) spring support, (c) linear spring, (d) elastomeric bearing.

For B2 elastomeric bearing, the computed springs' stiffness for linear and single spring are as follows.

1 DOF: $K_s = E_c . A_s/L_s = 10{,}335 * (12.72*16)/(9*1) = 234$ kip/in (4.41)

Linear Spring Supports: $K_{ls} = K_s/L_s = 234/12.72 = 18.4$ kip/in^2 (4.42)

The maximum dynamic response for these four different models is shown in Table 4.7 and 4.8 for both types of elastomeric bearing, B1 and B2. The results show that for these two bridges, the 2-D models with an equivalent spring support lead to satisfactory results. For bearing B1, which is stiffer than B2, the dynamic results with elastomeric bearing are nearly identical to the results of the simply supported beam. For B2 bearing, which is softer than B1, acceleration and velocity are slightly higher than the simply supported bridge, while the impact factor is identical.

Table 4.7 Bridge Dynamic Results with Elastomeric Bearing B1, $k_b = 2.98$

K_s = 1090 kip/in	bearing with Ec = 24,117 psi			
	f (Hz)	dis/d_{st}	$vel/\omega.d_{st}$	$acc/\omega^2.d_{st}$
3-D bearing	2.40	1.14	0.31	0.35
Rigid Support	2.40	1.15	0.32	0.33
Single Spring Support	2.39	1.15	0.31	0.37
Line Spring Support	2.40	1.15	0.33	0.87

Table 4.8 Bridge Dynamic Results with Elastomeric Bearing B2, $k_b = 2.89$

K_s = 234 kip/in	bearing with Ec = 10,335 psi			
	f (Hz)	dis/d_{st}	$vel/\omega.d_{st}$	$acc/\omega^2.d_{st}$
3-D bearing	2.33	1.15	0.37	0.60
Rigid Support	2.40	1.15	0.32	0.33
Single Spring Support	2.34	1.14	0.39	0.54
Line Spring Support	2.35	1.14	0.39	0.89

For these two bridges with their elastomeric bearing supports, the ratio of beam stiffness to bearing stiffness, stiffness ratio (k_r), is computed. The bridge to bearing stiffness ratio (k_r) for a bridge (Yang et al. 2004) is defined as:

$$k_r = \frac{EI\pi^3}{K_s {L_b}^3} \tag{4.43}$$

Where, k_r is the stiffness ratio, E is the modulus of elasticity, I is the moment of inertia, K_s is the spring support stiffness, and L is the bridge span length. It is reported by Yang et al. (2004) that the bridge response is identical to the response for simply supported bridge when k_r is very small. For larger values of k_r the effect of resonance is more sever for some specific speed parameters. The computed stiffness ratio for B1 and B2 bridges is very small. These ratios are computed as follows:

$$k_{r\ (B1)} = \frac{29000*28442*\pi^3}{1090*1577^3} = 0.006$$

$$k_{r\ (B2)} = \frac{29000*28442*\pi^3}{234*1577^3} = 0.028$$

If the same investigation is performed for a bridge with 460 in. span length while E, I, and V are kept the same as B1 and B2 bridges, stiffness ratio would be equal to:

$$\text{Stiffness Ratio-460}_{\ (B3)} = \frac{29000*28442*\pi^3}{1090*460^3} = 0.244$$

Stiffness ratio indicates the ratio of bearing deflection to bridge deflection and for most of the bridges, this ratio is less than 0.3. Therefore, considering 0.244 for k_r is a reasonable value for highway bridges. Table 4.9 shows the results obtained from 2D and 3D models. As can be seen, the results from spring support model no longer match the results of 3D elastomeric bearing models. The acceleration results for spring supports are significantly higher than the actual results obtained from 3-D models. Therefore, the equivalent spring support cannot provide appropriate dynamic results for higher values of k_r.

Table 4.9 Bridge Dynamic Results with Elastomeric Bearing B3, k_b = 7.34

Ks = 1090 kip/in	bearing with Ec = 24,117 psi			
	f (Hz)	dis/d_{st}	vel/$\omega.d_{st}$	acc/$\omega^2.d_{st}$
3-D bearing	20.3	1.14	0.29	0.28
Rigid Support	27.7	1.03	0.12	0.15
Single Spring Support	24.3	1.14	0.34	0.92

Bridge k-parameters for B1 and B2 are 2.97 and 2.89, respectively, while k_b for B3 is equal to 7.3. The smaller values of velocity and acceleration responses in B3 bridge as compared to B1 and B2 bridges are due to the larger value of k_b. As was shown in previous sections, higher k_b for one axle loading results in smaller dynamic responses.

If k_b in B3 bridge is altered by varying the bridge mass, dynamic responses can be graphed for different values of k_b and can then be compared with the results of simply supported bridge. Figures 4.42 to 4.44 show the dynamic response of bridges with different k_b and two extreme values of k_r, $k_r = 0.03$ and $k_r = 0.244$.

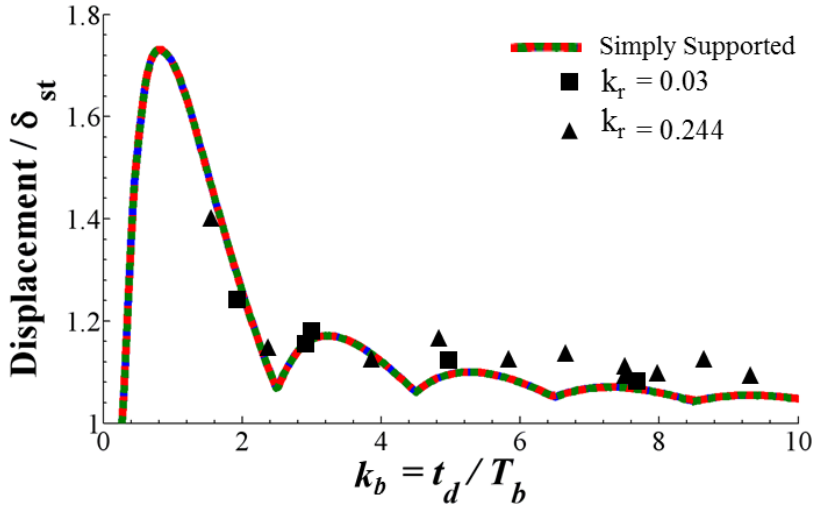

Figure 4.42 Dimensionless displacement for simply supported bridge and elastomeric bearing with stiffness ratios of 0.224 and 0.03.

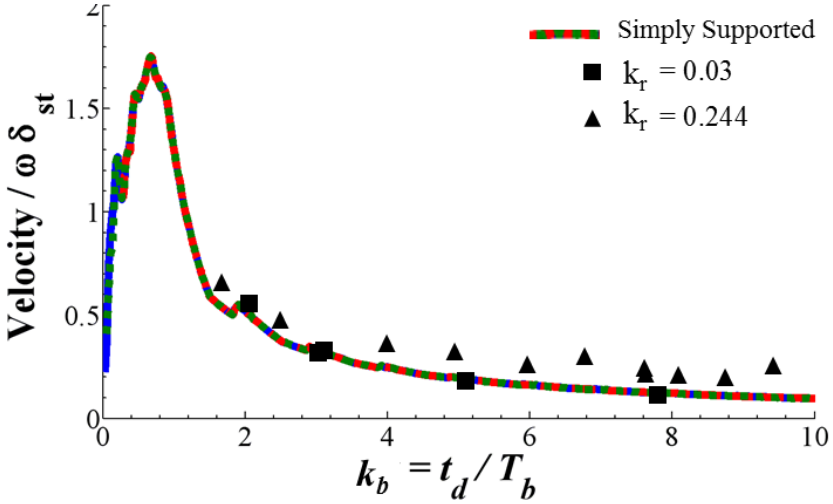

Figure 4.43 Dimensionless velocity for simply supported bridge and elastomeric bearing with stiffness ratios of 0.224 and 0.03.

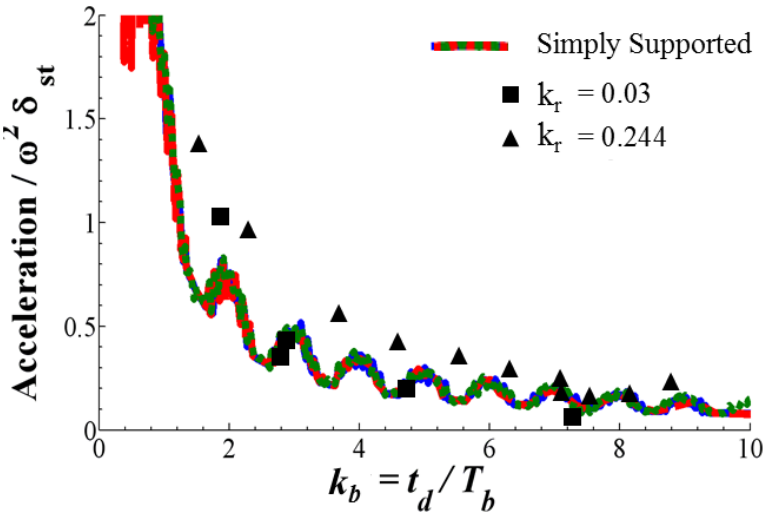

Figure 4.44 Dimensionless acceleration for simply supported bridge and elastomeric bearing with stiffness ratios of 0.224 and 0.03.

As can be seen, stiffness ratio affects bridge response to some extent. However, the response increases not more than 0.1 for displacement and velocity. The acceleration response increases about 0.3 in some cases. It is apparent that for larger values of k-parameter, acceleration is less influenced by stiffness ratio and bearing stiffness.

A more flexible superstructure design and stiffer sub structure design in vertical direction would decrease the bridge to bearing stiffness ratio and the effect of bearing flexibility to bridge dynamic response can be reduced

CHAPTER 5

STRUCTURAL PERFORMANCE

5.1 Fatigue Problem Due To Vibration

Fatigue is the active structural damage that occurs when a material is subjected to repeated loading and unloading. The stresses due to cyclic loading are less than the ultimate stress limit and may be below the yield point of the material. When the stresses are above a certain threshold, microscopic cracks may appear locally where the stress concentration exists. When loading and unloading condition is continued, the cracks sizes will increase and eventually the structure will collapse. The higher the stress ranges, due to cyclic loadings, the lower the fatigue life.

Sharp corners, the edges that separate different cross sections throughout a member, notches, welded areas, and material rough surfaces lead to stress concentration, which causes fatigue damage. Some manufacturing processes involving heat or deformation, such as casting, may produce shrinkage voids which initiate fatigue cracks inside the material. Cutting and welding can also produce a high level of residual tensile stresses that decrease fatigue life.

Structures with high cycles of vibration are more sensitive to fatigue failure. The fatigue criterion in AASHTO Specifications is based on experimental data and it is about five decades old. Since bridge vibration is significantly affected by other parameters such as k-parameters, k_b, k_v ($k_b = Lf/V$, $k_b = L_v.f/V$), and damping ratio (ζ), these parameters have to be taken into account for fatigue calculations. In this chapter, it is shown that

bridges with specific k-parameters and low damping ratio risk the possibility of fatigue failure after 10 years while they are designed for a 75-year fatigue life by AASHTO.

5.1.1 Fatigue Loads

The worst case of fatigue loading is the case known as fully reversing load in which a tensile stress of some value is applied to an unloaded part and then released; then a compressive stress of the same value is applied and released; and this process continues until the failure occurs. Since the bridge self-weight causes constant stresses, the fatigue failure on bridges cannot be of this kind.

Other types of fatigue loads are less severe but not negligible. When the transient part of the vibration is considerably high in amplitude, fatigue due to the transient part of the vibration should be also taken into account. Figure 5.1 shows different types of fatigue loading. The loading shown at the left side of the graph is more similar to the one that occurs in bridges due to the vibration caused by live load.

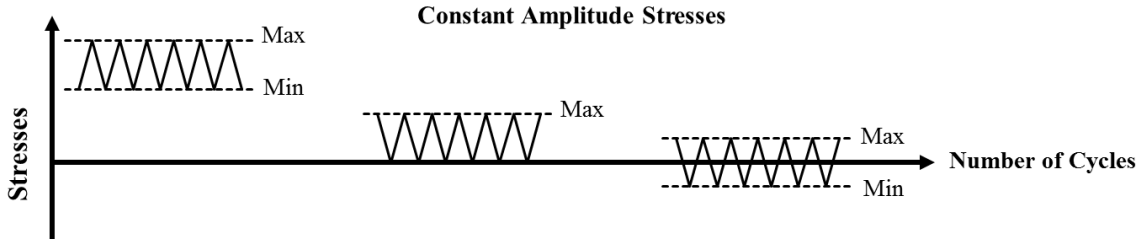

Figure 5.1 Types of fatigue loads.

Bridges fatigue stresses under moving truck loads cannot be simplified as a single stress range as shown in Figure 5.1. The stresses vary with respect to different k-parameters and truck types. Figure 5.2 shows the bridge time history response when a

three-axle truck passes over a short span bridge. The stresses increase when the 1st two axles enter the bridge, and the stresses decrease when the 1st two axles exit the bridge. Consequently, when the rear axle enters the bridge, the stresses increase and then decrease until the rear axle also exits the bridge.

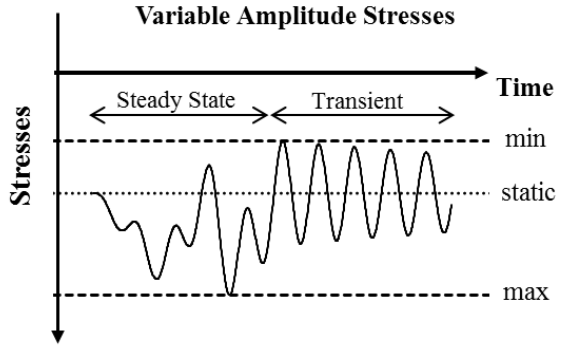

Figure 5.2 Variable stress range in bridge response due to a truck.

As can be seen in Figure 5.2, the stresses in the steady state part of the vibration do not fluctuate as much as they do in the transient part of the vibration. Since the fatigue life depends on the number of cycles and the range of stresses, neglecting the transient part of the vibration leads to overestimating the fatigue life.

5.1.2 AASHTO LRFD Fatigue Criteria

The first fatigue criterion was introduced in the 1965 Specifications. Revisions were made in 1971 and 1974 based on experimental data. In LRFD Specifications, fatigue limit state is used to calculate fatigue stresses and only one truck is considered in the calculation. The design is based on an expected 75 year structure life and one to two cycles of vibration per truck is considered in calculations. Nominal fatigue resistance is taken as:

$$(\Delta F)_n = (\frac{A}{N})^{\frac{1}{3}} \geq \frac{1}{2}(\Delta F)_{TH} \quad (5.1)$$

Where:

$(\Delta F)_n$ = Allowable fatigue stress.

N = Number of cycles the structure is subjected to the truck load for a 75 year design life. N can be calculated as:

$$N = (365)\,(75)\,n\,(ADTT)_{SL} \quad (5.2)$$

$(ADTT)_{SL}$ = Single-lane Average Daily Truck Traffic.

A= Detail category constant in ksi (Table 5.1)

$(\Delta F)_{TH}$ = Constant amplitude fatigue thresholds in ksi (Table 5.1).

n = Number of cycles per truck passage (for span length shorter than 40 ft, n=2. For span length larger than 40 ft and near interior continuous supports, n=1.5, otherwise, n = 1).

Table 5.1 Fatigue Constant A and Threshold Amplitude for each Detail Category

Detail Category	Detail Category Constant A (* 10^8 ksi^3)	Constant-Amplitude Fatigue Thresholds (ksi)
A (Rolled beams and base metal)	250.0	24.0
B (Welded girders)	120.0	16.0
B' (See AASHTO LRFD)	61.0	12.0
C (stiffeners and short 51 mm attachments)	44.0	10.0
C' (See AASHTO LRFD)	44.0	12.0
D (102 mm attachments)	22.0	7.0
E (cover plated beams)	11.0	4.5
E' (See AASHTO LRFD)	3.9	2.6
A325 Bolts	17.1	31.0
A 490 Bolts	31.5	38.0

The fatigue limit values computed by Equation 5.1 are also graphed in Figure 5.3. Noting that rolled beams and base metal are in Category A, welded girders are in

Category B and B', stiffeners and short 2 inch attachments are in Category C, 4 inch attachments are in Category D, and cover plated beams are in Category E and E'.

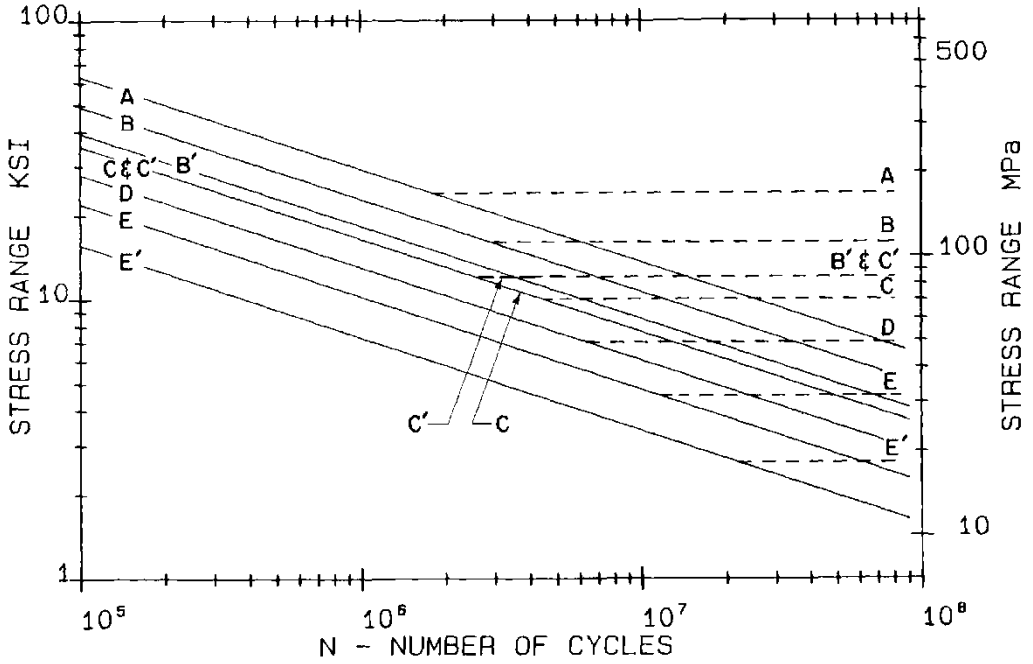

Figure 5.3 S-N curve and threshold limits for each design category (AASHTO LRFD).

In fatigue design calculations, AASHTO design truck HL-93 with a constant spacing of 30.0 ft between the rear and middle axles is considered. The design truck is considered on one interior stringer and distribution factor is applied. Live load factor for the design truck is less than 1, because the fatigue damage due to a small number of heavy trucks is relatively less than the fatigue damage due to a large number of lighter trucks. Therefore, the live load factor in AASHTO Specifications is equal to 0.75 of the design truck (low stress and high cycles loading). If the rear and middle axle weights of the HL-93 truck are multiplied by the fatigue live load factor of 0.75, the middle and rear axle weight of NJ122, which is used as the most common truck in this study, is obtained as follows:

$$32 \text{ kips} * 0.75 = 24 \text{ kips} \quad (5.3)$$

Note that, live load impact factor is equal to IM = 0.15 and multiple presence factor (m) is neglected for fatigue limit state.

5.2 Analytical Studies on Fatigue

As it was shown in Chapter 4, the bridge response in the transient part of the vibration is a variable of k_b and k_v. Noting that, the live load stress range in the steady state part of the vibration is equal to the maximum live load stress in the steady state part of the vibration. The stress value does not fluctuate much in the steady state part of the vibration (see Figure 5.2). However, in the transient part of the vibration, the live load stress range is twice as much as the maximum live load stress in the transient part of the vibration, considering the vibration fluctuation around the static equilibrium. Figure 5.4 shows the ratio of transient response to steady state response for live load stress range. The values in this graph were obtained from Figure 4.13, which was discussed in Chapter 4.

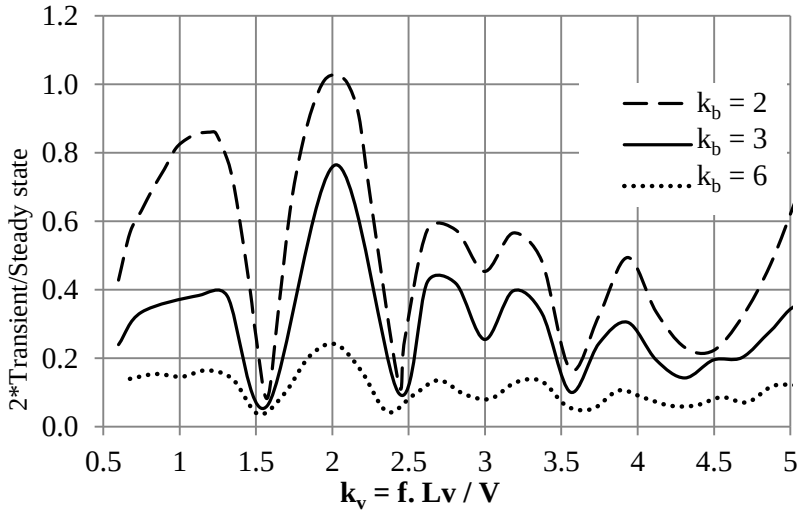

Figure 5.4 Stress range for the transient with respect to the steady state part of the vibration.

The number of vibration cycles per truck passage, considered by AASHTO, is 1 for long span bridges and 2 for short span bridges (Table 5.2); therefore, the effect of the transient part of the vibration was not considered in AASHTO fatigue criteria.

Table 5.2 Number of Vibration Cycles per Truck by AASHTO

Span Length	Simple span	Continuous span	
		not near interior support	near interior support
span > 40 ft	1	1	1.5
span < 40 ft	2	2	2

When span length is less than 40 ft, the truck length exceeds the span length (30+14>40). At the time that the last axle enters the bridge the first axle has already left the bridge and the second axle is also about to exit. Therefore, one truck causes two vibration cycles in the steady state part of the vibration. As can be seen, in Figure 5.2, the fluctuation during the steady state part of the vibration contains two cycles. However, the stress fluctuation is much more in the transient part of the vibration and can significantly affect fatigue life.

The number of cycles that should be taken into account for each truck depends on both the steady state and the transient parts of the bridge vibration. Thus, all the stress ranges greater than threshold limit should be taken into account, whether they are in the steady state or the transient part of the vibration. For this, the complex stress range shown in Figure 5.2 should be reduced to a series of simple cyclic stresses. Then a histogram of cyclic stresses should be created to form a fatigue damage spectrum. For each stress level, the degree of cumulative damage incurred from the S-N curve (Figure 5.5) should

be calculated. Finally, Miner's rule can be used to combine the individual contribution of each stress level.

The Miner's rule states that where there are k different stress magnitudes in a spectrum, S_i ($1 \leq i \leq k$), each contributing n_i cycles, then if N_i is the number of cycles to failure for each stress range (Figure 5.5), failure occurs when:

$$\sum_{i=1}^{k} \frac{n_i}{N_i} = C \tag{5.4}$$

C is experimentally found to be between 0.7 and 2.2. Usually for design purposes, C is assumed to be 1.

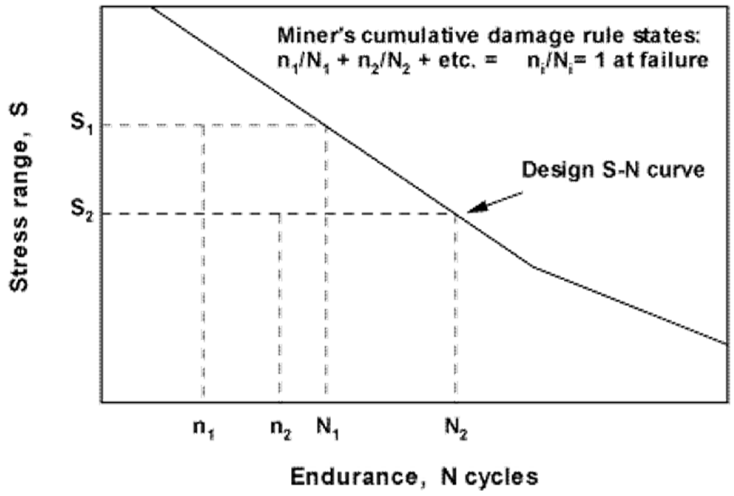

Figure 5.5 Stress range spectrum and S-N curve to find out the cumulative damage due to each stress range (Maddox 2003).

Assuming that the maximum stress in the steady state part of the vibration, due to the most common truck weight, is equal to f_{ss}, the cumulative damage due to the transient part of the vibration can be calculated. Table 5.3 shows the computed values of Transient Cumulative Damage (TCD) for k_v equal to 2 and various k_b and damping ratios. The ratio of $f_{transient}$ / f_{ss} is obtained from Figure 5.4 for each k-parameter. The values of cumulative

damage due to the transient part of the vibration are expressed as a percentage of the amount of damage due to the stresses in the steady state part of the vibration. As can be seen, the transient part of the vibration significantly affects fatigue life for k_b up to 4 and smaller damping ratios.

Table 5.3 Cumulative Damage Due To Transient Part of the Vibration (TCD) for k_v =2

k_b	$f_{transient} / f_{ss}$	Damage due to the transient part of the vibration with respect to the damage due to steady state stresses -TCD (%)				
		ζ=1%	2%	3%	4%	5%
2	1.05	672	369	268	219	190
3	0.75	245	134	98	80	69
4	0.50	73	40	29	24	20
5	0.35	25	14	10	8	7
6	0.25	9	5	4	3	3
7	0.15	2	1	1	1	1
8	0.10	1	0	0	0	0

To understand the values stated in Table 5.3, the case of k_b = 3, k_v = 2 with 3% damping ratio is explained in detail. Noting that the cumulative damage due to the transient part of the vibration for this case is equal to 98%. This percentage shows that the transient part of the vibration may increase the damage up to 98% of the value calculated by AASHTO, which only represnets the stress ranges in steady state part of the vibration. When the cumulative damage is increased to 1.98 of the damage due to steady state stresses, the fatigue life is decreased by 1/1.98 = 50%, from 75 years to 37.5 years.

$$\left(\sum \frac{n_i}{N_i}\right)_1 = C \tag{5.5}$$

$$\left(\sum \frac{n_i}{N_i}\right)_2 = 1.98\,C \quad \rightarrow \quad \left(\sum \frac{n_i}{N_i}\right)_2 . \frac{1}{1.98} = \left(\sum \frac{50\% n_i}{N_i}\right)_2 = C \tag{5.6}$$

To consider the amount of damage caused by all stress ranges above the threshold limit in the transient part of the vibration, the stress range in each cycle should be calculated. Stress reduction per each cycle can be calculated using Equation 5.7, where j is the number of cycles, ζ is the damping ratio, u_i is the stress range amplitude at the first cycle, and u_{i+j} is the stress range amplitude after j cycles.

$$j = \frac{1}{2\pi\zeta} \ln \frac{u_i}{u_{i+j}} \tag{5.7}$$

For one cycle, j =1, the stress is damped out to 82.82% of the initial value when damping ratio is equal to 3%.

$$\ln \frac{u_i}{u_{i+j}} = 2\pi.\zeta.j \rightarrow \frac{u_i}{u_{i+1}} = e^{2\pi.\zeta.1} = e^{2\pi*0.03*1} \rightarrow u_{i+1} = 0.8282\, u_i \tag{5.8}$$

Assuming that the maximum stress in the steady state part of the vibration is equal to f_{ss}, for k_b and k_v equal to 3 and 2, respectively, the stress range ratio at the first cycle of the transient part of the vibration is equal to 0.75 f_{ss} (Figure 5.4). If N_1 cycles are required to result in failure for the stress range equal to f_{ss}, the number of cycles which results in failure for a stress range equal to 0.75 f_{ss} can be obtained using the following equation:

$$\text{Stress} = \left(\frac{A\ constant\ based\ on\ \text{the}\ detail\ categories}{Number\ of\ Cycles}\right)^{\frac{1}{3}} \tag{5.9}$$

$$\text{Number of Cycles} \sim \frac{1}{Stress^3} \tag{5.10}$$

Hence, it takes ($1/0.75^3$) N_1 cycles for the bridge to exhibit fatigue failure under a stress range equal to $0.75f_{st}$. the stress in the second cycle of transient vibration is 82% of the stress in the first cycle, and equal to 0.75* 82% f_{ss}. Since the number of cycles , which result in failure, is inversely proportional to the cube of stress range, the number of cycles required to result in fatigue failure for a stress range equal to 0.82 * 0.75* f_{ss} , is equal to ($\frac{1}{0.8282^3} * \frac{1}{0.75^3} N_1$). The number of cycles to failure for each stress range in the transient part of the vibration is calculated and shown in Table 5.4.

Table 5.4 Number of Cycles to Fatigue Failure for $k_b = 3$, $k_v = 2$ and $\zeta = 3\%$

Cycle in Transient Part	Stress range	Number of cycles required to cause failure (N)
1st	$f_{1\ (transient)} = 0.75f_{ss}$	$\frac{1}{0.75^3} N_1$
2nd	$f_{2(transient)} = 0.8282 * 0.75f_{ss}$	$\frac{1}{0.8282^3} * \frac{1}{0.75^3} N_1$
3rd	$f_{3(transient)} = 0.8282^2 * 0.75f_{ss}$	$\frac{1}{0.8282^{3*2}} * \frac{1}{0.75^3} N_1$
….	…….	……..
λ^{th}	$f_{\lambda(transient)} = 0.8282^{\lambda-1} * 0.75f_{ss}$	$\frac{1}{0.8282^{3*(\lambda-1)}} * \frac{1}{0.75^3} N_1$

Accordingly, the cumulative damage in the transient part of the vibration can be computed as the sum of all damages due to all stress ranges above the threshold limit, $f_\lambda > \Delta F_{TH}$.

$$\sum \frac{n_i}{N_i} = \left(\frac{n_1}{\frac{1}{0.75^3}N1} + \frac{n_1}{\frac{1}{0.8282^3} * \frac{1}{0.75^3}N1} + \frac{n_1}{\frac{1}{0.8282^{3*2}} * \frac{1}{0.75^3}N1} + \cdots + \frac{n_1}{\frac{1}{0.8282^{3*(\lambda-1)}} * \frac{1}{0.75^3}N1}\right. \quad (5.11)$$

$$\sum \frac{n_i}{N_i} = \frac{n_1}{N1}\left(0.75^3 + 0.8282^3 * 0.75^3 + 0.8282^{2*3} * 0.75^3 + \cdots + 0.8282^{(\lambda-1)*3} * 0.75^3\right) = 0.75^3 * \frac{1-(0.8282^3)^{\lambda-1}}{1-(0.8282^3)} \quad (5.12)$$

$$= 2.32\frac{n_1}{N1}\,(0.75^3) = 0.98\,\frac{n_1}{N1}$$

The total cumulative damage due to the transient part of the vibration when k_v = 2, k_b = 3, and ζ = 3%, would be equal to 98% of the damage due to the steady state part of the vibration. This results in 50% life reduction for the structure.

In order to consider the fatigue stress threshold in computing the actual fatigue life, only the stress ranges above the threshold limit should be considered in calculations. For this, the number of cycles (λ) that has to be considered in the transient part of the vibration can be computed using Equation 5.13.

$$\lambda - 1 = \frac{\log(\frac{\Delta F_{TH}}{R.f_{ss}})}{\log(e^{-2\pi.\zeta})} \quad (5.13)$$

This equation is as a result of solving for λ-1 when the magnitude of $f_{\lambda(transient)}$ is equal to ΔF_{TH} , Equation 5.14. Noting that R is the ratio of the first cycle stress range in the transient part of the vibration to the maximum stress range in the steady state part of the vibration.

$$f_{\lambda(transient)} = \Delta F_{TH} = (e^{-2\pi.\zeta})^{\lambda-1}\ R\ f_{ss} \quad (5.14)$$

As can be seen in Table 5.3, the cumulative damage due to the transient part of the vibration varies from 0% to 672%. Therefore, for bridges with higher transient vibration (k_b less than 4), the effect of transient part and damping ratio should be taken into account for fatigue calculations.

The fatigue life decreases as a result of cumulative damage due to the transient part of the vibration. Actual fatigue life can be obtained using Equation 5.15.

$$\text{Actual life} = \frac{1}{1+\frac{TCD}{100}} \ \text{Life}_{\text{AASHTO}} \tag{5.15}$$

Where TCD is equal to the Transient Comulative Damage in percentage, which is shown in Table 5.3 for some k-parameters.

Figure 5.6 shows the effective life of the structure due to fatigue failure for the bridges designed by AASHTO criteria. The structure life time in AASHTO is assumed to be 75 years while ,as can be seen, only in some cases does the structure life reach to 75 years. In some cases, the structure life would be even less than 20 years. Therefore, considering k_b and the damping ratio is very important to calculate the fatigue life. The fatigue life for bridges with integer k_b would be much less than the calculated fatigue life.

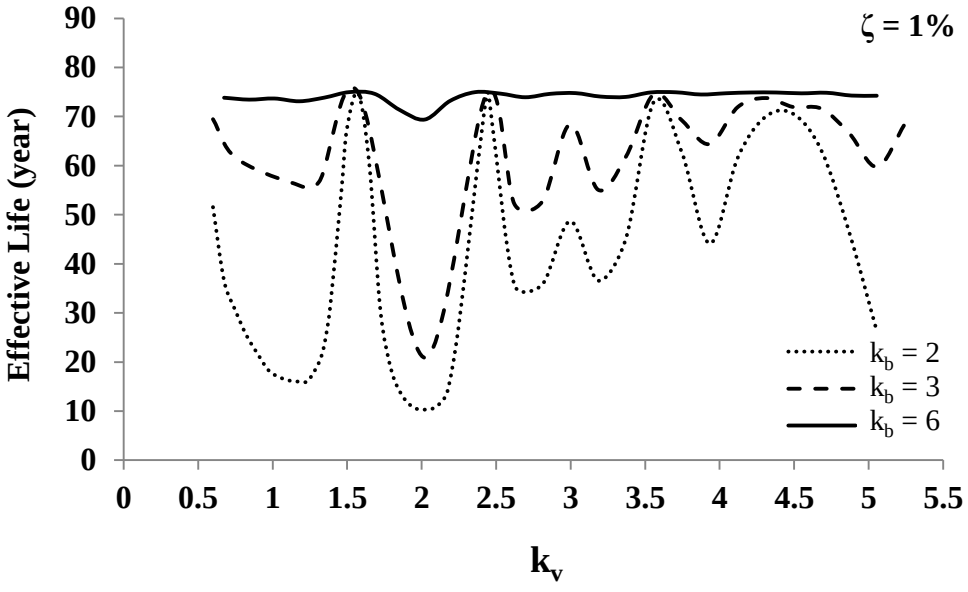

Figure 5.6 Effective fatigue life vs. k-parameters due to both steady state and transient parts of the vibration.

5.3 Fatigue Modification

To conclude the results of this chapter, it is suggested to calculate the fatigue stress limit based on the procedure proposed below.

- Find f_{ss} (computed using HL-93 truck, live load factor, distribution factor, and impact factor suggested by AASHTO).
- Find k_b and k_v using span length, maximum axle distance, bridge frequency, and average vehicle velocity (65 mph = 1144 in/sec).
- Using k_b and k_v , find the ratio of transient displacement response to the steady state response (R), Figure 5.4.
- Assume damping ratio (ζ).
- Find ΔF_{TH} from Table 5.1 for a specific detail category which is being designed.
- Find λ-1 using Equation 5.13. λ is the number of cycles in which the stresses are higher than ΔF_{TH}. Note that ΔF_{TH} should be greater than $R.f_{ss}$ in order to use Equation 5.13.

$$\lambda - 1 = \frac{\log(\frac{\Delta F_{TH}}{R.f_{ss}})}{\log(e^{-2\pi.\zeta})}$$

- Compute TCD, Transient Comulative Damage, using Equation 5.16.

$$TCD = R^3 . \frac{1 - (e^{-6\pi\zeta})^{\lambda-1}}{1 - e^{-6\pi\zeta}} \quad (5.16)$$

- Modify N, number of cycles that the structure is subjected to the truck load for the 75-year design life, by using Equation 5.17, instead of Equation 5.2.

$$N = (365)\,(75)\,(n + TCD)\,(ADTT)_{SL} \quad (5.17)$$

CHAPTER 6

CASE STUDIES

The procedure introduced in Chapter 5 would provide a better estimation for number of vibration cycles. Fatigue life can be better predicted by the method provided in Chapter 5. In previous chapters it was shown that the bridge dynamic response under the most common truck can be predicted using the bridge natural frequency, span length, and vehicle velocity. The predicted bridge vibration should then be limited to the threshold affecting human comfort. The objective of this chapter is to assess the validity of the results of previous chapters through a case study and suggest a reasonable acceleration limit for bridges.

Still there is no limitation that is agreed upon by all researchers which can confidently provide human comfort due to vibration. Some codes or researchers assert that limiting deflection would provide a good control on bridge vibration. Some others believe that velocity or acceleration limitation would control the excessive vibration felt by humans. In this chapter, a comparison is made between all available studies to better address the vibration issues.

6.1 Dynamic Response

As was mentioned, many researchers investigated the dynamic displacement response due to moving loads. In this section, some of these studies were chosen for verification.

6.1.1 Study by Yang et al. (1997)

Yang et al. (1997) considered a simple beam made of prestressed concrete with L = 20 m, I = 3.81 m^4, E = 29.43 GPa, m_b = 34,088 kg/m, for which the first frequency of vibration is ω = 44.75 rad/s (7.12 Hz). This beam is subjected to a train with 5 cars (10 axles) of length d = 18 m with a distance of 6 m between the cars. Each axle weight is equal to P = 215.6 kN. For the purpose of verification, two cases with speed parameters (S) equal to 0.27 and 0.6 are considered.

The results are shown in Figure 6.1. As can be seen, the current study's results match perfectly with the results obtained by Yang et al. (1997). For the speed parameter equal to 0.6, vehicle speed is equal to 170.88 m/s (615 Km/hr or 382 mph) which does not seem realistic for highway bridges. k_b for this case is equal to 0.83 and k_v is equal to 1. The integer value of k_v indicates that a high dynamic response should be expected. As was shown in Figure 4.6, for integer values of k_b, the maximum velocity and acceleration responses occur.

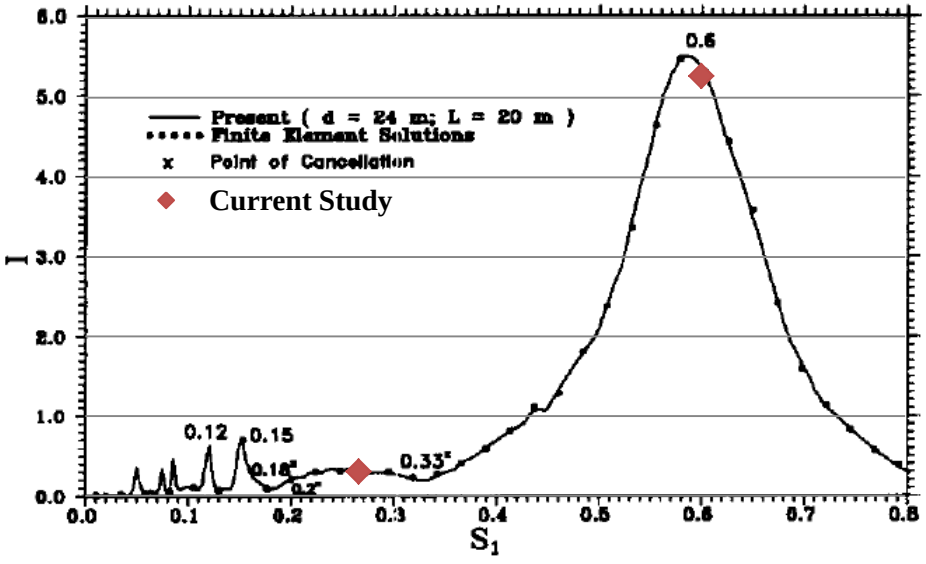

Figure 6.1 Impact factor versus speed parameter comparison with Yang et al. (1997).

The highest peak in Figure 4.6 corresponds to the k_b equal to 0.85. This value of k_b was not discussed earlier, as it is not reasonable for highway bridges. This case represents a condition in which the vehicle crosses through the span length in 85% of the bridge natural period. Note that for highway bridges, k_b is always greater than 2. and it is not realistic to consider this range of k_b for highway bridges.

6.1.2 Study by Yau et al. (1999)

In 1999, Yau et al. examined the moving load model versus the sprung mass to model a train on a simply supported beam. They concluded that "the moving load model can be reliably used to predict the bridge response."

The simply supported beam used in Yau et al.'s study is investigated and the results are compared with the original study. The beam has a span length of 30 m, a cross-sectional area of 7.94 m^2, a moment of inertia of 8.72 m^4, a mass per unit length of 36,056 kg/m, and a frequency of 29.3 rad/sec (4.66 Hz). The road irregularity was defined by a function shown in Equation 6.1, where x is the distance from the first support, x_0=1.0 m, r_0 is the amplitude of irregularities and is equal to 0.5 mm, and the wavelength of γ_0 = 1 m.

$$r(x) = -r_0 \left[1 - \exp(-\frac{x}{x_0})^3\right] sin\frac{2\pi x}{\gamma_0} \quad (6.1)$$

The bridge is subjected to T18 and S25 trains. The T18 train consists of 8 axles of 30 ton weight and equal distances of 18 m. The S25 train consists of 10 axles of 24 ton and axle distances of 18 and 7, alternating from axle to axle. The results are compared

with the original study in Figure 6.2. As can be seen, the results match perfectly. When the speed parameter for the bridge is equal to 0.3, the maximum response occurs under the T18 train. This speed parameter corresponds to the vehicle speed of 84 m/s (302 Km/hr, 188 mph). The vehicle and bridge k-parameters (k_v and k_b) corresponding to this vehicle speed are equal to 1 and 1.67. As can be seen, the results for a sprung mass are marginally smaller than the results from a moving load. This is due to the fact that the elastic behavior of tires interacting with the bridge surface absorbs some of the impact force on the bridge superstructure. Therefore, the results from moving load model are more conservative than sprung mass models.

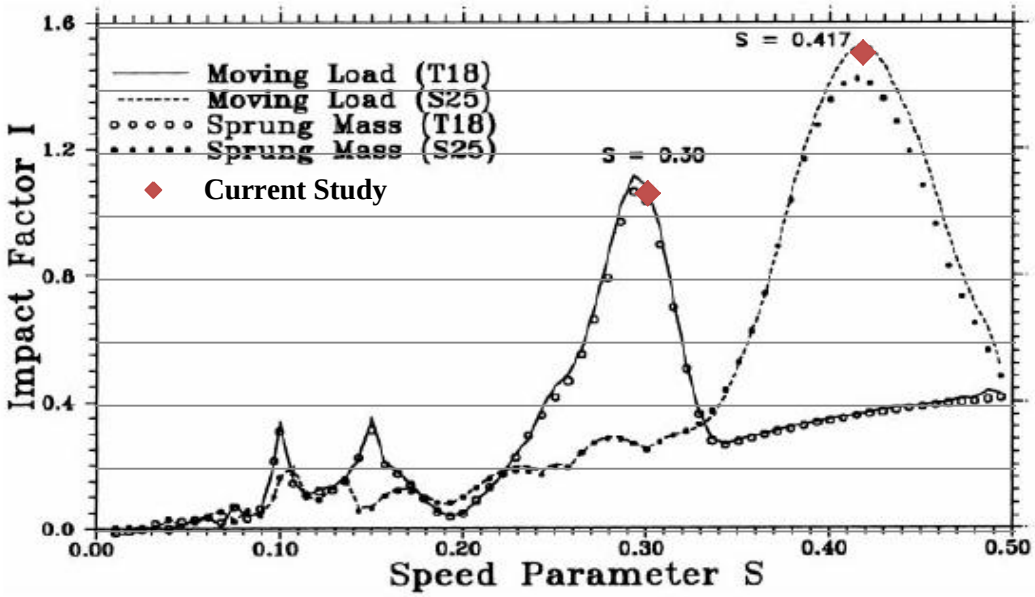

Figure 6.2 Impact factor for midspan deflection of a beam subjected to different vehicle models (Yau et al. 1999).

6.1.3 Study by Pan and Li (2002)

The effect of speed parameters on bridges dynamic response was also investigated by Pan and Li (2002). The properties of the single span beam used in this study are as follow:

Table 6.1 Bridge Parameters in Pan and Li (2002)

L (m)	EI (Nm^2)	m_b (kg/m)	m_v (kg)	V(km/hr)	K_{tire} (N/m)	ζ_{tire}
11.68	$1.72e^8$	3105	8900	68.4 (19 m/s)	104290	0.02

Vehicle-structure interaction was investigated in four different models. Dynamic Vehicle Element (DVE), Dynamic Nodal Loading (DNL), and Moving Load (ML) method were investigated in their study. They concluded that the proposed method of DVE provided the most accurate results, because "the DVE method treats the vehicle as a moving part of the entire system, which considers the vehicle influence at the element level by incorporating the detailed interaction between multiple vehicles and the structure induced by irregular road profiles."

The same bridge parameters are used for verification using the moving load utilized in this study. Figures 6.3 to 6.5 indicate that the results obtained by this study match very well with the results obtained by Pan and Li.

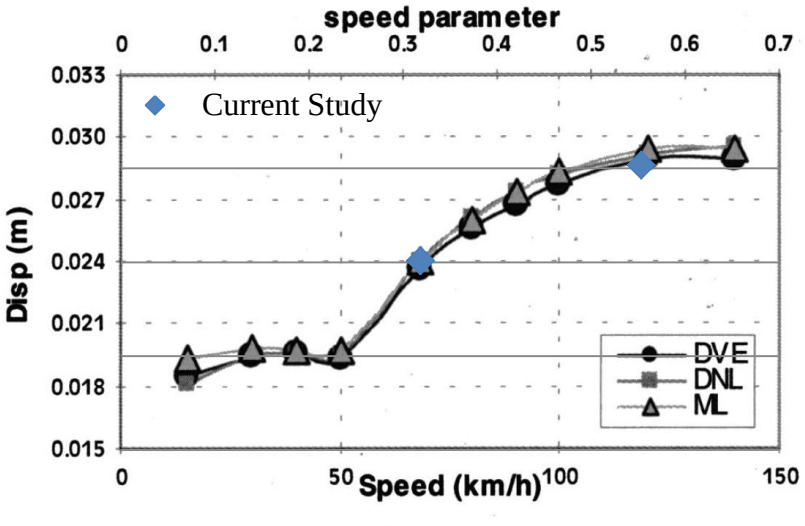

Figure 6.3 Midspan displacement of simply supported beam with different vehicle speeds (Pan and Li 2002)

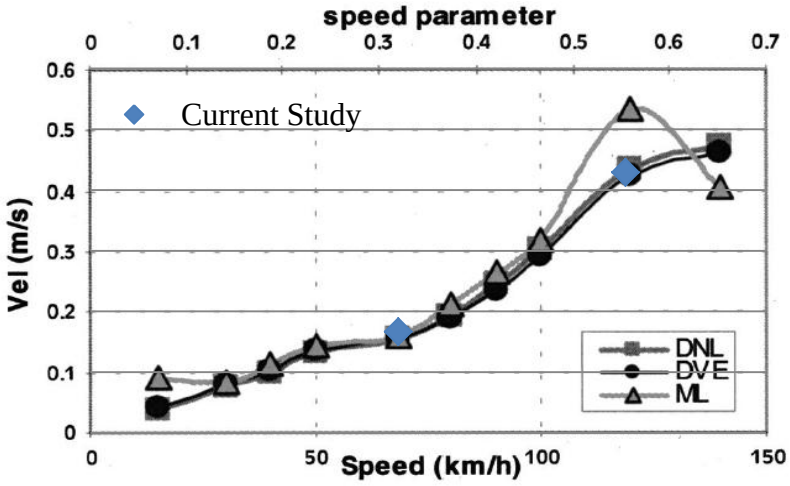

Figure 6.4 Midspan velocity of simply supported beam with different vehicle speeds (Pan and Li 2002)

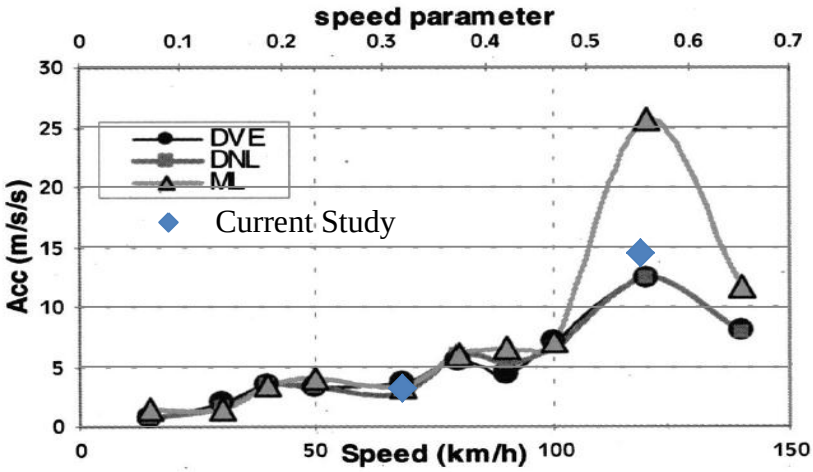

Figure 6.5 Midspan acceleration of simply supported beam with different vehicle speeds (Pan and Li 2002)

6.2 Human Comfort and Limitations

In Chapter 2 several studies were investigated for vibration limitation. These studies can be categorized into four types, those limiting static displacement (AASHTO 1998; Reiher and Meister 1931; Goldman 1948; Write and Green 1964); those limiting velocity (Gaunt

and Sutton 1981; Manning 1981; New Zealand 1994); those limiting acceleration (Postlethwaite 1944; Blanchard et al. 1977; Goldman 1948; BD 37/01; Ontario 1991; ISO 1989; Billing and Green 1984); and those limiting a combination of frequency and static deflection to provide human comfort (Gaunt and Sutton 1981; Janeway 1950, Wiss and Parmelee 1974). However, as limiting static deflection is more convenient for engineers, because no dynamic analysis is required, this limitation has been more popular among all others. Noting that, almost all research and regulations, including Canadian and British codes, require calculating the deflection limits as a function of frequency except AASHTO LRFD, which still does not use bridge frequency in the deflection criteria.

As was shown in Chapter 4, velocity and acceleration responses are proportional to dynamic displacement. Referring to Figure 5.4, the maximum ratio of transient stress "range" to steady state stress range is equal to 1. Thus, the ratio of the maximum transient displacement to steady state displacement is equal to 0.5.

$$\frac{\delta_{\max(\text{Transient})}}{\delta_{\max(\text{Steady State})}} = 0.5 \quad (\text{for } k_b \text{ and } k_v \text{ equal to } 2)$$

Considering that the value of the impact factor (IM) is equal to a constant 33% and the maximum displacement in the steady state part of the vibration is the maximum dynamic displacement, maximum transient response can be obtained thusly:

$$\delta_{\max(\text{Transient})} = 0.5 \ \delta_{\max(\text{Steady State})} = \ 0.5\,(\text{IM} + 1) \ \delta_{st}$$

Figures 4.14 and 4.15 show that the velocity and acceleration responses in the steady state part of the vibration are nearly identical to the vibration in transient part. Therefore, Equations 4.8 and 4.9 can be used in both the transient and the steady state

part of the vibration. Equation 6.2 can be used to compute the velocity and acceleration responses when k_b and k_v both equal to 2.

$$k_b, k_v = 2 \begin{cases} \text{Vel} = \omega.\delta_{\text{Transient}} = 0.5\ (\text{IM} + 1)\ \omega.\delta_{st} \\ \text{Acc} = (1 + 5\%)\omega^2.\delta_{\text{Transient}} = 0.5\ (\text{IM} + 1)(1 + 5\%)\ \omega^2.\delta_{st} \end{cases} \quad (6.2)$$

Note that the factor 0.5 in Equation 6.2 is only used for bridges with k_v and k_b equal to 2. For all other bridges this factor is less than 0.5 and varies depending on the values of k_b and k_v.

Equation 6.2 highlights the same fact as that shown in Figures 2.1, 2.2, and 2.10. As can be seen for higher values of bridge frequency, static deflection must be smaller in order to provide the same comfort level for pedestrians. In order to have a constant value for velocity or acceleration, when bridge frequency is higher, static deflection should be lower to compensate. This shows that limiting static deflection indirectly limits velocity or acceleration responses. Acceleration or velocity responses are directly influenced by both static deflection and natural frequency. The use of high performance materials would increase static deflection and decrease bridges natural frequency. The effect of these two parameters on bridges designed for HPS are in contradictory; meaning that although static deflection would be higher for HPS design, the lower frequency may result in the same acceleration value.

There are three limitations that are of interest to this study; they are an acceleration limitation of 100 in/sec^2 suggested by Wright and Walker (1972), a velocity limitation of 2.2 in/sec by New Zealand code (Wu 2003), and an acceleration limit of $0.5\sqrt{f}$ (m/sec^2) by British . The acceleration limit by BS code can be converted to US units and be written as $20\sqrt{f}$ (in/sec^2). These three limits are used for acceleration and

velocity values in Equation 6.1, and the static deflection is graphed with respect to frequency in Figures 6.6 and 6.7 combined with the graphs by other researchers.

Figure 6.6 indicates that the acceleration limit of 100 in/sec^2 is the most accurate limit to provide human comfort based on Goldman's graph (1948).

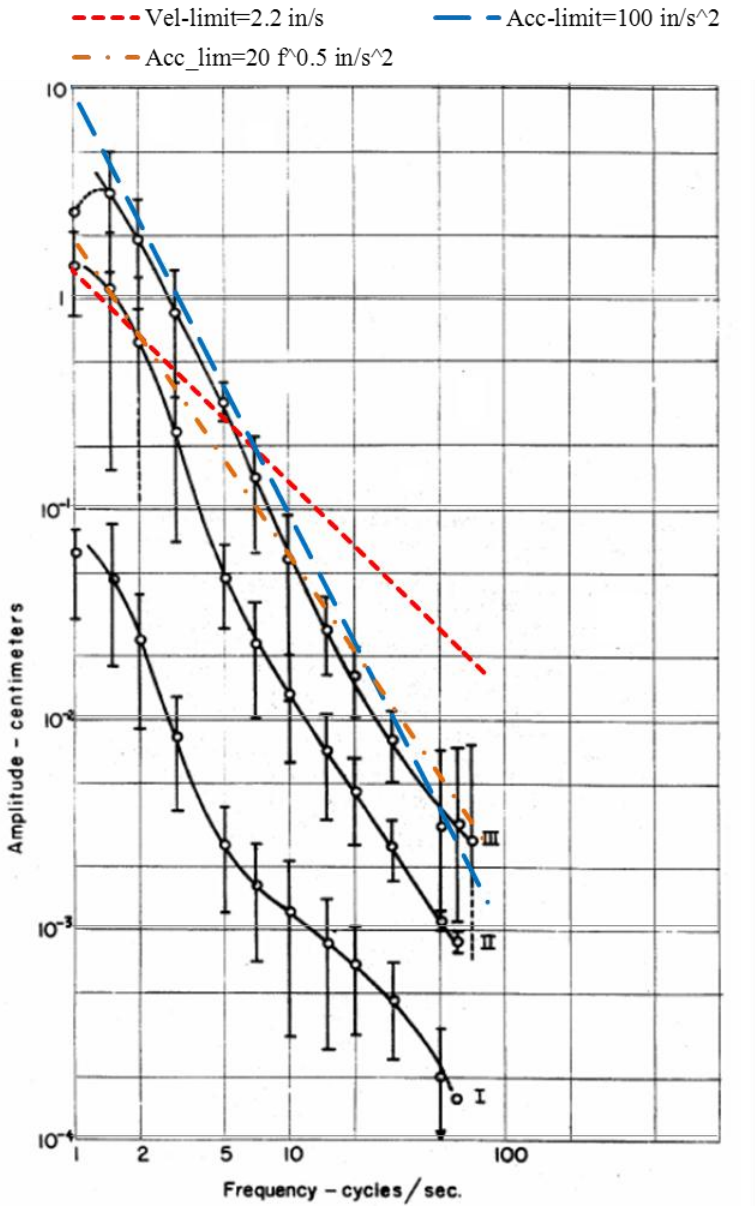

Figure 6.6 Comparison with average amplitude of vibration suggested by Goldman.

As can be seen the acceleration limit of 100 in/sec^2 matches the threshold of discomfort (III). A velocity limit of 2.2 in/sec and British acceleration limits do not seem to be accurate enough compared with the results obtained from a constant acceleration limit of 100 in/sec^2.

Figure 6.7 indicates that the limits suggested by Reiher and Meister (1931) match the British code for typical bridge frequencies of 2 to 10 Hz. An acceleration limit of 100 in/sec^2 is slightly higher than the threshold limits for very disturbing vibration. However, in highway bridges where excessive vibration is expected higher limits may be used.

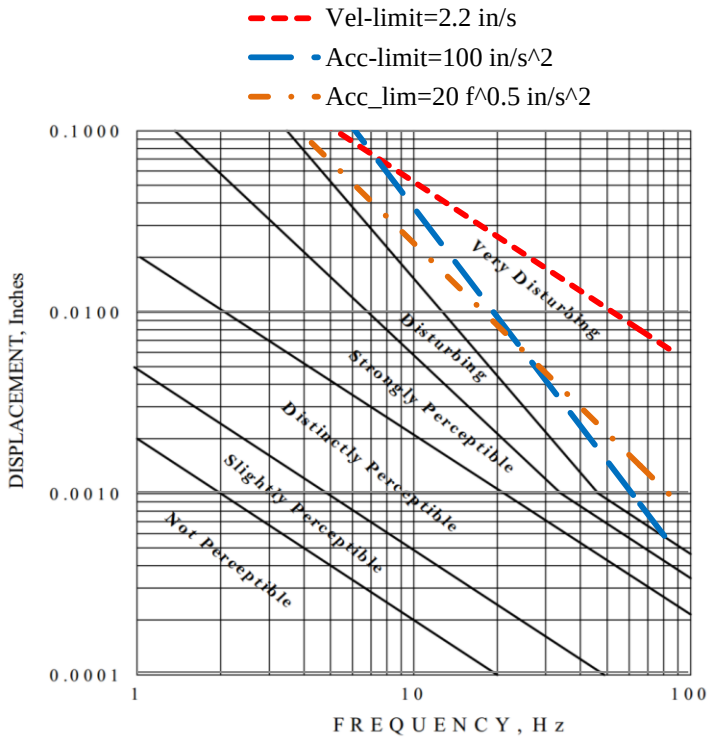

Figure 6.7 Comparison with the human perceptible vibration introduced by Reiher and Meister.

Figure 6.8 shows that neither acceleration nor velocity limits match Ontario limits. However, Write and Walker acceleration limit seems to be the closest match.

The deflection limits of L/800 or L/1000 suggested by AASHTO LRFD, and L/600 by Australian Specifications seem to be the least accurate method to control vibration in order to provide human comfort, due to the lack of frequency term in those criteria.

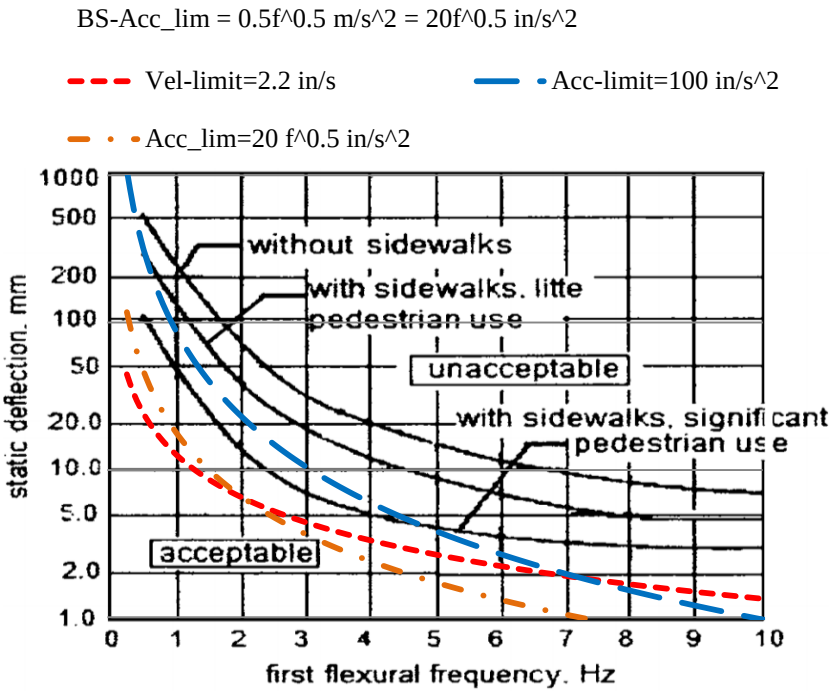

Figure 6.8 Comparison with Ontario Code deflection limits.

The acceleration limit suggested by Wright and Walker matches the deflection limits suggested by Goldman while it is about three times larger than the values suggested by Reiher and Meister. This could be attributed to the fact that humans discomfort threshold is different for bridges than for the buildings. The limitation suggested by Reiher and Meister is for a general human response. On bridges, where more vibration is expected, human tolerance for vibration is higher. Wright and Walker acceleration limit falls between two threshold limits used by Ontario Code.

British Standard acceleration limit matches Goldman deflection limits for the frequencies larger than 10 Hz while for frequencies less than 10 Hz it matches the deflection limits suggested by Reiher and Meister. British acceleration limit is far smaller than the limits suggested by Ontario code. Ontario threshold for sidewalk with significant pedestrian use is three times higher than the British acceleration limit.

Among all these limitations, the acceleration limit suggested by Wright and Walker seems to be the best limit to provide human comfort, as it is in the closest agreement with available deflection criteria. Note that, this acceleration limit corresponds to the "very strongly noticeable" threshold in German code, DIN 4150. This value is 140 in/s^2 and is shown in Table 2.4.

CHAPTER 7

RATIONAL SERVICEABILITY CRITERIA

As previously mentioned, the existing AASHTO deflection serviceability criteria are more than a century old and their origin is not known. Prior studies dispute their effectiveness in reducing dynamic effect and/or damage to bridges and they do not address the issues related to the application of high-performance materials. Thus, there is a need for a more rational serviceability requirement that accurately considers important dynamic parameters such as acceleration and frequency in addition to bridge deflection.

The research by Wright and Walker (1971) is the only work that proposed an equation to estimate bridge acceleration. However, it has not been implemented due to the lack of consensus and the limitation in its application. In this dissertation, a more general method is proposed to estimate the dynamic response of bridges subjected to moving loads.

In previous Chapters it was shown that the bridge vibration is solely dependent on k-parameters, bridge frequencies, damping ratios and static deflections. It was shown that the vibration in a single-span bridge is higher than a continuous-span bridge. Bracing and bridge stiffness in transverse directions do not affect bridge vibration. Also, for those bridges with smaller bridge to bearing stiffness ratio, bearing stiffness do not affect bridge dynamic responses.

The bridge maximum velocity and acceleration responses in the steady state part of the vibration are nearly identical to the maximum velocity and acceleration in the transient part of the vibration. To estimate the maximum dynamic response, Equations 7.1 and 7.2 are proposed to compute the bridge transient vibration for a rigid-support

single-span bridge with 1% damping ratio. It is recommended that the bearings are designed such that the bridge to bearing stiffness ratio is less than 5%. However, if this ratio is higher than 5%, bearing amplification response should be added to the computed values.

In Equations 7.1 and 7.2, the bridge natural frequency and static deflection for the heaviest axle of the truck are utilized. k_b is computed using the average truck speed and span length. k_b needs to be rounded to the nearest integer value in order to count for the response due to different truck speeds and the practical bridge frequency.

$$k_v \leq 2 \begin{cases} \delta_{Transient} = \frac{2}{k_b}(0.3k_v + 1.2).\delta_{st} \\ Vel = \omega\delta_{Transient} \\ Acc = (1 + 5\%)\omega^2\delta_{Transient} \end{cases} \quad (7.1)$$

$$k_v > 2 \begin{cases} \delta_{Transient} = \frac{2}{k_b}\left(0.2{k_v}^2 - 1.75k_v + 4.5\right).\delta_{st} \\ Vel = \omega\delta_{Transient} \\ Acc = (1 + 5\%)\omega^2\delta_{Transient} \end{cases} \quad (7.2)$$

The computed acceleration value should then be limited to the acceleration limit suggested by Wright and Walker, 25%g or 100 in/sec^2. If other values than 1% of damping ratio exist, a modification factor should be applied to the results obtained by Equations 7.1 and 7.2. As mentioned in Chapter 4, every 1% change in damping ratio influences displacement and acceleration by approximately 1.2% and 10%, respectively. Velocity is not noticeably influenced by damping ratio.

As examples, four actual bridges in New Jersey are investigated for this proposed serviceability criteria, on two of which an acceleration measurement was performed and the detailed results were included in the NJDOT report by Saadeghvaziri et al. (2012).

7.1 Example I- Magnolia Avenue Bridge

Magnolia Avenue Bridge is located over Route 1 & 9. It is a composite bridge with a single effective span of 129' 6". The bridge has two 15-foot lanes with two sidewalks. The NJDOT Bridge Manual required that the live load deflection under HL-93 Live Load be less than L/1000 (1.5 in). The bridge has 7 stringers with a depth of 42 in and a 6.5 ft distance between stringers. The deck thickness in 8.5 in. and the flanges of the stringers are composed of 70W steel and stringers webs are in 50W. The computed moment of inertia for one stringer with the proportional transformed concrete deck is equal to 68,121 in^4. The frequency, k_b and k_v for this bridge are equal to 2.0 Hz, 2.72 and 0.75, respectively. The deflection due to truck load was computed using CsiBridge software (CsiBridge 2012) and is equal to 2.76 in. Impact factor (IM) or dynamic load allowance is only applied to the deflection resulting from a truck load and is equal to 1.33 according to AASHTO LRFD. Therefore, the deflection due to truck load plus impact would be equal to 3.67 in. Deflection due to 0.64 kips/ft lane load is equal to 2.05 in.

$$\Delta_{\text{lane}} = \frac{5\omega L^4}{384EI} = \frac{5(\frac{0.64}{12})(1554)^4}{384(29000)(68121)} = 2.05 \text{ in}$$

The deflection resulted from the design truck itself (3.67 in) is higher than the deflection resulted from the design lane plus 25% of the design truck (2.97 in). The multiple presence factor for two lane bridge is equal to m = 1. The distribution factor is

computed assuming all girders deflect equally as suggested in AASHTO LRFD (AASHTO LRFD article 2.5.2.6.2).

$$\mathrm{DF} = \frac{\#\ \text{of Lanes}}{\#\ \text{of Stringers}} = \frac{2}{7} = 0.286$$

By applying DF and m factors to the maximum deflection resulting from HL 93 design truck plus impact, the final computed deflection would be equal to 1.05 in, which is less than 1.55 in (L/1000 limit) and acceptable by AASHTO LRFD and NJDOT Manual.

As k_v is smaller than 2, Equation 7.1 is used to estimate the dynamic response. Note that δ_{st} in this equation is computed using a 1-axle load, which is equal to 16 divided by 2 (to count for a line load in HL 93 truck).

$$k_v \leq 2 \begin{cases} \delta_{\mathrm{Transient}} = \frac{2}{3}(0.3\ (0.75) + 1.2).\frac{16 * 1554^3}{48\ (29000)(68121)} = 0.6\ \text{in} \\ \mathrm{Vel} = \omega\delta_{\mathrm{Transient}} = 2\pi(2)(0.6) = 7.5\ \text{in/sec} \\ \mathrm{Acc} = (1 + 5\%)\omega^2\delta_{\mathrm{Transient}} = 99\ \text{in/sec}^2 \end{cases}$$

As can be seen, velocity is higher than the New Zealand limit of 2.2 in/sec. Acceleration value does not meet the BS criteria which is equal to 20 $f^{0.5}$ in/sec^2. $20\ f^{0.5} = 28\ \text{in/s}^2$. The value of acceleration just meets Wright and Walker's acceleration limit of 100 in/sec^2.

7.2 Example II- Route 130 over Route 73

Route 130 over Route 73 is a simply-supported single-span bridge with a 128.3 ft span length, six stringers, and three lanes. The slab thickness and width are 9 in and 46 ft,

respectively. Stringers distance is 8 ft and haunch is equal to 1.5 inch. The bridge is designed with 70W for flanges and 50W for webs. The equivalent moment of inertia for this bridge is equal to 86,898 in^4 for one stringer and the proportional transformed concrete deck. Deflection has been computed using the same procedure as used for the Magnolia bridge for both lane and truck loads and the governing maximum deflection is equal to 1.19, which is less than the AASHTO deflection limit of L/1000, 1.54 in. The natural frequency, k_b and k_v for this bridge are equal to 2.11 Hz, 2.85 and 0.8, respectively. Considering Equation 7.1, dynamic responses for this bridge can be predicted.

$$k_v \leq 2 \begin{cases} \delta_{Transient} = \frac{2}{3}(0.3\,(0.8) + 1.2).\frac{16 * 1540^3}{48\,(29000)(86898)} = 0.466 \text{ in} \\ vel = \omega\delta_{Transient} = 2\pi(2.11)(0.466) = 6.17 \text{ in/sec} \\ Acc = (1 + 5\%)\omega^2\delta_{Transient} = 86 \text{ in/sec}^2 \end{cases}$$

The acceleration value satisfies the Wright and Walker acceleration limit. However, It is more than the BS acceleration limit of 29 in/sec^2 and not acceptable.

$$20\ f^{0.5} = 20(2.11)^{0.5} = 29 \text{ in/s}^2$$

The velocity is higher than 2.2 in/sec and does not satisfy the New Zealand velocity limitation either.

7.3 Examples III and IV - Field Measurements

The experimental acceleration data from two bridges in New Jersey, one with concrete stringers and the other with steel stringers were obtained. The steel-stringer bridge is located on Interstate I-80E over Interstate I-287N and the concrete-stringer bridge is

located on the same highway, Interstate I-80, but over Smith Road. The bridges are very close to each other and there is no exit or entrance ramp between them. The span lengths and computed frequencies and k-parameters for these two bridges are very similar to each other. Remarkably, the vibration in the steel-stringer bridge was much more substantial than the concrete-girder bridge.

The bridge on I-80 over I-287 is a simply-supported steel-stringer bridge with an 87.75 ft span length, 51 ft deck width, and 8 inch deck thickness. The concrete deck is supported by 7 steel stringers with grade 50 steel at a distance of 7.75 ft. Haunch is equal to 1.5 in and the bridge has 4 traffic lanes. The moment of inertia for one stringer cross section with its proportional deck is equal to 72,488 in^4, considering the transformed concrete deck to steel material. The steel bridge is without a sidewalk and the deflection limit, based on AASHTO LRFD, is equal to L/800 = 1.32 in. New Jersey deflection limit is more conservative than AASHTO LRFD and it is equal to L/1000 for all bridges, with or without sidewalk. Therefore, the deflection limit based on the NJ Design Manual is equal to 1.05 in.

The static deflections for this bridge under HL93 truck and lane load are equal to 0.781 in and 0.406 in, respectively. Therefore, the maximum governing deflection is resulted from the truck load alone. By applying m=0.65, DF=0.57 and IM=1.33 to the deflection resulting from the design truck, the final computed deflection would be equal to 0.38 in. As it can be seen, the computed deflection is significantly less than the limit provided by the NJ Design Manual. However, vibration on this bridge is strongly noticeable. The computed frequency, k_b, and k_v are equal to f = 4.6 Hz, k_b = 4.23, and k_v = 1.73, respectively.

Dynamic response can be computed using Equation 7.1:

$$k_v \leq 2 \begin{cases} \delta_{Transient} = \frac{2}{4}(0.3\,(1.73) + 1.2).\frac{16 * 1053^3}{48\,(29000)(72488)} = 0.154 \text{ in} \\ vel = \omega\delta_{Transient} = 2\pi(4.6)(0.154) = 4.5 \text{ in/sec} \\ Acc = (1 + 5\%)\omega^2\delta_{Transient} = 135 \text{ in/sec}^2 \end{cases}$$

As can be seen, the acceleration value for this bridge is much higher than the acceleration values for the Magnolia and Rt. 130 over Rt. 73 Bridges. This value does not satisfy the acceleration limit proposed by Wright and Walker. The acceleration and velocity values do not satisfy the BS and New Zealand limits either.

$$20\,f^{0.5} = 20(4.6)^{0.5} = 43 \text{ in/s}^2$$

Other field study was on the bridge on I-80 over Smith Road. This bridge is a simply-supported, 80.8 ft long and 51 ft wide bridge over concrete stringers. This bridge is less than a mile away from Rt. I-80 over Rt. I-287 (east side) and has 4 lanes, 7 concrete stringers with the moment of inertia of 686,061 in^4 , frequency of 4.74 Hz, k_b of 4.02, and k_v of 1.79. This bridge is the least flexible bridge among all the examples in this dissertation. Bridge to bearing stiffness ratio ($k_r = \pi^3 EI/L^3 k_s$) for this bridge is equal to 0.4 considering the minimum bearing stiffness of 234 kip/in. The deflection limit of L/800 is equal to 1.21 in and L/1000, stated by NJ manual, is equal to 0.97 in. Static deflection due to the design truck governs and it is equal to 0.514 in. The distribution factor, DF = 0.57, dynamic load allowance, IM = 1.33, and multiple presence factor, m = 0.65 should be applied to the deflection caused by truck load which result in 0.25 in deflection. This value is 26% of the NJ limit and 20% of the AASHTO limit.

$$k_v \leq 2 \begin{cases} \delta_{Transient} = \frac{2}{4}(0.3\,(1.79) + 1.2).\frac{16 * 960^3}{48\,(4000)(686{,}061)} = .09 \text{ in} \\ vel = \omega\delta_{Transient} = 2\pi(4.74)(0.09) = 2.8 \text{ in/sec} \\ Acc = (1 + 5\%)\omega^2\delta_{Transient} = 87 \text{ in/sec}^2 \end{cases}$$

As can be seen, the computed acceleration satisfies Wright and Walker's acceleration limit. However, it does not satisfy the BS and New Zealand acceleration and velocity limits.

$$20\ f^{0.5} = 20(4.74)^{0.5} = 43 \text{ in/s}^2$$

The results from field measurements indicate that the computed frequency for the concrete bridge is significantly less than the frequency obtained from test results. The experimental value is 10 Hz, while the computed value is 4.7 Hz. The Fast Fourier Transform (FFT) for both Rt. 80 over 287 and Rt. 80 over Smith Rd. bridges are provided in Figures 7.1 and 7.2. As can be seen, the experimental frequency for the steel bridge matches the computed frequency while the experimental frequency for concrete bridge is nearly twice as much as the computed one. This could be attributed to the support conditions with respect to the end diaphragms.

For this value of bridge frequency, k_b is equal to 8.4, and k_v is equal to 3.8. Therefore, Equation 7.2 is used to compute the dynamic response. Note that k_b for this bridge is a close value to an integer number plus 0.5 and dynamic response for this value of k_b is very close to zero for the average truck speed.

$$k_v > 2 \begin{cases} \delta_{Transient} = \frac{2}{8}(0.2(3.8)^2 - 1.75(3.8) + 4.5).\frac{16 * 960^3}{48\,(4000)(686{,}061)} = 0.02 \text{ in} \\ vel = \omega\delta_{Transient} = 2\pi(10)(0.02) = 1.256 \text{ in/sec} \\ Acc = (1 + 5\%)\omega^2\delta_{Transient} = 82.82 \text{ in/ sec} \end{cases}$$

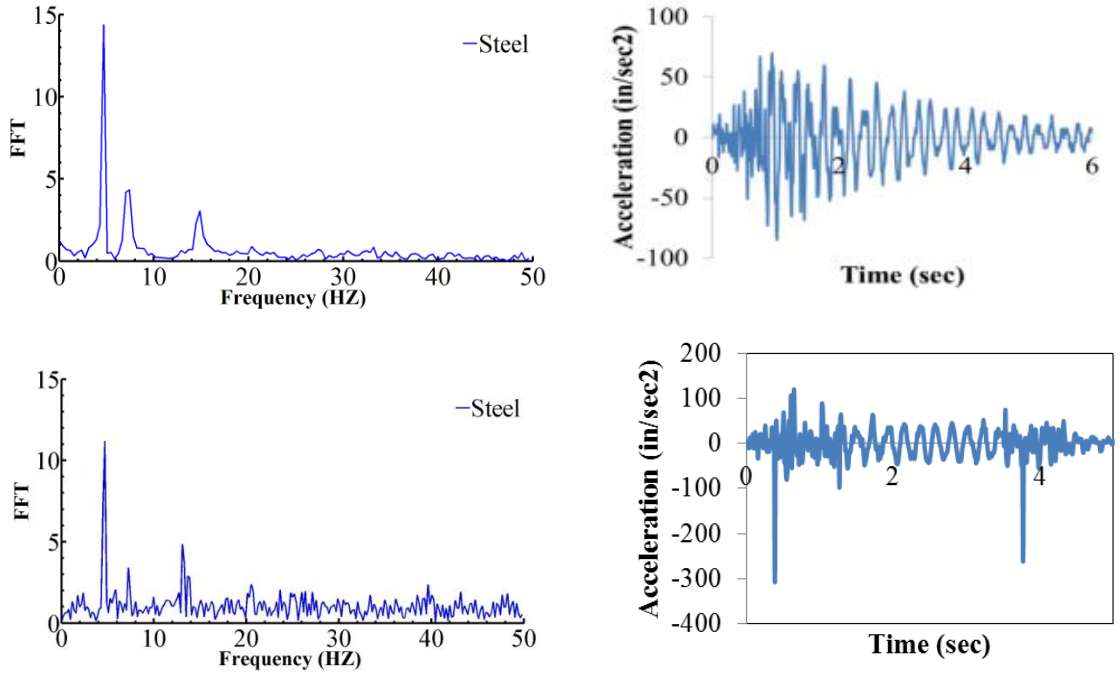

Figure 7.1 Fast Fourier Transform for Rt. I-80 over Rt. I-287 steel bridge.

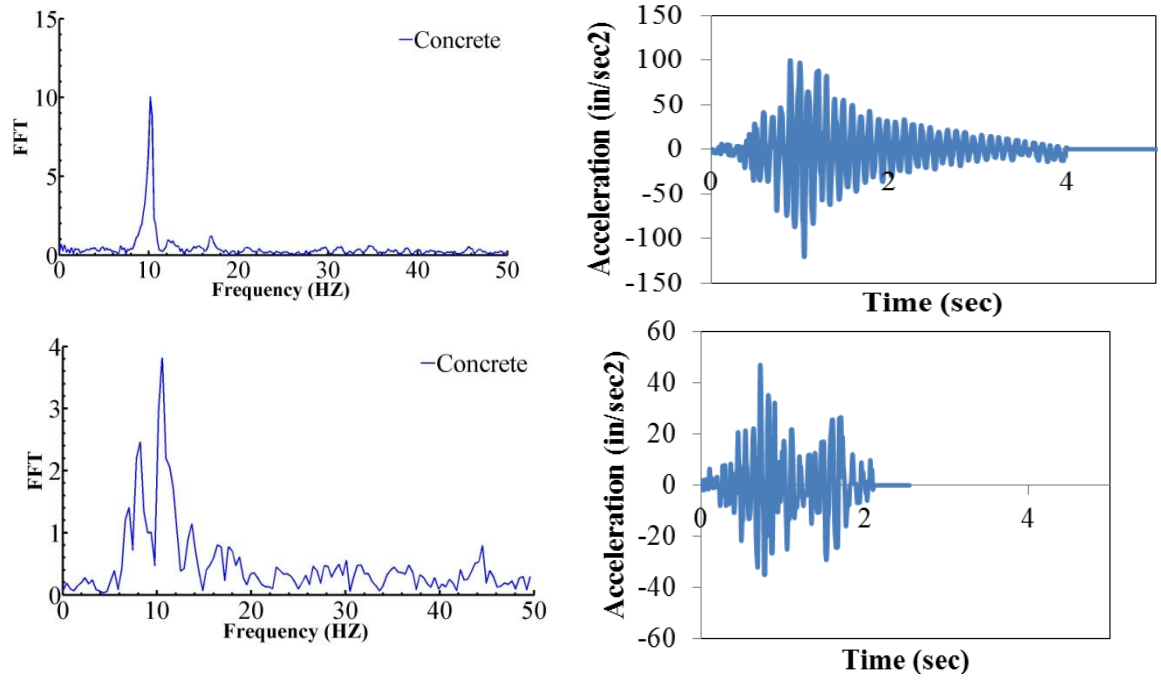

Figure 7.2 Fast Fourier Transform for Rt. I-80 over Smith Rd. concrete bridge.

The less-severe vibration observed in the concrete bridge is probably due to its higher frequency and lower vibration duration compared to the steel bridge. Although vibration duration after a truck exits the bridge is an important factor for human response, it does not influence the bridge structural performance. Bridge structural performance is influenced by the number of vibration cycles regardless of duration. Field measurements showed that vibration duration for concrete bridge does not exceed 2 seconds while the duration on steel bridge is more than 5 seconds. This is due to a higher measured frequency for the concrete bridge than the steel bridge.

The damping ratio for both bridges is less than 1.5% which is less than the values suggested by British code, which is 4% for steel composite bridges and 5% for concrete bridges.

Figure 7.3 and 7.4 show the end diaphragms in a typical concrete bridge versus a typical steel bridge. As can be seen, the end diaphragms in steel bridges do not provide enough supports for concrete deck. This provides and initial oscillation or impact on steel bridges which may significantly increase the dynamic responses.

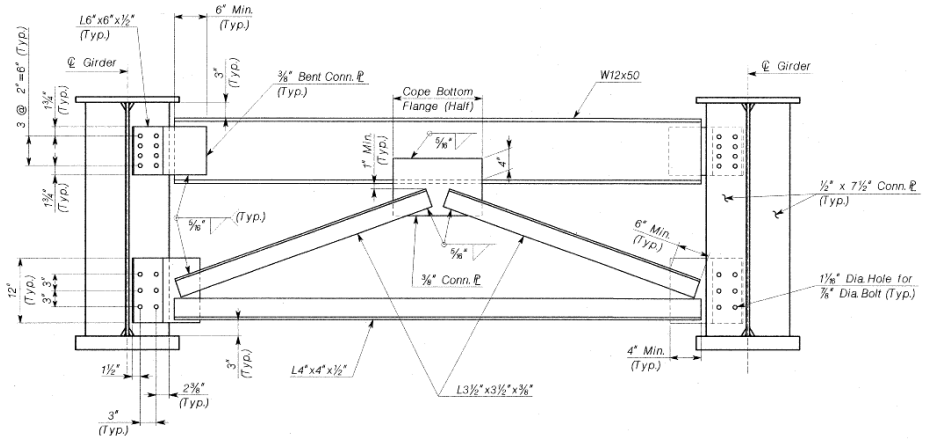

Figure 7.3 Typical end diaphragm detail for steel girder bridges.

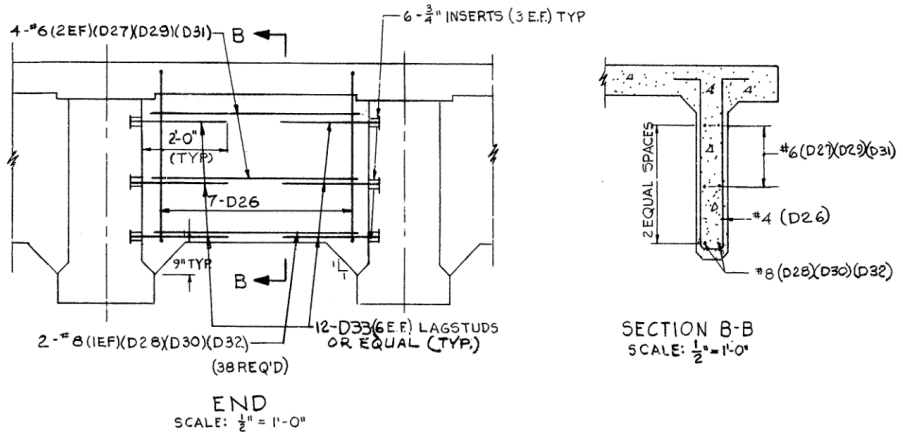

Figure 7.4 Typical end diaphragm detail for concrete girder bridges.

CHAPTER 8

CONCLUSIONS AND FUTURE WORK

With continued development of High Performance Steel (HPS), design for lighter and more economical bridges is unavoidable. HPS offers high-yield strength, high-fracture toughness, good weldability, and an ease of fabrication with the choice of weathering performance. In order to take advantage of these characteristics, some modifications are required in design codes so that they do not negate the use of such newly-innovated materials. AASHTO LRFD optional deflection criterion, which is implemented in the Bridge Design Manual of some states, including New Jersey, as a mandatory criterion, is based on experimental data which were obtained several decades ago. In the intervening time, not only have bridge construction, materials, and design changed, but so have vehicle type, weight, and flexibility.

Literature review shows no correlation between bridge structural damages and excessive deflection. Damages are due to connection rotations and local deformations which cannot be controlled by limiting the global deflection. It is now generally agreed by most researchers that deflection limits were based on the reactions of people to the bridge vertical acceleration rather than the structural effects.

Although the human body is more sensitive to the derivatives of displacement rather than the displacement itself, it is believed that deflection limits have been established and used for decades: computing deflection was much easier than computing the acceleration of a bridge under a moving truck load. While a few researchers such as Wright and Walker suggested simple methods to compute acceleration, these methods

have not been adopted by AASHTO Specifications because of the lack of consensus and the limitation on their application.

A comprehensive analytical parameter study has been performed under this study to investigate a bridge dynamic response under a moving truck load. Existing finite element (FE) software programs provide an ideal platform for such a parameter study. However, one has to be careful in selecting the modeling parameters as the acceleration and velocity time histories are quite sensitive to specific parameters such as time step, mesh quality, number of modes, and load representation. Therefore, to study acceleration and velocity responses, it is important to correctly select the finite element model parameters. In this study, first, the results of finite element models have been compared to the exact solution for single-axle loading where exact solution exists. Once confidence was established in the accuracy of the models, they were used for parameter study. The dynamic results are in dimensionless values for all acceleration, velocity and deflection responses for bridges at their mid-span.

Parameters considered are: vehicle velocity, span length, bridge natural frequency, speed parameter, damping ratio, number of spans, stringers distances, bracing effect, support conditions, and load sequence. Vehicle velocity (V), span length (L), and bridge frequency (f) have the most influence on bridge dynamic response.

The results indicate that k_b and k_v which are the bridge and vehicle k-parameters have the most influence on dynamic response. k_b can be obtained by natural frequency multiplied by span length divided by vehicle velocity (k_b =Lf/V),. This parameter is equal to half the inverse of the speed parameter, which has been established by several other researchers as an important parameter to bridge response under moving loads. k_v can be

computed using the truck length multiplied by natural frequency divided by the truck speed. It was noticed that the bridges with k-parameters equal to an integer number plus one half, i + 0.5, exhibited lower amplitudes of vibration under any types of trucks traversing the bridge. Thus, the intention is to design the bridges with i+0.5 k-parameters. For these bridges, the vibration in the transient part (after the truck exits the bridge) is nearly equal to zero and impact in the steady state part (while the truck is still over the bridge) is at the minimum value. This is true for all displacement, velocity, and acceleration responses.

For bridges with integer numbers of k-parameters, the dynamic response is at its maximum. For trucks with several axles, the dynamic amplification caused by one axle may be cancelled out by another axle. Hence, the arrangement of axles on the bridge is an important factor to estimate the bridge dynamic response.

Load sequence is a vast area for research with a large number of possibilities in vehicle types and bridge dynamic parameters. In particular, highway bridges can be investigated under the most common truck, which is similar to the AASHTO fatigue truck with one axle of 8 to 12 kips at the front, two axles of 12 to 16 kips at the middle, and two other axles of 12 to 16 kips at the back of the truck. The distance between the two axles at the middle and the two axles at the rear are normally 4-5 feet, the distance between the first axle to the second axle is equal to 14-18 feet, and the distance between the third axle and the forth axle is equal to 30-35 feet. After investigating three types of trucks with k-parameters equal to 2, 3 and 6, it was noticed that the bridges with frequencies equal to 2.7 and 5.4 Hz exhibit the highest vibration due to NJ 122 truck for

the speed limit of 65 mph. This truck was the most common truck in New Jersey and it is nearly the same as AASHTO fatigue truck.

Bridge acceleration and velocity are at their maximum or minimum when the vehicle k-parameter ($k_v = \frac{L_v}{V}.f$) is equal to an integer number or an integer number plus one half, respectively. The maximum deflection decreases when the axles are further from each other. In the vicinity of an integer number for k_v, deflection is the maximum; and in the vicinity of an integer number plus 0.5 for k_v, deflection is the minimum. As a truck speed is not always an exact value of 65 mph and the practical frequency may be slightly varied from the computed value, a range of k-parameters should be considered in practical approach. It is suggested to round the computed k_v and k_b to the closest integer values and utilize the integer values in the proposed equations. Equations 7.1 and 7.2 are proposed to estimate a bridge dynamic response under a moving truck. It is suggested that a higher value of impact factor is considered for k_v equal to two, similar to Canadian code.

Damping ratio, boundary condition, and number of spans were also among the parameters considered in this dissertation. The number of spans did not significantly affect dynamic response. However, dynamic response in the transient part of the vibration decreased slightly as the number of spans increased.

For large span bridges, the bridge flexibility is much larger than the bearings flexibility and the bridge to bearing stiffness ratio is very small (less than 5%). Therefore, support flexibility slightly influences the bridge natural frequency and the frequency of higher modes in a bridge. In such cases, bridge response under a moving truck is not influenced by support conditions. However, for short span bridges or those that the bridge

to bearing stiffness ratio is high, more flexible bearings would dramatically increase bridge responses. Therefore, design of a more flexible superstructure and a less flexible substructure is required to decrease dynamic responses under moving loads. Use of HPS and more flexible structures would be beneficial in this case.

It was shown that a higher damping ratio not only decreases the dynamic response, but also decreases vibration duration. If the damping ratio increases by the order of n, the number of vibration cycles decreases by the order of 1/n. For instance, if damping ratio increases from 1% to 2%, the number of vibration cycles decrease to half. This can significantly reduce fatigue problem caused by a high number of cycles.

Although previous research does not include enough acceleration response, deflection and impact factor results of some other studies were compared to the present study. The results are in agreement. The acceleration limit proposed by Wright and Walker (1971) and British Standard (BD 2001) and the velocity limit used by New Zealand code were converted to deflection based controls using the results obtained by this study. These deflection controls were then compared with the deflection limits suggested by Goldman (1948), Reiher and Meister (1931), and Ontario Code (1991). It was concluded that New Zealand velocity limit does not match any of the deflection limitations. Among all these limitations, the acceleration limit suggested by Wright and Walker seems to be the best limit to provide human comfort, as it matches the other criteria.

Two actual bridges, the Magnolia Bridge over Rt. 1 & 9 and the Route 130 Bridge over Route 73, were considered in the case study. Both bridges are located in New Jersey and constructed using hybrid girders of 70W for flanges and 50W for webs. The

proposed equations were used to compute both acceleration and velocity responses. The results were compared to the limits suggested by Wright and Walker (1971), New Zealand, British Codes. Neither of the computed acceleration or velocity for these two bridges satisfied British acceleration or New Zealand velocity limits. However, the computed acceleration for both bridges satisfied limit suggested by Write and Walker.

Acceleration response was measured on two bridges on Route 80, east side of Rt. I-80 over Rt. I-287, a steel girder bridge; and Rt. I-80 over Smith Rd which is a concrete-girder bridge, both located in New Jersey. Some of the observations on these two bridges were used as practical examples in this dissertation. These two bridges are less than one mile away from each other with the same frequency, number of girders, number of lanes, and span length. Vibration over the steel bridge was significantly more noticeable than vibration over the concrete bridge.

The steel girder bridge did not satisfy the acceleration limit suggested by Wright and Walker, nor did it satisfy the limits by British and New Zealand codes. Concrete bridge satisfies Wright and Walker acceleration limit while it did not satisfy the British and New Zealand limits.

Although both bridges satisfy the AASHTO and NJ design manual deflection limit criteria, the steel bridge exhibited much higher vibration under the same truck load than the concrete bridge. The computed frequency for the steel bridge corresponded to the frequency determined by the field test. Surprisingly, the frequency determined by the field test for the concrete bridge was twice as much as the computed frequency. In fact, this could be attributed to support conditions or the fact that the concrete deck is thoroughly supported by end diaphragms while the concrete deck in the steel girder

bridge is only connected to end diaphragms through stringers. In either case, more investigation is required to obtain a more solid conclusion on this matter.

Damping ratios for both bridges were less than 1.5%. Therefore, for those bridges that the value of damping ratio is not known, it is recommended that the damping ratio is taken as 1%. This provides a more conservative design for a bridge.

Future Work

Significant parameter study was performed in this dissertation. As a result, new serviceability equations were proposed that can have national implications. However, the proposed method, which appears to be consistent with other national efforts, will require determination of bridge frequency. To facilitate day-to-day implementation by engineers there is a need for easy and practical determination of bridge frequency. Bridge frequency can be computed for simply-supported bridge using the available equation. However, there is still no simple equation to estimate higher mode frequencies or the frequencies for multi-span bridges with various span lengths.

As the measured bridge frequency for concrete bridge was nearly twice as much as the computed frequency on this bridge, more investigation is required on this aspect to find the reasons for such a difference. There is also a need for more measurements of response of highway bridges to moving loads, especially the acceleration response as more rational serviceability requirements tend to consider this aspect of bridge response too. Acceleration should be measured by accurate ground accelerometers so that the exact value can be compared with finite element results.

Moreover, the results are required to be expanded to include curved and skewed bridges. Similar to existing parameter study both 2-D and 3-D models with different boundary conditions, girder distances, and cross bracing spacing should be investigated.

APPENDIX A

HYPERELASTIC MODEL

In a stress relaxation test, the stress is measured under a constant strain. The schematic time-dependent stress function for the relaxation test is shown in Figure A.1.

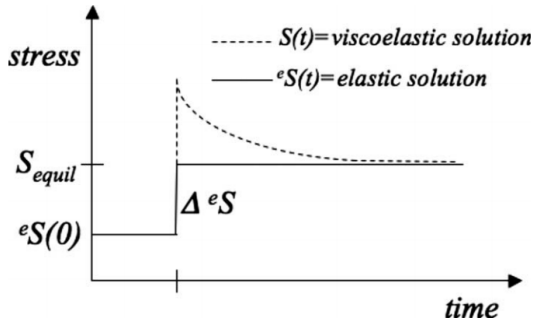

Figure A.1 Elastic and viscoelastic stress responses due to a strain step function.

The viscoelasticity property of the material models can be represented by simple spring and dashpot models. The linear-elastic component follows Hook's law in which:

$$\sigma = E \cdot \varepsilon \tag{A.1}$$

The equation for the viscous component of the material model is as shown in Equation A.2, in which η represents the viscosity constant.

$$\sigma = \eta \cdot \frac{\partial \varepsilon}{\partial t} \tag{A.2}$$

To define the viscoelasticity behavior of a material, two models may be used, separately considering the material's elastic and viscous components. These two models

are based on either relaxation or creep tests and are known as Maxwell and Kelvin models, respectively (Figure A.2).

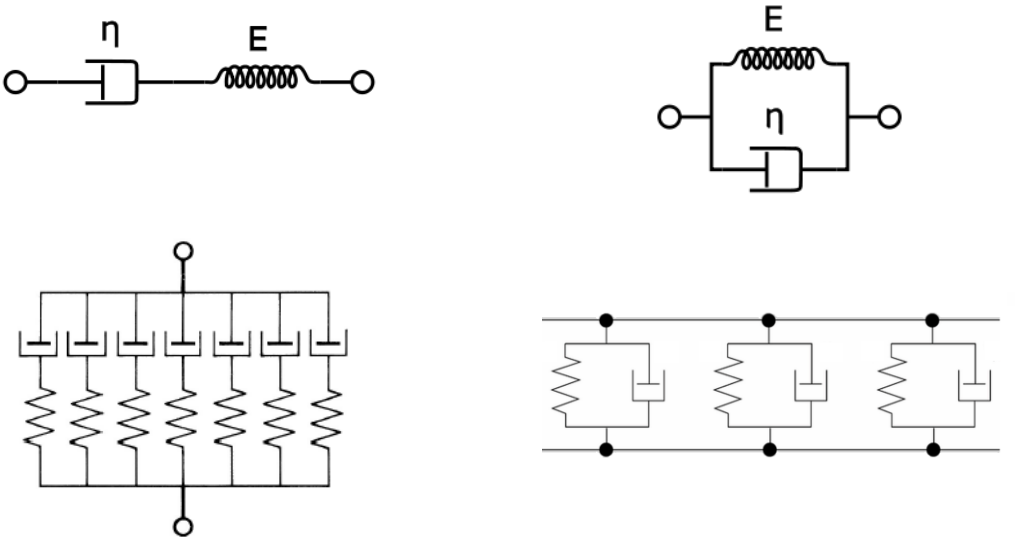

(a) (b)

Figure A.2 Maxwell model for one mode and the generalized model (a) and Kelvin Model (b).

In Maxwell models, the viscous and elastic components of a material are in serial combination with each other and the total strain is equal to the sum of the viscous and elastic strains; while the stresses in dashpots and springs are equal to each other and equal to the total stress.

$$\varepsilon_{\text{total}} = \varepsilon_{\text{elastic}} + \varepsilon_{\text{viscos}} \tag{A.3}$$

By differentiating Equation A.3 with respect to time and substituting Equations A.1 and A.2 in it, the following equation is obtained:

$$\dot{\varepsilon} = \frac{\dot{\sigma}}{E} + \frac{\sigma}{\eta} \tag{A.4}$$

In order to simulate the relaxation test data for viscoelastic material models, solving the differential Equation A.4 for $\dot{\varepsilon} = 0$ is required, in which the strain is held constant over time, and stress is a function of time. Solving this differential equation results in the following equations:

$$\sigma_{(t)} = E.\varepsilon_0 . e^{-\frac{E}{\eta}t} \tag{A.5}$$

$$E_{(t)} = E. e^{-\frac{E}{\eta}t} \tag{A.6}$$

The viscoelastic function can be estimated as shown in Equation A.5. In this equation, $\sigma_{(t)}$ is the stress function with respect to time, E is the modulus of elasticity, ε_0 is the constant strain, and η is the material viscosity constant.

The ratio of $\frac{\eta}{E}$ can be shown by τ and is called relaxation time. This time corresponds to the time in which the material has lost 63% of its final stiffness loss and 37% of the final stiffness loss remains. The computation can also be performed for shear stress and strain and the loss in shear modulus with respect to time can be computed (Equation A.7).

$$G_{(t)} = G_0. e^{-\frac{t}{\tau}} \tag{A.7}$$

However, a real material model does not lose all its stiffness in infinity. Therefore, Equation A.7 can be written as follows:

$$G_{(t)} = G_\infty + G_0. e^{-\frac{t}{\tau}} \tag{A.8}$$

The Generalized form of the Maxwell model does not consider one relaxation time for the material. In this model, it is assumed that different molecular segments of different lengths contribute differently to relaxation time. Therefore, more springs and dashpots contribute in the material model. Figure A.2a shows the generalized Maxwell model as well as the single model. The corresponding equation for the generalized Maxwell model is as follows. This series is also known as Prony series.

$$G_{(t)} = G_{\infty} + \sum_{i=1}^{N} G_i \, . \, e^{-\frac{t}{\tau_i}} \tag{A.9}$$

In the Kelvin model, it is assumed that the same strain is felt by both viscous and elastic elements and that the stresses are additive, as seen in Equations A.10 and A.11. The Kelvin model represents a creep experiment in which the strain reaches a limiting value after a very long time.

$$\sigma_{total} = \sigma_{elastic} + \sigma_{viscous} \tag{A.10}$$

$$\sigma = E.\varepsilon + \eta \, . \, \dot{\varepsilon} \tag{A.11}$$

For hyperplastic materials, stress-strain relationship can be defined by different strain energy density functions, W, the derivative of which with respect to strain gives the stress values in the material. The strain energy function can be composed of two separate terms representing the energy due to shear deformation and the energy due to volumetric change. These two terms are called deviatoric (shear) and dilatational (volumetric) components of the strain energy function.

$$W_{total} = W_{deviatoric} + W_{dilatational} \quad \text{(A.12)}$$

The deviatoric strain energy function can be defined using many mathematical models such as the Neo-Hookean model, applicable for a strain range less than 30%, the Mooney Rivlin model for the strain range between 30-200%, the Polynomial and Arruda Boyce model for a strain range up to 300%, and the Yeoh and Ogden model for a strain range up to 700%.

Since the ultimate strain for the Natural Rubber used in elastomeric bearings should be larger than 400%, according to AASHTO, the higher orders of strain energy functions such as Ogden or Yeoh should be used to make an acceptable curve fit based on experimental data. Curve fitting for various hyperelastic models are performed to choose the best model which matches the provided experimental data.

For the test results used in this study, Yeoh strain energy function resulted in the best curve fit for the material model. Therefore, the 3rd order of this function is used for the elastomer material model.

The Yeoh function is used for nearly incompressible hyperplastic materials and is defined as:

$$W_{deviatoric} = C_{10}\,(I_1 - 3) + C_{20}\,(I_1 - 3)^2 + C_{30}\,(I_1 - 3)^3 \quad \text{(A.13)}$$

Where C_{10}, C_{20}, and C_{30} are the material constants and I_1 is the first stretch invariant which is expressed as:

$$I_1 = {\lambda_1}^2 + {\lambda_2}^2 + {\lambda_3}^2 \quad \text{(A.14)}$$

For uniaxial test, the first stretch invariant is defined as:

$$\lambda_1 = \lambda\,;\ \lambda_2 = \lambda_3 = \sqrt{\frac{J}{\lambda}}\,;\ I_1 = \lambda^2 + \frac{2J}{\lambda} \tag{A.15}$$

In the case of equi-biaxial extension, the first stretch invariant is defined as:

$$\lambda_1 = \lambda_2 = \lambda\,;\ \ \lambda_3 = \frac{J}{\lambda^2}\,;\ I_1 = 2\lambda^2 + \frac{J^2}{\lambda^4} \tag{A.16}$$

Volumetric component of strain energy function can be obtained using Equation A.17:

$$W_{dilatation} = \sum_{n=1}^{3} D_n\,(J-1)^{2n} \tag{A.17}$$

Where D_n is the material incompressibility constant and J is the volume ratio (V_2/V_1) due to hyperelastic pressure and is equal to:

$$J = \sqrt{I_3} = \lambda_1.\lambda_2.\lambda_3 \tag{A.18}$$

Where I_3 is the third stretch tensor invariant and $\lambda_1, \lambda_2, \lambda_3$ are stretch values. Stretch values are defined as strain values plus 1, as stretch is defined as the final length divided by the original length, whereas strain is defined as the change in length divided by the original length.

APPENDIX B

DESIGN OF ELASTOMERIC BEARINGS

To design a bridge's elastomeric bearings, the following procedure is performed by AASHTO LRFD:

1. The area is computed such that the total compressive stress due to total load does not exceed 1.75 ksi.

2. The total height of the elastomers should be larger than $2\Delta_s$, in which Δ_s is equal to the total shear deformation.

3. The maximum elastomer height should be considered such that the criteria in Equations B.1 and B.2 are satisfied.

$$\sigma_s \leq 2GS \tag{B.1}$$

$$\sigma_L \leq GS \tag{B.2}$$

4. Bearings shall be designed to prevent from uplift due to rotations. Equation B.3 should be satisfied.

$$\sigma_s > 1.0GS\left(\frac{\theta_s}{n}\right)\left(\frac{B}{h_{ri}}\right)^2 \tag{B.3}$$

5. The thickness of the steel reinforcement, h_s, shall satisfy the provisions of Article 14.7.5.3.7 of the AASHTO LRFD Bridge Construction Specifications, and:

At the service limit state: $$h_s \geq \frac{3h_{max}\sigma_s}{F_y} \tag{B.4}$$

At the fatigue limit state: $$h_s \geq \frac{2.0h_{max}\sigma_L}{\Delta F_{TH}} \tag{B.5}$$

Where:

S = the shape factor for the thickest layer of the elastomers.

n = number of interior layers of elastomer.

h_{ri} = thickness of the i^{th} elastomer layer (in.).

σ_s = service average compressive stress due to the total load (ksi).

σ_L = service average compressive stress due to live load.

B = length of pad if rotation is about its transverse axis, or width of pad if rotation is about its longitudinal axis (in.).

θ_s = maximum service rotation due to the total load (rad.).

ΔF_{TH} = constant amplitude fatigue threshold for Category A as specified in Article 6.6 (ksi)

h_{max} = thickness of thickest elastomeric layer in elastomeric bearing (in.)

F_y = yield strength of steel reinforcement (ksi)

REFERENCES

AASHTO (1996). *Load Factor Design: Bridge Design Specifications*, American Association of State Highway and Transportation Officials, Washington, D. C.

AASHTO (1998). *Load Resistance and Factor Design: Bridge Design Specifications*, American Association of State Highway and Transportation Officials, Washington, D.C.

Alampalli, A. (2001). "Correlation between bridge vibration and bridge deck cracking: a qualitative study." *Report FHWA/NY/SR-01/136*, Transportation Research and Development Bureau, New York State Department of Transportation, Albany, NY.

Aluri, S., Jinka, C., and GangaRao, H.V.S. (2005). "Dynamic response of three fiber reinforced polymer composite bridges." *Journal of Bridge Engineering*, 10(6), 722-730.

ANSYS. < http://www.ansys.com/>, (Nov 30, 2012)

Aramraks, T. (1975). "Highway bridge vibration studies." *Report FHWA/IN/JHRP-75/02* ,*Joint Highway Research Project*, Indiana State Highway Commission, Purdue University, West Lafayette, IN.

Amin, A.F.M.S., Lion, A., Sekita, S., and Okui, Y. (2006). "Nonlinear dependence of viscosity in modeling the rate-dependent response of natural and high damping rubbers in compression and shear: Experimental identification and numerical verification." *International Journal of Plasticity*, 22(9), 1610-1657.

ASCE (1958). "Deflection limitation of bridges." *Journal of the structural division*, ASCE, 84(3), 1-20.

Ashebo, D. B., Chan, T. H. T., and Ling, Y. (2007). "Evaluation of dynamic load on a skew box girder continuous bridge. Part I: Field test and modal analysis." *Journal of Structural Engineering*, 29(6), 1052–1063.

Au, F. T. K., Jiang, R. J., and Cheung, Y. K. (2004). "Parameter identification of vehicles moving on continuous bridges." *Journal of Sound and Vibration*, 269(1-2), 91-111.

Azizinamini, A., Barth, K., Dexter, R., and Rubeiz, C. (2004). "High performance steel: research front-historical account of research activities." *Journal of Bridge Engineering ASCE*, 9(3), 212-217.

Barker, M. G., Gandiaga, L., and Staebler, J. (2008). "Serviceability limits and economical steel bridge design." *Interim Report, University of Wyoming, in cooperation with U.S. Department of Transportation Federal Highway Administration, Washington, DC.*

Barker, M. G., Staebler, J., and Barth, K. E. (2011). "Serviceability limits and economical steel bridge design." *Publication No. FHWA-HIF-11-044,* West Virginia University and *University of Wyoming, in cooperation with U.S. Department of Transportation Federal Highway Administration, Washington, DC.*

Bartos, M. J. (1979). "Ontario write new bridge code." *Journal of Civil Engineering, ASCE*, 49(3), 56-61.

BD 37/01 (2001). *Design Manual for Roads and Bridges*. 2(2), part 8. Highway Agency, London, UK.

Billing, J. R. and Green, R. (1984). "Design provisions for dynamic loading of highway bridges." *Second Bridge Engineering Conference*, Transportation Research Record 950, National Research Council, Washington, DC, 94-103.

Blanchard, J., Davies, B. L. and Smith, J. W. (1977). "Design criteria and analysis for dynamic loading of footbridges." *Transport and Road Research Laboratory Supplementary Report 275*, Symposium on Dynamic Behavior of Bridges, Crow Thorne, UK, 90-106.

Brown C. W. (1977). "An engineer's approach to dynamic aspects of bridge design." *Transport and Road Research Laboratory Supplementary Report 275*, Symposium on Dynamic Behavior of Bridges, Crow Thorne, UK, 107-113.

Chopra, Anil K., 2007. *Dynamics of Structures: Theory and Applications to Earthquake Engineering.* 3rd ed., Prentice Hall, NJ.

Clingenpeel, B. F. (2001). "The economical use of high performance steel in slab-on-steel stringer bridge design." MS thesis, West Virginia University, Morgantown, WV.

CsiBridge. "Computers and Structures. Inc structural and Earthquake Engineering Software". <www.csiberkeley.com/csibridge>, (Nov. 30, 2012).

Dexter, R. J., Wright, W. J., and Fisher, J.W. (2004). "fatigue and fracture of steel girders." *Journal of Bridge Engineering*, ASCE, 9(3), 278-286.

Ebrahimpour, A.; and Sack, R. L. (2005). "A review of vibration serviceability criteria for floor structures." *Computers and Structures*, 83(28-30), 2488-2494.

Esmailzadeh, E. and Jalili, N. (2003). "Vehicle-passenger-structure interaction of uniform bridges traversed by moving vehicle." *Journal of Sound and Vibration*, 260(4), 611-635.

Fisher, J. W. and Wright W. J. (2007). "High toughness of HPS: Can it help you in fatigue design" *Journal of Constructional Steel Research*, 63, 922-940.

Fountain, R.S. and Thunman, C.E. (1987). "Deflection Criteria for Steel Highway Bridges." *Proceedings of the National Engineering Conference and Conference of Operating Personnel*, New Orleans, LA, 20.1-20.12.

Fryba, P. L. (1999). *Vibration of solids and structures under moving loads*. 3rd Edition, Thomas Telford, Westminster, London.

Fushun, L., Huajun, L., Guangming, Y., Yantao, Z., Weiying, W., and Wanqing, S. (2007). "New Damage-locating Method for Bridges Subjected to a Moving Load." *Journal of Ocean University of China*, 6(2),199-204.

Gaunt, J. T. and Sutton, C. D. (1981), "Highway Bridge Vibration Studies." *Joint Highway Research Project, FHWA/IN/JHRP-81/11*, Engineering Experiment Station, Purdue University, West Lafayette, IN.

Gergess, A. N. and Sen, R. (2009). "Cold bending HPS 485W steel bridge girders." *Journal of constructional steel research*, 65 (8-9), 1549-1557.

Goldman, D.E. (1948). "A Review of Subjective Responses to Vibratory Motion of the Human Body in the Frequency Range 1 to 70 Cycle per Second." *Naval Medical Research Institute*, National Naval Medical Center, Bethesda, MD.

Goodpasture, D.W., and Goodwin, W.A. (1971), "An evaluation of Bridge Vibration as Related to Bridge Deck Performance." *Final Report, No. 440.924*, The Tennessee Department of Transportation, The University of Tennessee, Knoxville, TN.

Griffin, M. J. (1996). *Handbook of human vibration.* Elsevier academic press, London, UK.

Homma, K. (1994). "Potential for high performance steel in plate-girder bridge designs under the LRFD code." MS Thesis, Department of Civil Engineering, Lehigh University, Bethlehem, Pennsylvani.

Homma, k., Tanaka, M., Matsuoka, K., Kasuya, T. and Kawasaki, H. (2008). "Development of application technologies for bridge high-performance steel, BHS." *Nippon steel technical report No. 97*, Special Issue on Construction and Architectural Materials, 51-57.

ISO, International Standards Organization (1989). "Evaluation of human exposure to whole-body vibration _ part 2: Continuous and shock-induced vibration in buildings (1_80 Hz)." International Standard ISO- 2631/2, Geneva, Switzerland.

ISO, International Standards Organization (2002). "Mechanical vibration - Evaluation of measurement results from dynamic tests and investigations on bridges." *International Standard ISO/DIS 18649:2002(E),* Geneva, Switzerland.

Janeway, R.N. (1950). "Vehicle Vibration Limits for Passenger Comfort. From Ride and Vibration Data." *Special Publications Department (SP-6),* Society of Automotive Engineers Inc., Warrendale, PA.

Kawatani, M., Kobayashi, Y., and Kawaki, H. (2000). "Influence of elastomeric bearings on traffic-induced vibration of highway bridges." *Fifth International Bridge Engineering Conference*, Tampa, Florida, 76-82.

Kirkcaldie, D. K., and Wood, J. H. (2008) "Review of Australian standard AS 5100 Bridge design with a view to adoption – Volume 2." *NZ Transport Agency Research Report 361*, NZ Transport Agency, Wellington, New Zealand.

Kou, J, -W., and DeWolf, T. (1997). "Vibrational behavior of continuous span highway bridge- influencing variables." *Journal of Structural Engineering*, 123(3), 333-344.

Krauss, P. D., and Rogalla, E. A. (1996). "Transverse Cracking in Newly Constructed Bridge Decks" *National Cooperative Highway Research Program Report NCHRP Report No. 380,* Transportation Research Board, National Research Council, Washington, DC.

Machado, M. A. (2006). "Alternative Acceleration-Based Serviceability Criterion for Fiber Reinforced Polymer Deck-on-Steel girder Bridges." PhD Dissertation, Perdue University, West Lafayette, Indiana.

Maddox, S. J. (2003). "Review of fatigue assessment procedures for welded aluminum structures." *International Journal of Fatigue*, 25(12), 1359-1378

Majka, M., and Hartnett, M. (2008). "Effects of speed, load and damping on the dynamic response of railway bridges and vehicles." *Journal of Computers and Structures* 86(6). 556-572.

Manning, D. G. (1981). "Effects of Traffic-Induced Vibrations on Bridge-Deck Repairs." *National Cooperative Highway Research Program Synthesis of Highway Practice, No. 86,* Transportation Research Board, National Research Council, Washington, DC.

MATLAB, <http://www.mathworks.com/>, (Nov. 30, 2012).

Matsuda, A. (2004). "Evaluation for Mechanical Properties of Laminated Rubber Bearing Using Finite Element Analysis." *Journal of Engineering Materials and Technology,* Transactions of (ASME), 126(1), 134-140.

Michaltsos, G. T., and Raftoyiannis, I.G. (2010). "The influence of a train's critical speed and rail discontinuity on the dynamic behavior of single-span steel bridges." *Engineering Structures*, 32(2), 570-579

Moghimi H., Ronagh H. R. (2008). "Development of a numerical model for bridge_vehicle interaction and human response to traffic-induced vibration." *Journal of Engineering Structures*, 30, 3808-3819.

Munirudrappa, N., and Iyengar, H.N.D. (1999). "Dynamic analysis of continuous span highway bridge." ISET Journal of Earthquake Technology, 36(1), 73-84.

Museros, P., and Alarcón, E. (2005). "Influence of the second bending mode on the response of high-speed bridges at resonance." *Journal of Structural Engineering*, 131(3), 405-415.

Nagy, G. I. (2008). "Development of an optimized short-span steel bridge design package." Department of Civil and Environmental Engineering, College of Engineering and Mineral Resources at West Virginia University, Masters' Thesis, Morgantown, WV.

Nishikawa, K., Murakoshi, J. and Matsuki, T. (1998)." Study on the fatigue of steel highway bridges in Japan." *Construction and Building Materials*, 12(2-3), 133-141.

Nevels, J.B., and Hixon, D.C. (1973). "A Study to Determine the Causes of Bridge Deck Deterioration." *Final Report,* State of Oklahoma Department of Highways. Oklahoma City, OK.

Nowak, A.S. and Grouni, H.N. (1988). "Serviceability Considerations for Guide ways and Bridges." *Canadian Journal of Civil Engineering*, (4), 534-537.

Oehler, L.T. (1957). "Vibration Susceptibilities of Various Highway Bridge Types." *Project 55 F-40, No. 272*, Michigan State Highway Department, Lansing, MI.

Oehler, L.T. (1970). "Bridge vibrations: summary of questionnaire to state highway departments." *Project No. 107*, National Research Council, Highway Research Board, Washington, DC.

Ontario Highway Bridge Design Code (1991). 3rd ed., Ontario Ministry of Transportation and Communications Highway Engineering Division, Toronto, Ontario, Canada.

Pan, T. –C. and Li, J. (2002). "Dynamic Vehicle Element Method for Transient Response of Coupled Vehicle-Structure Systems." *Journal of Structural Engineering*, 128(2), 214-223.

Postlethwaite, F. (1944). "Human Susceptibility to Vibration." Engineering, 157(4072), 61-63.

Elias, P., and Villot, M. (2010). "Review of existing standards, regulations and guidelines, as well as laboratory and field studies concerning human exposure to vibration." *RIVAS SCP0-GA-2010-265754*, Railway-Induced Vibration Abatement Solutions Collaborative Project, Paris, France.

Roeder, C. W., Barth, K. and Bergman A. (2002). "Improved Live Load Deflection Criteria for Steel Bridges." *NCHRP Web Document 46 (Project 20-7(133))*, National Cooperative Highway Research Program Transportation Research Board of the National Academies.

Reiher, H. and Meister, F.J. (1931). "The Effect of Vibration on People." *Report No. F-TS-616-RE,* Headquarters Air Material Command, 2(II), Translation: Wright Field, Ohio, 1946.

Saadeghvaziri, M. A., and Hadidi, R. (2002). "Cause and Control of Transverse Cracking in Concrete Bridge Decks." *FHWA-NJ-2002-19, Final report*, Federal Highway Administrat ion U.S. Department of Transportation Washington, D.C.

Saadeghvaziri, M. A. (1993). "Finite Element Analysis of Highway Bridges Subjected to Moving Loads." *Journal of Computers and Structures*, 49(5), 837-842.

Saadeghvaziri, M. A., Darjani, S., Saigal, S.,and Khan, A. (2012). "Design for deflection control vs. use of specified span to depth ratio limitations." *FHWA-NJ-2012-009*, Final report, New Jersey Department of Transportation Bureau of Research, Trenton, NJ, and U.S. Department of Transportation Federal Highway Administration, Washington, DC.

Smith J.W. (1988). *Vibration of structures, application in civil engineering design.* Chapman and Hall, London.

Takayama, M., Tada, H., and Tanaka, R. (1992). ''Finite element analysis of laminated rubber bearing used in base-isolation system.'' *Rubber Chemistry and Technology*, 65(1), 46–62.

Tilly, G. P., Cullington, D. W. and Eyre, R. (1984). "Dynamic Behavior of Footbridges." *IABSE Surveys*, IABSE, S-26/28, 13-23.

Wei, J. and Chen, B. (2007). "Estimation of dynamic response for highway CFST arch bridges" *5th International conference on arch bridges*, Madeira , Portugal.

Wiss, J. F. and Parmelee, R. A. (1974). "Human perception of Transient Vibrations." *Journal of the Structure Division*, ASCE, 100(4), 773-787.

Wright, D.T. and Green, R. (1959). "Human Sensitive to Vibration." *Report No.7, Ontario Department of Highway and Queen's University*, Kingston, Ontario, Canada.

Wright, D. T. and Green, R. (1964). "Highway Bridge Vibration. Part II" *Report No., Ontario Test Program*, Ontario Department of Highways and Queen's University. Kingston, Ontario, Canada.

Wright, R. N. and Walker, W. H. (1971). "Criteria for the deflection of steel bridges." *American Iron and Steel Institute*, Bulletin No. 19, Washington, DC.

Wu, H. (2003). "Influence of live load deflection on superstructure performance of slab on steel stringer bridges." PhD Dissertation, College of Engineering and Mineral Resources at West Virginia University, Morgantown, WV.

Zhou, S., Rizos, D. C. and Petrou, M. F. (2004). "Effects of superstructure flexibility on strength of reinforced concrete bridge decks." *Computers and Structures*, 82(1), 13-23.

Zivanovic, S.; Pavic, A.; and Reynolds, P. (2005). "Vibration Serviceability of Footbridges under Human-Induced Excitation: a Literature Review." *Journal of Sound and Vibration*, 279(1-2), 1-74.

Yang, Y.B., Lin, C.L, Yau, J.D., and Chang, D.W. (2004). "Mechanism of resonance and cancellation for train-induced vibrations on bridges with elastic bearings." *Journal of Sound and Vibration*, 269(1-2), 345-360.

Yang, Y., -B., Yau, J., -D., and Hsu, L., -C. (1997). "Vibration of simple beams due to trains moving at high speeds." *Engineering Structures*, 19(11), 936-944.

Yau, J.-D., Wu, Y.-S., Yang, Y.-B. (2001). "Impact response of bridges with elastic bearings to moving loads." *Journal of Sound and Vibration*, 248(1), 9-30.

Yau, J.-D., Yang, Y., -B., and Kuo, S. -R. (1999). "Impact response of high speed rail bridges and riding comfort of rail cars." *Journal of Engineering Structures*, 21(9), 836-844.

Yau, J.-D. and Yang, Y.-B. (2006). "Vertical accelerations of simple beams due to successive loads traveling at resonant speeds." *Journal of Sound and Vibration*, 289, 210–228

Yoshida, J., Abe, M., Fujino, Y. (2004). "Constitutive Model of High-Damping Rubber Materials." *Journal of Engineering Mechanics ASCE*, 130(2), 129-141.